A GENERALIZED THEORY OF SORPTION PHENOMENA IN BIOLOGICAL MATERIALS

Thesis for the Degree of Ph. D.
MICHIGAN STATE UNIVERSITY
PATRICK OBI NGODDY
1969

This is to certify that the

thesis entitled

A GENERALIZED THEORY OF SORPTION
PHENOMENA IN BIOLOGICAL MATERIALS

presented by

Patrick Obi Ngoddy

has been accepted towards fulfillment
of the requirements for

Ph.D. degree in Agr. Eng.

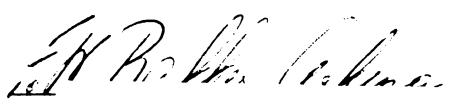

Date Sept. 24, 1969

ABSTRACT

A GENERALIZED THEORY OF SORPTION PHENOMENA IN BIOLOGICAL MATERIALS

by Patrick Obi Ngoddy

A moisture sorption model unifying three basic concepts in adsorption, is developed and verified for biological materials.

The B-E-T and Capillary Condensation theories are combined into an integral isotherm equation for porous biological materials. In order to solve the integral equation explicitly, it was necessary to (a) characterize the physical structure of sorbing bio-materials mathematically, and (b) to derive an explicit density function for water sorbed by biological materials, utilizing the general framework of the Adsorption Potential theory in conjunction with the fundamental laws of thermodynamics.

Application of the moisture adsorption model to adsorption data of a wide variety of biological materials led to the following specific conclusions:

1. The pores of biological materials are best modeled as interconnected spheroidal ink-bottles.
2. The numerical distribution of pore-size in biological materials can be described by a power law type analytical function.
3. The density of water adsorbed by biological materials may be expressed by the semi-theoretical relation:

$$\rho/\rho_o = \mu^* \ (\Delta H_{st}/\Delta H^\circ_{st})$$

where ρ is the density associated with the isosteric heat of

ads

iso

def

4. The

iso

5. A t

of

"sw

suc

adsorption ΔH_{st}, ρ_o and ΔH°_{st} are the corresponding density and isosteric heat values at saturation, and μ^* is empirically defined for the class of bio-materials of interest.

4. The three basic concepts in adsorption can be unified into an isotherm equation of the type:

$$M_a = \frac{\rho \bar{\xi}}{\eta} (Z^{\eta} - \lambda^{\eta})$$

$\bar{\xi}$ and η are characteristic parameters of the physical structure of the sorbent, and Z and λ are functions of relative vapor pressure.

5. A theory of sorption hysteresis based on the superposition of the so-called "capillary condensation" hysteresis and "swelling fatigue" hysteresis is developed and used to predict successfully the desorption isotherms of whole corn kernels.

Approved F. W. Bakker-Arkema
Major Professor Sept 24, '69

Approved Carl W. Hall
Department Chairman

A GENERALIZED THEORY OF SORPTION PHENOMENA IN BIOLOGICAL MATERIALS

By

Patrick Obi Ngoddy

A THESIS

Submitted to
Michigan State University
in partial fulfillment of the requirements
for the degree of

DOCTOR OF PHILOSOPHY

Department of Agricultural Engineering

1969

661755
2/-27-70

To

The people of BIAFRA

at their moment of supreme anguish.

ACKNOWLEDGEMENTS

It gives the author special pleasure to acknowledge with sincere gratitude, the indispensable help and guidance of Dr. Fredrick W. Bakker-Arkema (Agricultural Engineering), a truly inspiring teacher and counselor, whose attitude and friendship made this investigation a very rewarding and delightful experience.

The personal interest and unfailing assistance of Dr. J. B. Kinsinger (Chairman, Chemistry) who guided the author's study of the fascinating field of Surface Chemistry is gratefully acknowledged.

Sincere appreciation is extended to Dr. W. G. Bickert (Agricultural Engineering) and Dr. D. R. Heldman (Agricultural Engineering and Food Science) for serving on the author's guidance committee.

The author is indebted to Dr. Carl W. Hall (Chairman, Agricultural Engineering) and his staff for making available the graduate assistantship and for their kind cooperation and help in innumerable other ways.

Grateful acknowledgement is due Dr. Bakker's group of graduate students, David Farmer, Gonzalo Roa, John Rosenau, and David Thompson, whose lively participation in several brain storming sessions helped to crystallize many of the concepts presented in this dissertation.

It seems appropriate to recognize here, members of the author's family: his parents, Mr. and Mrs. H. O. Ngoddy and sister, Mrs. R. A. Akudu, who were directly responsible for his early education; his wife, Omogo, without whose understanding and kind support this study could not have been accomplished.

Finally, thanks go to the members of the M.S.U. Glass Shop for their unfailing assistance, to Mr. M. P. Palnitkar for his assistance in the laboratory experiments, and to Mrs. Nancy Hodge for her extraordinary patience and diligence in typing the manuscript.

****

TABLE OF CONTENTS

Table

2.1

2.2

2.3

2.4

4.1.1

4.1.2(a)

4.1.2(b)

4.1.3

4.2.1

4.2.2

4.3.1

4.3.2

LIST OF TABLES

Tab

LIST OF FIGURES

NOTATION

d	average diameter of sorbate molecule, [A°]
f	factor of pore geometry
d.b.	dry basis
H	enthalpy, [calories]
$\Delta H_{st}, Q_{st}$	isosteric heat of sorption, [calories/mole]
ΔH, $\Delta' H$	enthalpy change, [calories/gram]
$\Delta H_m, \Delta' H_m$	molar enthalpy change
E	elastic modulus, [psi]
ΔF	surface free energy
K	bulk modulus, [psi]
K_1	pore-size distribution parameter, eqn. (2.3.16)
K_{12}	parameter defined by eqn. (4.1.5)
$L(R)$	length of pore of radius, R, [A°]
M	molecular weights of sorbate, [grams]
M_a	specific adsorbed mass [grams]
M_d	specific desorbed mass
M_o	equilibrium moisture content, [M.C.d.b.]
M.C.	moisture content
n, n'	number of sorbate molecules, number of adsorbed multi-layers
P	vapor pressure
P_m	vapor pressure corresponding to the mono-layer capacity
P_a	adsorption vapor pressure
P_d	desorption vapor pressure
P_s	swelling pressure, eqn. (2.5.5)
R	pore radius, [A°]
R_g	universal gas constant
R_a	radius of curvature of meniscus during adsorption
R_d	radius of curvature of meniscus during desorption [A°]
r	generalized radius of meniscus [A°]
r_c	Cohan radius [A°]
r_k	Kelvin radius [A°]
r_{12}	parameter defined by eqn. (4.1.4)
S	entropy, [Cal./degree]
S_{BET}	B-E-T surface area $(A°)^2$
S_m	molar entropy, [Cal./degree-mole]
$\Delta S, \Delta' S$	entropy change
$\Delta S_m, \Delta' S_m$	molar entropy change

$N(R)$	number of pores of size, R
0	used as a subscript or superscript implies saturation conditions
V_a	specific adsorbed volume, eqn. (2.3.13) [cc]
V	volume, [cc]
V_m, $\overline{V}$	molar volume [cc]
v_R	volume of pore of radius, R
v_{12}	finite volumetric step
Δv	volumetric hydro-expansion
X	in chapter I used as relative vapor pressure; elsewhere used as specific adsorbed mass
X_m	specific adsorbed mass at the mono-layer capacity
X_L	specific adsorbed mass at hygroscopic or fiber saturation point
Z	variable, defined by eqn. (2.3.23)
α	identification for a component of a thermodynamic system
β_o	coefficient of linear hydro-expansion, [in./in. % M.C.d.b.]
σ	surface tension of condensed sorbate
σ_H	normal stress, [psi]
S_{12}	surface area pores associated with a given adsorption step, $[(A°)^2]$
T	temperature, [°K]
t	thickness of adsorbed multi-layer, [A°]
χ_1	variable defined by eqn. (2.3.25)
χ_2	variable defined by eqn. (2.3.26)
ω	factor of pore geometry
Ω	empirical constant of the Halsey eqn. (2.3.5)
τ	average thickness of a single layer of adsorbed molecules, [A°]
γ	pore-size distribution parameter, eqn. (2.3.16)
λ	constant defined by eqn. (2.3.24)
η	primary characteristic parameter of pore structure, eqn. (2.3.20)
ξ	secondary characteristic parameter of pore structure, eqn. (2.3.19)
$\varphi_1(R)$	function of pore geometry
$\varphi_2(R)$	pore-size distribution function
ν	Poisson's ratio

σ_m	area which one adsorbed molecule will occupy $(A°)^2$	Ψ,φ	contact angle
		π	two dimensional spreading pressure in chapter I
ρ	density of sorbed water, [gm./cc.]		
		θ	fraction of surface covered by mono-molecular adsorption
μ^*	function defined by eqn. (2.4.26)		
μ,μ'	chemical potential	$\varkappa$	factor of pore geometry

I. INTRODUCTION

1.1 General Remarks

The growing socio-economic importance of food and fibres together with the complexity of the technology for their production, handling, processing, preservation and distribution has brought about a new and exacting emphasis among Agricultural and Food Engineers on the study of BIOLOGICAL MATERIALS SCIENCE. The primary intent of this endeavor is to provide higher quality food and fibre products more economically, while the methodology consists of the basic engineering approach to problems involving the handling and processing of biological materials. It appears logical that the physical laws governing the response of biological materials to handling and processing must be well understood in order to optimize harvesting, processing, handling and storage systems.

It is now well established that the moisture content of biological products exerts a profound influence on their mechanical, physical, chemical and enzymic behaviors. This recognition has, in the main, provided the stimulus for the large body of scientific work to be found on the subject. The work, with a few limited exceptions, has been primarily experimental in nature. In consequence, while there exists a vast quantity of confirmatory data on the relationship between biological products and those molecules of water associated with them, the exact nature of water in food, and even such fundamental datum as the adsorption isotherm itself has not been satisfactorily derived from a theoretical point of view. The cause

of the sigmoid shape of this isotherm and of the distinctively pronounced hysteresis effect must still be considered the subject of conjecture rather than the consequence of an established theory. A large body of isolated data still exists which to a greater or lesser degree has refused to fit any general treatment. Yet, in view of its all pervading influence, it is fundamental to the entire field of biological materials science, that the laws which underlie the hygroscopic phenomena in biological materials be well understood and particularly that these laws be rendered more concise, understandable and useable by expressing them in more precise mathematical terms. The present work was undertaken in the attempt to weld some of the data - old and new - into a coordinated theory of adsorption for biological materials.

1.2 Hygroscopic Phenomena - Moisture Retention and Transport in Bio-Materials

Kuprianoff (1958) in his treatment of bound water in foods, suggests that moisture in biological materials may exist as free moisture, chemically bound moisture, and adsorbed moisture. In appraising the relative contribution of each type of moisture to the overall role of water in food, he concludes that adsorbed moisture is by far the most important category of water in biological products. The extensive body of scientific work on the subject amply vindicates the point that problems associated with moisture transport and retention in bio-materials above the so-called hygroscopic point lend themselves to relatively easy theoretical treatment. The hygroscopic point has been defined by Lewis (1921) as the product moisture content

corresponding to a relative humidity of 100 percent. Above this point, the physical laws of osmosis, liquid diffusion and capillarity govern the motion or retention of water molecules in organic materials. These laws are coordinated with remarkable success (Lykov, 1955) into a moisture transport theory. This theory has been variously used (Van Arsdel and Copley, 1963) to reconstruct the so-called constant rate drying period which characterizes the drying of biological materials above the hygroscopic point.

In contradistinction with the so-called "free or removable" moisture discussed above, water associated with biological products below the hygroscopic point is subject to intense surface phenomena called sorption. This explains why this type of moisture is called adsorbed moisture. The removal of this type of moisture is characterized by a falling rate drying period. The motion and retention of adsorbed moisture in biological materials have eluded rigorous theoretical treatment for a long time. The reason why this is the case will become apparent in subsequent discussions in this chapter.

1.3 The Nature of Adsorption

When a solid is exposed to a vapor at a definite pressure, the concentration of the vapor is higher at the solid - vapor interface than it is in the vaporous atmosphere. This is the phenomenon called adsorption. It is not confined to solid-gas interface alone, but must be expected to occur in gas-liquid, liquid-solid, liquid-liquid and even in some circumstances solid-solid interactions (Brunauer, 1945).

Adsorption is described phenomenologically in terms of an empirical general adsorption function, $m = f(P,T)$ where m is the amount of vapor adsorbed under conditions specified by pressure P and temperature T. As a matter of experimental convenience the relationship between the amount of vapor adsorbed by a solid and vapor pressure is often represented by the so-called moisture equilibrium isotherm, $m = f_T(P)$. This isothermal function can be generated for several temperatures making it thereby possible for alternative plots of the data as isobars, $m = f_p(T)$ or isosteres, $P = f_m(T)$ to be developed. While a major body of experimental and theoretical work has focused on the precise reconstruction of the adsorption isotherm, the isostere has almost exclusively been used in conjunction with the Clausius-Clapeyron equation to obtain the heats of adsorption.

It is customary to divide adsorption into two broad classes, namely physisorption and chemisorption. Physical adsorption as the former is alternately called, takes place relatively rapidly, and, apart from hysteresis, the process is reversible. It is further supposed that adsorption is induced by the same type of relatively nonspecific intermolecular forces responsible for condensation phenomena. Thus, in physical adsorption, the heat of adsorption should be in the range of the heats of condensation. Physical adsorption is important only for gases below their critical temperatures, i.e., for vapors (Adamson, 1967). Chemisorption, on the other hand, may occur below or above the critical temperature of the sorbate. It may be slow or rapid. It is qualitatively distinguishable

from physisorption in that the chemical specificity is higher and the energy of adsorption so large to suggest the presence of an activation energy necessary for full chemical bonding. While the probability of chemisorption playing at least some role has been considered by some investigators (Rodriquez-Arias, 1956), it is now generally agreed that is is adsorption of the van der Waal's type which is almost wholly in effect in the adsorption of water vapor by biological products.

Even though no definitive concensus is discernible from the literature on the state of the solid-adsorbate complex, certain directive conclusions can be drawn regarding moisture retention in biological materials by a careful comparison of available experimental data and existing adsorption theory. While such conclusions are at best tentative and must be updated as the frontiers of uncertainty in surface phenomena shrink, they remain essential if our present modelistic conceptualization of adsorption in biological materials is to continue its steady advance. Bearing this in mind, observations regarding moisture retention by biological materials can be summarized as follows: their predominant sigmoid shape together with their pronounced hysteretic behavior distinguish the moisture equilibrium isotherms of biological products as belonging to the type II (sometimes type IV) classification of the Brunauer type. If the combined consequences of (a) the B-E-T theory of multimolecular adsorption, (b) Polanyi's adsorption potential theory, and (c) Zsigmondy's capillary condensation theory are now admitted into the picture, it becomes rather obvious that moisture is held in organic materials by intermolecular and capillary adsorption forces.

Molecular adsorption occurs when the water molecules adhere to the pore walls as result of the divergent force field at the surface of the cell walls. When moisture is adsorbed by organic materials, it is compressed due to strong intermolecular forces of attraction. The adsorption compression is highest at low relative humidities, so that there is a net decrease in the volume of the water-solid aggregate. As layers of water molecules on the cell wall increase with rising vapor pressure, the force of attraction is decreased and the resultant adsorbate compression is correspondingly diminished. This simplified picture of molecular adsorption is essentially in harmony with the "hydrogen bonding" theory of adsorption as discussed by Ward (1962).

Capillary adsorption occurs when voids in the cellular structure of a material are of a size large enough to hold water in liquid form, under reduced vapor pressure, by the forces of surface tension. The tensions originating in the capillary water are transmitted to the capillary walls and there produce stresses within the cell walls. These stresses combined with swelling stresses culminate in what Hammerle (1968) termed the HYDRO-STRESS in biological materials. It will be shown later in this work that the hydro-stress can be used as a basis for the quantitative estimation of hysteresis in biological materials.

1.4 Adsorption as a Function of the Nature of the Adsorbent

The quantity of the vapor adsorbed by a given weight of adsorbent varies greatly from one adsorbent to another. Since, as has been amply discussed in the preceding sections, adsorption is a surface

phenomena, this variation must be due to the active operation of at least two factors: the area of the interface and the specific adsorbing properties of the substance per unit area. Because the present interest lies in the class of organic plant or animal materials, it must be quickly recognized that these are characterized by a great complexity and heterogeneity in physical structure. Each being an assemblage of strongly hydrated high-molecular-weight compounds, mostly belonging to the classes called proteins, carbohydrates, and lipids. Complete quantitative representation of even a single one of these systems is not possible. Consequently, the average or combined behavior of a large number of individual units or pieces must be dealt with in practice.

Bearing this limitation in mind, both plant and animal tissues can be considered on the microscopic level as being fundamentally cellular in their natural state. These fundamental building blocks are interposed with a complex labyrinth of passageways making them microscopically intricate porous bodies (Babbitt, 1942). While it is impossible to estimate from a priori considerations the potential surface area that plays a part in adsorption phenomena, the present state of the art has made possible the rough estimation of the relative pore size distributions in such porous complexes. If this tool is used with caution, it is now entirely within the realms of possibility to characterize the physical structure of biological materials mathematically in terms of a pore-size distribution function and an idealized pore geometry. It is the thesis of this study

that if the structure of an adsorbing biological material can be so mathematically characterized, its equilibrium isotherm shape can be predicted accordingly. The details of this structural characterization will be pursued in a subsequent chapter.

1.5 Adsorption as a Function of the Nature of the Adsorbate - the Water Molecule

As has become evident from the foregoing discussions, the adsorbability of water vapor by organic tissues must depend in a very high degree upon the nature of water itself. While within the context of a lumped or averaged treatment of the subject, water must necessarily be conceived as an ubiquitous and fundamental part of the structure of biological products (Kuprianoff, 1958; Barkas, 1953), cognizance must here be taken of the fact that scientists and engineers often find it convenient to assume a double superposition effect in defining the various properties of water-binding biological products (see for example Hammerle, 1968). It becomes therefore expedient to consider at this point, the nature and properties of the water molecule.

Water is, in many respects, a unique compound. Chemical reactions and physical interactions in which it participates on the molecular scale influence every gross characteristic of organic materials. Except for a slight natural ionization which leads to the formation of minute amounts of hydrogen and hydroxyl ions, pure water consists of molecules made up of two atoms of hydrogen and one atom of oxygen. These molecules may be aggregated by weak

forces into quasi-crystalline combinations whose size and form depend upon the physical conditions prevailing at the time.

Thermochemical data show that the heat of formation of gaseous water from hydrogen and oxygen gases is 57.8 K Cal./Mole. Since the heats of dissociation of hydrogen and oxygen gases are 103.4 and 118.2 K Cal./Mole., respectively, the bond energy for each O-H bond is one-half of the sum:

57.8 + 103.4 + 59.1 or 110.2 K Cal./Mole.

The chemical bonds are formed by completion of two electron pairs, each of the two unpaired electrons of the oxygen atom associating with the electron of a hydrogen atom. Four of the remaining six electrons of oxygen are much farther apart from the nucleus than the other two. These four plus the four electrons involved in the chemical bonds tend to form four pairs that are as far apart as they can be while still attracted by the oxygen nucleus. They form the corners of an imaginary tetrahedron.

The water molecule is schematically represented in Figure 1.1. The distance of the boundary shell from the center of the atom is equal to the so-called van der Waal's radius. The equivalent diameter of the molecule as determined from the density of ice is about 3.2 Å. The cross-sectional area of the water molecule is given either as 14.8 $(\text{Å})^2$, corresponding to its chemisorption as O-H groups or 10.6 $(\text{Å})^2$, corresponding to physical adsorption as H_2O molecule along its longest axis (Gregg and Sing, 1967). These are important quantities which will be used extensively later in this work.

Water vapor exhibits phenomena which can be most satisfactorily explained by assuming that the molecules involved therein contain

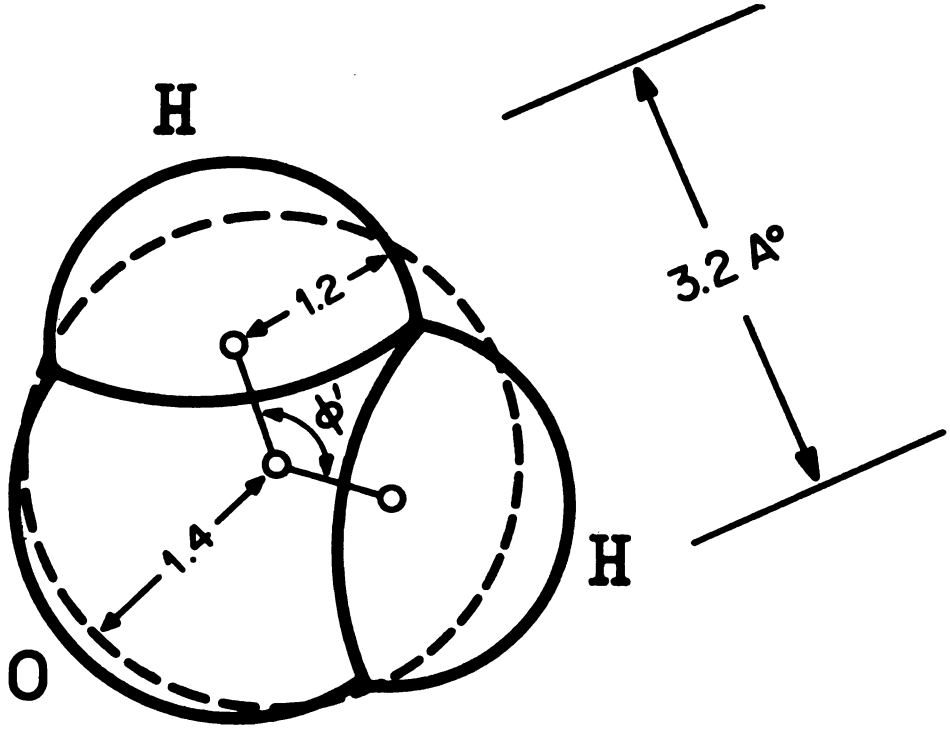

$\emptyset' = 104^\circ\ 31'$

Figure 1.1. Molecule of water vapor.

rigid, or nearly rigid, electrical dipoles. The distance between the dipoles being significantly less than the diameter of the molecule. The magnitude of these moments can be obtained from a study of the dielectric constants (Dorsey, 1940). The unique properties of water with respect to molecules of similar size, such as NH_3, H_2S and CH_3OH, have been attributed (Bernal and Fowler, 1933) not only to its dipole character, but also to the geometrical structure of the molecule. In the present context, the later characteristic together with the polarizability of the water molecule (i.e., the distortion in the molecular charge distribution and the resultant distortion of molecular geometry due to external force fields) may in fact be more important than the dipole qualities (Adamson, 1967).

In the vapor, the molecules are separated by relatively great distances and are moving at high velocities. The translational energy of these molecules is so great that the van der Waal forces are inadequate to hold them together when they collide. Thus the vapor expands and exerts pressure in conformity with the kinetic theory of gases and in the first approximation behave in accordance with the ideal gas laws.

In the liquid the molecules are held in intimate contact with one another by combined intermolecular forces. Each molecule in liquid water occupies a volume of $29.7(\mathring{A})^3$ which indicates a porosity between molecules of about 36.7% (Matz, 1965). The nature of the bonding forces is not well understood. Some contribution is probably made by the weak forces of the van der Waal's type (with

bond energies of about 5 K Cal./Mole.) and must be, to a considerable extent, nondirectional, since the molecules are free to move in the liquid. The magnitude of the attractive forces between the molecules must be relatively large, since the vapor pressure of the liquid is negligible compared to the pressure which is implied by the gas laws.

In organic products hydrogen bonding exists between water molecules, between water and small and large molecules and ions, and as the direct link between these latter micromolecular components (Ward, 1962). There is, therefore, competition between the components for the available hydrogen bonding sites. The rate at which water may break or promote particular intermolecular hydrogen bonds, and the extent to which this can be carried out, together with the converse process of displacement of water from bonding sites, affect all practical dehydration and rehydration processes. Coulson (1959) reduced the intermolecular forces to (a) electrostatic interactions (b) dispersion forces (c) repulsive forces and (d) delocalization interaction. Under the combined influence of these forces the water molecule in its adsorbed state appears to have undergone a definite thermodynamic transformation (Ewing and Spurway, 1930). While there exists no satisfactory theory of the liquid state, the detailed treatment of the adsorbate-adsorbent complex is even farther away.

1.6 Review of Related Literature

In view of the extensiveness of the subject, it is not intended here to give complete coverage of the voluminous literature

on the general subject of gas adsorption. Instead, the principal models or theories which have been advanced to account for the sorptive behavior of biological materials or from which such theories are directly or indirectly derivable, will be taken up partly for their own sakes and partly as a means of introducing a new generalized model to be presented in a later chapter.

In order to expedite the task in this section, it is necessary to outline some criteria against which the works to be examined can be evaluated. As was previously mentioned, the adsorption isotherm is not only the most convenient form in which to obtain and plot experimental data, it is also the form in which theoretical treatments are most easily developed. The first demand of a theory of adsorption then, is that it gives an experimentally correct adsorption isotherm. Adamson (1967), however, points out that this is a necessary but insufficient test of the validity of the premises underlying a theory. Since quite differently based models have been found to yield equations which are experimentally indistinguishable and even algebraically identical, he suggests that data on the heats and possibly entropies of adsorption be used as a more discriminating test of an adsorption model. The characteristic hysteresis observed in adsorption by porous systems provides a third criterion of evaluation in the case of porous biological materials. This demands that the hysteresis phenomenon be both qualitatively and quantitatively derivable from a given adsorption model.

Labuza (1968) in a recent review of the subject, points out that theoretical treatment of sorption has primarily come under three modelistic frameworks, namely:

1. The Kinetic concept of Langmuir;
2. Polanyi's Adsorption potential theory;
and 3. Zsigmondy's capillary condensation theory.

The Kinetic Concept: Langmuir (1918) proposed the classical kinetic model of adsorption based on his belief that adsorption was in essence, induced by unbalanced chemical forces on the surface of crystals leading to a unimolecular layer of the adsorbate. Assuming that (a) adsorbed molecules are localized, (b) colliding adsorbate molecules are reflected elastically, and (c) the heat of adsorption for every adsorbate molecule striking the bare surface of a solid adsorbent is the same and equal to the heat of vaporization, Langmuir equated the rate of evaporation to the rate of condensation at the surface of the adsorbing solid under conditions of dynamic equilibrium. The resultant isotherm equation is of the form:

$$P/v = 1/b\ v_m + P/v_m \qquad [1.1]$$

where v is the volume of gas adsorbed isothermally at vapor pressure P; v_m is the volume adsorbed at the monolayer point; and b is a constant of adsorption dependent on both the heat of adsorption as well as the isotherm temperature.

In spite of the limitations inherent in its simplifying assumptions, the Langmuir isotherm equation is perhaps the most important single equation in the field of adsorption, serving in many cases as the starting point in the derivation of other equations.

Type I adsorption isotherms are best interpreted in terms of Langmuir's equation and accordingly, are sometimes referred to as Langmuir isotherms.

While Langmuir's pioneering adsorption model may be considered a perfectly acceptable one at very low P/P_o values, its greatest merit lies in the fact that it forms the basis of the more universally accepted B-E-T theory of multimolecular adsorption. This theory has, with varying degrees of success, been used to account for the occurence of types II, III, IV and even V adsorption isotherms of the Brunauer classification. Brunauer, Emmett and Teller (1938) extended Langmuirs kinetical approach to multilayer adsorption. The basic assumptions in the B-E-T model are: (a) the Langmuir equation applies to each layer, (b) for the first layer the heat of adsorption, q, may take a unique value, whereas for all succeeding layers, it is equal to q_v, the heat of vaporization of the liquid adsorbate and (c) evaporation and condensation can occur only from or on exposed surfaces. A detailed balancing of the forward and reverse rates of adsorption on a surface where the number of adsorbed layers is restricted to n by walls of pores having finite diameters leads to the equation:

$$v = \frac{v_m C X}{1 - X} \cdot \frac{1 - (n+1) X^n + n X^{n+1}}{1 + (C-1) X - C X^{n+1}} \qquad [1.2]$$

where X is the relative vapor pressure, P/P_o; v is total volume adsorbed at the measured pressure, P; v_m is the volume adsorbed in the monolayer; and C is a constant related exponentially to the heats of adsorption and liquifaction of the adsorbate. Relation

[1.2] is the so-called B-E-T 3-parameters equation. It reduces to the Langmuir relationship when n = 1. Under conditions in which the surface is free and adsorption is not limited [n = ∞], it reduces to the more familiar 2-parameters equation:

$$\frac{X}{v(1-X)} = \frac{1}{v_m C} + \frac{(C-1)\,X}{v_m C} \qquad [1.3]$$

from which values of v_m and C are obtainable from straight line plots of adsorption data in the low-pressure region. In a subsequent extension of the theory by Brunauer, Deming, Deming and Teller (1940), a much more elaborate equation was obtained to account for isotherms of Types IV and V. The multi-layer theory thus became the first unification of physical-adsorption concepts which applied to the complete isotherm from the monomolecular region through the multi-layer and capillary condensation regions to the saturation pressure. The B-E-T relationship works very satisfactorily in the relative vapor pressure region from 0.05 to 0.3 (Adamson, 1967), and is extensively used as a general method for the determination of surface areas of adsorbents.

The considerable success of the B-E-T equation stimulated investigators to consider modifications that would give a better fit to type II isotherms. Among these modifications are those of Pickett (1945), Huttig (1948), McMillan and Teller (1951), Clampitt and German (1958) and Dellyes (1963). A detailed summary of these modifications is contained in a book by Young and Crowell (1962).

In spite of its considerable success, the assumptions of the B-E-T theory are not realistic. It does not give the correct variation of either the heat or entropy of adsorption with the amount of gas adsorbed. While the B-E-T assumption correctly reflects the approach of the adsorbed film to bulk liquid properties as P approaches P_o, its assumption of localized multilayers is not consistent, leading to erroneous configurational entropy values (Hill, 1960). Related to this is a catastrophe that Cassel (1944) has pointed out, namely, that the B-E-T model predicts infinite adsorption at saturation.

In view of the fact that these same general criticisms apply to the Huttig equation and indeed to the various modifications of the B-E-T equation, the opinion of Gorter and Frederikse (1949) that "the kinetical B-E-T theory gives a simple and valuable first picture of the phenomenon of adsorption, but it seems difficult to correct its obvious short comings without destroying the simplicity which perhaps constitutes its chief attraction", seems very appropriate. Halsey (1950) concludes that the B-E-T and related isotherms should be regarded as merely convenient algebraic tools for locating the point "B", which, he feels, marks the monolayer stage, since it is the point of most rapid change in the affinity of the solid for the adsorbate.

The Potential Model: At approximately the same time that Langmuir developed his monomolecular theory, Polanyi (1914, 1916, 1920) formulated an entirely different concept known as the potential theory.

This concept recognizes the existence of multi-layer adsorption, and considers that there is a pontential field at the surface of a solid into which adsorbate molecules fall. The adsorbed layer thus resembles the atmosphere of a planet, being most compressed at the surface of the solid and decreases in density outward.

Polanyi defined the adsorption potential at a point on the solid, as the work done by adsorption forces in bringing an adsorbate molecule from the vapor phase to that point. This work is conceived as a work of compression, and mathematically is given by the so-called hydrostatic equation:

$$\epsilon = \int_{\rho_o}^{\rho} V \, dp \qquad [1.4]$$

where ϵ is the adsorption potential at a point where the density of the adsorbed film is ρ; ρ_o is the density of the gas phase; and V is the molar volume of the adsorbate. It is fundamental to Polanyi's theory that the adsorption potential at any given point is characteristic of the adsorbent alone and is temperature independent as well as unaffected by the presence of foreign molecules. It is hence possible to map out the entire adsorption space into a number of equipotential surfaces, the nature of which would be characteristic of the adsorbent.

On qualitative grounds, the potential theory appears to be fundamentally correct. It accounts for the empirical fact that systems at the same values of $R_g T \ln (P/P_o)$ are in essentially corresponding states (Brunauer, 1945) and that the multi-layer approaches the bulk liquid in properties as P approaches P_o.

However, in specific treatments, functions must be assumed to represent the equation of state in the adsorbed phase. Since the adsorbent - adsorbate complex still remains a major thermodynamic puzzle, functions used can only be approximate. From this point of view, the original formalism of Polanyi its subsequent modifications by Frenkel (1946), Halsey (1948), McMillan and Teller (1951) and Hill (1952) together with the adjoint so-called two-dimensional film theory of Harkins-Jura (1944), must be regarded as still somewhat primitive in specific applications.

Capillary Condensation: It has long been recognized that the vapor pressure over the miniscus of a liquid contained in a narrow capillary is lower than the vapor pressure of the free liquid at the same temperature, provided that the liquid wets the capillary and forms a concave meniscus. In other words, a vapor is liable to condense in a capillary at a lower pressure than it would on a plane surface. This phenomenon is called capillary condensation.

The quantitative relationship between the vapor pressure, P, over a liquid confined in a capillary and the corresponding saturation vapor pressure in a free space at the same temperature was given by Lord Kelvin (1871) in the form:

$$\ln (P/P_o) = \frac{-2\,\sigma\,\bar{V}\cos\varphi}{r\,R_g\,T} \qquad [1.5]$$

where σ is the surface tension of the liquid; $\bar{V}$ is the molecular volume of the adsorbate in its liquid state; r is the radius of the cylindrical capillary; R_g is the universal gas constant; T is temperature in degrees Kelvin and φ is the contact angle.

Zsigmondy (1911) and later Foster (1932) applied the capillary condensation theory to relationships between adsorption and pore structure in porous adsorbents. They argued that in porous structures, the same relationship between vapor pressure and meniscus radius exists as in the case of ordinary cylindrical capillaries. As the equilibrium pressure is increased in an adsorption experiment, condensation occurs in successively larger pores. This rationalization leads directly to the calculation of pore-size from adsorption isotherm data employing the Kelvin equation [1.5]. The principal assumption is that the adsorbate exists as a condensed liquid in the pores of the adsorbent and has properties characteristic of the bulk liquid phase.

Zsigmondy (1911) attributed the hysteresis phenomenon characteristic of adsorption in porous systems, to contact angle hysteresis due to impurities. While this may well be true in some cases, it fails to account for systems having retraceable closed hysteresis loops. The schemes of Barret et al. (1951), Pierce (1953) and Cranston and Inkley (1957) for calculating pore-size distributions from adsorption isotherms represent refinements of Zsigmondy's original theory. In spite of the warning by Everett (1958) that the bundle of capillaries model can be outrageously wrong for real porous systems, these methods constitute in many cases, the only available estimation of the real pore structure. The "ink bottle" concepts of hysteresis as advanced by Kraemer (1931), McBain (1935) and Cohan (1938, 1944) remain to date, the most plausible qualitative description of the phenomenon. These too, are founded on the capillary condensation theory of Zsigmondy.

In conclusion, while the applicability of the Kelvin equation and the assumed bulk liquid properties of the adsorbed film remain subjects of controversy, most investigators (see Brunauer 1945, Adamson 1967) seem to agree that capillary condensation plays some role in physical adsorption. In general, it is believed to come into play approximately in the region of hysteresis.

The Polarization Theory: In the interest of completeness, the Polarization theory of de Boer and Zwikker (1929), and Bradley (1936) is briefly taken up here. This theory explains the adsorption of non-polar molecules on ionic adsorbents by assuming that the uppermost layer of the adsorbent induces dipoles in the first layer of the adsorbed molecules, which in turn induce dipoles in the next layer, and so on until several layers are built up. Brunauer (1945) severely criticized the polarization theory on the ground that the effect was not large enough and consequently the theory has largely been ignored. Even though some recent work by Bewig and Zisman (1964) and Benson and King (1965) suggest that this neglect may be either mistaken or premature, Hill (1952) points out that there exists no satisfactory theory of the liquid state, even for monatomic liquids, and the detailed treatment of a liquid in a combination electrical and dispersion long-range force field is still far away.

Secondary Theories

The models to be taken up in this section of the review, are designated secondary in so far as they are in varying degrees subordinate to one or in some cases a combination of the primary models

previously discussed. In the context of the present interest, these theories are especially relevant because each one of them has focussed on water vapor as the adsorbate and either polymeric or organic solids as the adsorbent.

Although as early as 1882 Müller had proposed an equation to predict the adsorption of water vapor by textile fibres, his equation turned out to be quite valueless (Swan and Urquhart, 1927) because his arbitrary assumptions - (a) a linear relationship between the amount of vapor adsorbed and relative vapor pressure and (b) zero adsorption at boiling point of water - were unsound.

The Smith Equation: It was not until 1947 that a partially successful treatment of water sorption by polymers was formulated by Smith who recognized the existence of two principal classes of sorbed moisture: (a) bound moisture, (α_b), held on the adsorbent surface by intermolecular forces in excess of forces responsible for condensation and (b) normally condensed moisture, (α_c). He assumed that the relationship between α_b and P/P_o can be approximated by the Langmuir equation. While accepting the multi-layer concept of Brunauer, Emmett and Teller as the structural framework of α_c and further adopting the B-E-T position that the multi-layer is essentially in the same thermodynamic state as the bulk liquid, he derived the following expression for α_c:

$$\alpha_c = - \alpha' \ln (1-P/P_o) \qquad [1.6]$$

and summed α_b and α_c to obtain:

$$\alpha = \alpha_b + \alpha_c = \alpha_b - \alpha' \ln (1-P/P_o) \qquad [1.7]$$

where α' is defined as the adsorbed mass per gram of the adsorbent in a unimolecular layer of normally condensed moisture, and α is the total specific adsorbed mass. In order to arrive at equation [1.6], Smith assumed that at any stage of sorption, the completed fraction of α' is a measure of the total potential evaporating surface - a perfectly valid assumption. However, his subsequent assumption that this fraction, (θ), is equal to P/P_o is thermodynamically unsound. While it is true that in the assumed thermodynamic state of α_c, both θ and P/P_o represent some measure of the escaping tendency of the vapor molecules, it can be shown that they do not reduce to an identity. All that can be deduced from thermodynamics is that: $\theta = \theta(P/P_o)$. Invoking (a) Lewis and Randall's representation (Lewis and Randall, 1961, p. 147) of fugacity as the molal free energy and (b) Gibb's definition of the surface free energy as the work done against surface tension forces by the spreading two - dimensional pressure on the adsorbing surface (Gregg and Sing, 1967, p. 234), the following approximation can be written:

$$\Pi\,\theta = \Delta F = -R_g T \ln (P/P_o) \qquad [1.8]$$

where θ is taken as a measure of the surface on which the spreading pressure, (Π), is active. Equation [1.8] suggests that Smith's fundamental simplification cannot be thermodynamically justified. It must therefore be concluded that even though the Smith equation has been found in certain cases (for example Becker and Sallans, 1955) to fit experimental isotherm data remarkably well in the

region $0.5 \leq P/P_o \leq 0.95$, his exponential representation of the multi-layer region is basically empirical. That empirical functions can be selected to fit a wide variety of isotherms has been demonstrated by Strohman et al. (1967) and Do Sup Chung et al. (1967), both of these works will be elaborated upon later in this section.

Other weaknesses of the Smith equation include (a) its inability to give the correct variation of either the heat or entropy of adsorption, (b) its inability to account for hysteresis and (c) the fact that temperature dependence is not inherent in the formulation.

The Henderson Equilibrium Equation: Perhaps the best known and most widely used equation for predicting the equilibrium moisture content of biological materials is the semi-empirical equation of Henderson (1952). Using the Gibb's adsorption equation as a starting point, Henderson derived an isotherm equation which can account for the temperature dependence of the experimental curve. His equation is of the form:

$$(1 - P/P_o) = e^{-kTM_a^{\bar{n}}} \qquad [1.9]$$

where T is absolute temperature in degrees Rankine; and k and $\bar{n}$ are empirical constants. When appropriate values of the parameters, k and $\bar{n}$, are available, the Henderson equation or its modifications by Day and Nelson (1965) and Thompson et al. (1967) have been found to fit isotherm data for cereal grains fairly well (see Rodrigues-Arias, 1956). However, the Henderson equation has been found to be

quite inadequate for certain biological products (see for example Pichler 1957, Bakker-Arkema 1961, Day and Nelson 1965). One deficiency of the Henderson equation is that it is totally based on thermodynamics, it is therefore not founded on a model and gives no information about the nature of the adsorbent or its surface.

The Young-Nelson Hysteresis Equation

A creditable effort to construct a theory of adsorption for biological materials to reflect their basic cellular nature was made by Young and Nelson (1967). These investigators considered the cell as the ultimate basis of adsorption and recognized the existence of three modes of adsorbed moisture: (a) the unimolecular-bound moisture of Langmuir, (b) the normally condensed or multiple-layer moisture of Brunauer, Emmett and Teller; and (c) an adsorbed moisture which results from a diffusional passage of moisture into the inner cell and which on account of the irreversibility of the diffusion process is responsible for the occurence of hysteresis.

The development of a representative expression for the first category of moisture is kinetical; being in essence identical to the B-E-T process. Their development of an expression for the normally condensed moisture, with only slight differences, parallels the Smith method of attack and implies the same basic assumptions. It is therefore not surprising that they arrived at an equation which has the properties of a combined B-E-T-Smith equation (Strohman et al., 1967) including the advantages of both but impeded by the fundamental empiricism of the Smith equation.

Although these authors by their perceptive introduction of the "absorbed moisture" have developed a comparatively straight forward quantitative representation of hysteresis, the simplifications and reasoning leading to their explicit expression for the absorbed moisture effectively destroyed their model. If the ultimate cell of a biological product is taken as the basis of sorption, it appears logical that moisture transfer across the semi-permeable cellular wall can take place only as a result of osmosis. From thermodynamic considerations, the osmotic pressure necessary to induce such transfer is given by: (see Guggenheim, 1967, pp. 183-184):

$$\Pi = \frac{R_g T}{V_1} \ln (P_1^{\circ}/P) \qquad [1.10]$$

where Π is osmotic pressure in atmospheres, R_g (the Universal gas constant) = 82.06 cc.atm. $^{\circ}K^{-1}mole^{-1}$; V_1 is the volume of adsorbed moisture in cc.; and T is absolute temperature in degrees Kelvin. For the 30°C isotherm, the values of Π corresponding to the relative vapor pressure values of 0.1, 0.3, 0.8 and 1.0 are respectively: 1.6×10^6, 4.6×10^5, 3.46×10^4 and 0.0 atmospheres. The values of V_1 corresponding to the above P/P_o values are obtained by conversion of the adsorption data for corn. The conversion constants will be developed later in this work. The specific values of V_1 used are 0.0351, 0.0654 and 0.1590 cc. Since the osmotic pressure must be exceeded or at least balanced for transfer across the cell wall to take place, it appears clear that except at saturation, infinite layers of adsorbed molecules will be necessary to create a sufficiently large hydrostatic force. Moisture transfer across the membrane

cannot therefore be justified prior to saturation. On the other hand, with a predicted zero osmotic pressure at saturation, all the normally condensed moisture on the surface would be expected to diffuse into the cell. In summary, our present line of reasoning allows for no adsorbed moisture except at saturation, at which point the normally condensed moisture begins to diffuse into the cell. This moisture passage should continue until the cell fills to its maximum absorptive capacity. The Young-Nelson picture of the absorbed moisture does not therefore agree well with thermodynamic reasoning. It must, however, be stressed that in spite of its apparent inability to stand up to its theoretical implications, the Young-Nelson model of hysteresis represents the best quantitative effort yet to solve explicitly the problem of hysteresis in water adsorption by biological materials.

The Chung-Pfost Equation: The general framework of the potential theory was utilized by Chung and Pfost (1967) to develop an isotherm equation for cereal grains and their derivatives. The equation is of the form:

$$\ln (P/P_o) = \frac{-A}{R_g T} \exp(-BM) \qquad [1.11]$$

where M is the specific adsorbed mass and the parameters A and B are product and temperature dependent empirical constants. Like the earlier but algebraically identical relation of Dubinin and coworkers (1955, 1965), the Chung and Pfost equation is semi-empirical being based on an over-simplified equation of state for the adsorbed film. While specific instances of success in the use of such equations can be cited, their wider usage cannot be justified on theoretical grounds.

The Empirical Equation of Strohman and Yoerger: Strohman and Yoerger (1967) using the Othmer linear plots as a starting point developed a purely empirical isotherm equation for corn. Since they had no working model, their method must be considered as essentially a curve fitting scheme which offers practically no descriptive picture of the phenomenon. While such schemes may become useful in secondary applications such as drying for example, they throw no light on the basic process of adsorption.

1.7 Statement of the Problem

While the three basic theories of adsorption and their subordinate equations have failed in their individual capacities to produce a generally satisfactory mathematical formulation of the sorptive response of biological materials when exposed to a vaporous atmosphere of water, their apparent complementary character indicates, as has been suggested by Kühn (1964), that the fundamental concepts may be successfully combined into a unified model of adsorption.

As a broad statement of the problem, it is attempted to construct an isotherm equation for biological materials based primarily on the B-E-T and capillary condensation theories and somewhat indirectly on the potential theory.

This integrated theory will be justified if the porous nature of a given biological material can be considered fundamental to its sorptive behavior. In the light of the best available knowledge in the area of sorption, it is reasonable to consider the adsorption process by biological products as resulting from mono and multi-layer

phenomena up to the incidence of hysteresis; the subsequent isotherm progress into the region of hysteresis is attributed to both multi-molecular adsorption as well as capillary condensation on the porous solid.

1.8 Objectives

The study reported in this dissertation was undertaken for the following specific objectives:

1. To construct, utilizing the B-E-T, and capillary condensation theories together with a working model of their pore structure, a moisture adsorption model for biological materials.
2. To derive, using the general framework of the potential theory in conjunction with the fundamental laws of thermodynamics, an explicit density function for adsorbed moisture. This function is then integrated into the moisture adsorption model to obtain a generalized isotherm equation for porous biological materials.
3. To verify the validity of the proposed model by showing that:
   (i) The heat of adsorption and its variation with the amount of vapor adsorbed are inherent in the formulation.
   (ii) Sorption hysteresis is both qualitatively and quantitatively expressible within its governing framework;
   (iii) The derived isotherm equation is experimentally correct.

II. THEORETICAL CONSIDERATIONS

2.1 Introduction

In this chapter the framework of a generalized model of adsorption is formed. The B-E-T and Capillary Condensation theories are combined into an integral isotherm equation accounting for molecular and capillary adsorbed moisture in porous biological materials. In order to solve the integral equation explicitly, it became necessary to:

(a) characterize the pore structure of adsorbing biological products mathematically;

(b) define an explicit density function to satisfy the fundamental postulates of the adsorption potential theory as advanced by Polanyi.

As a necessary self-consistency test for this line of attack, a concept of sorption hysteresis is constructed within the generalized framework, thereby making possible the quantitative estimation of hysteresis in swelling biological materials.

2.2 A Physical Model of Water Adsorption by Bio-materials

The physical picture advanced here is illustrated in Figure 2.1 which shows an organic tissue in a vaporous atmosphere of, for instance, water at a specified pressure and temperature. The tissue is visualized as a random network of small pores, the diameter of one of which has been magnified for illustrative purposes. The pores are interstices between ill-fitting cellular building blocks which make up the tissue. Although these intercellular passageways certainly are not cylindrical, a useful picture can be made in which they are

MAGNIFIED INTER-MICELLAR CAPILLARY, SHOWING

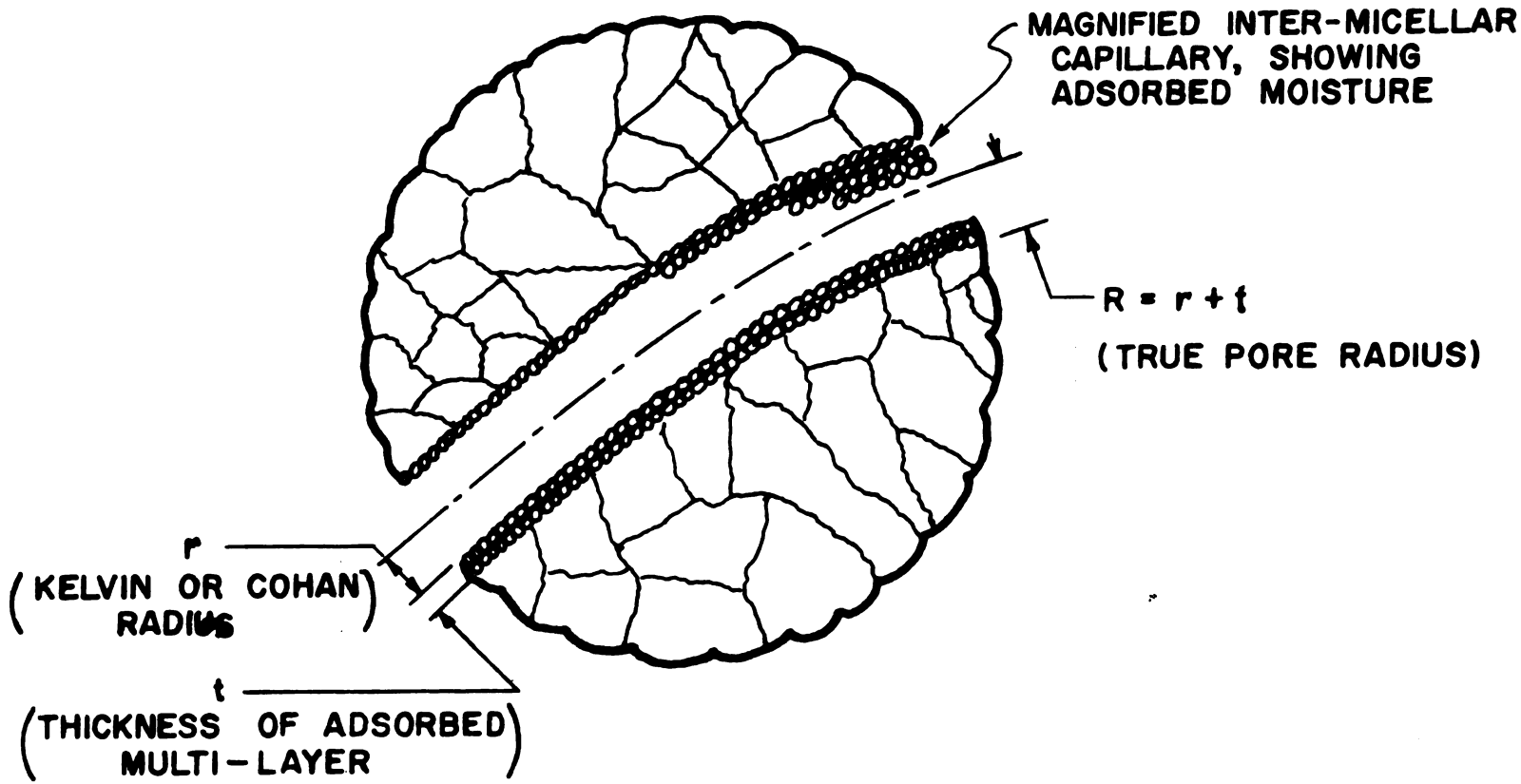

Figure 2.1. Pictorial representation of an organic tissue as a random network of small, irregular pores. The diameter of one pore is magnified for illustrative purposes.

treated as cylinders, parallelepipes (slitted pores) or interconnected spheroidal "ink bottles", with rough walls and intersecting with other pores.

The sorption of water vapor by the tissue can now be thought of as a process by which the pores are isothermally filled or emptied of water vapor under the influence of surface forces active on the pore walls. While this simplified picture classifies the tissue as essentially a porous body, it does not preclude its basic organic and biological nature. The position is taken here that unique modes of behavior such as respiration, and "water-active" sites which characterize biological materials in their natural state, exert a tremendous influence on the nature and distribution of surface forces. In consequence, it is logical to assume that at least some of the "live processes" find commensurate expression in the energy and entropy configurations associated with the sorptive process. The point is stressed here that in the gross treatment of physisorption in biological materials, the separate and detailed consideration of associated life phenomena may become superfluous since such processes are already inherent in energy or entropy terms.

As a microporous body, the pore filling process proceeds due to the operation of two mechanisms: (a) molecular adsorption, and (b) capillary condensation. At any stage in the process, its adsorptive capacity is measured by the adsorptively utilizable volume of the constituent pores. The practical objective of the physical model being developed is to characterize these pores sufficiently in terms of size, and size distribution to make the computation of the aforementioned volume possible.

2.3 Generalization of Molecular and Capillary Adsorbed Moisture

2.3 a. Pore Characterization - defining the size of a pore filled by Molecular and Capillary Adsorption:

In its strictest sense, the term "capillary condensation" is applied to the particular adsorption mechanism described by the Kelvin equation. In this mechanism the equilibrium vapor pressure of a liquid in a cylindrical capillary is reduced below its saturation value by negative hydrostatic pressure arising from tensile components of curved surfaces of tension of the liquid, i.e. from the menisci. The reduction in pressure is related to the radius of curvature of the menisci by the Kelvin equation (1.5). If complete wetting is assumed to occur so that φ is equal to zero, equation (1.5) can be reduced to the simpler form:

$$r_k = \frac{2\,\sigma\,\overline{V}}{R_g T \ln(P_o/P)} \qquad [2.3.1]$$

where r_k is the radius of curvature of a hemispherical meniscus.

Although equation (2.3.1) is basically descriptive of such microscopic phenomena as capillary rise and depression, Zsigmondy (1911) and later Foster (1932) applied it to relationships between adsorption and pore size in microporous adsorbents. Their principal assumption was that the adsorbate behaved as a single-component liquid in a potential field inside the microporous capillary of the adsorbent and possessed properties characteristic of the bulk liquid phase. In view of the undefined thermodynamic state of the adsorbent-adsorbate complex, this rationalization remains open to question. However, investigators consider that the Kelvin equation can be used with reliability for the

calculation of pore size along the desorption path of the isotherm (Flood, 1967, p. 55). This is particularly true in the case of H_2O where adsorbent contraction accompanying adsorption hysteresis is indicative of (a) the presence of a hemispherical meniscus, and (b) the active operation of a negative hydrostic pressure - both of which are consistent with the Kelvin mechanism.

Wheeler (1945) proposed an improved theory which took into account the effects of multi-layer adsorption. Two new assumptions were made. First, it is assumed that at any point on the desorption branch of the isotherm, all pores larger than a certain radius R, are covered with an adsorbed multi-layer of thickness t, whereas all pores smaller than R are filled by capillary condensation. Secondly, since all unfilled pore walls have an adsorbed layer of thickness t, the radius of the meniscus in a filled pore, where it joins a larger pore, is assumed not to be the pore radius R, but a smaller radius (R-t). This means in effect that under conditions of capillary adsorption it is not the pore of the true physical radius R which is important, but rather, a pore whose radius has been effectively diminished by the thickness of an adsorbed multi-layer. Wheeler thus argued that the Kelvin equation applied not to the actual pore radius but to the effective radius of the "inside annular tube" left after multi-layer adsorption has taken place. The maximum true pore radius R, which will be filled by both molecular adsorption and capillary condensation at a relative vapor pressure P/P_o is thus given by:

$$R = t + r_k \qquad [2.3.2]$$

where t = the thickness of adsorbed multi-layer, yet to be defined.

r_k = the Kelvin radius defined by equation (2.3.1). The summed radius is shown diagrammatically in Figure (2.2).

Because of its Kelvin component, the Wheeler equation (2.3.2) is applicable only to the desorption branch of the isotherm. However, Cohan (1938) and Coelingh (1938), working independently, concluded that capillary condensation occurred along both branches of the isotherm loop, and explained hysteresis in terms of the different shape of the meniscus during adsorption and desorption. Along the desorption branch the Kelvin mechanism is assumed - the meniscus being hemispherical - but along the adsorption branch, the meniscus assumes a cylindrical shape, the pore being open at both ends (see Figure 2.3). Cohan by (a) specializing the Young-Laplace equation for the case of a cylindrical meniscus (see Gregg and Sing, 1967, p. 149), and (b) employing the same basic thermodynamic argument as Kelvin, arrived at the equation:

$$r_c = \frac{\sigma \bar{V}}{R_g T \ln(P_o/P)} \qquad [2.3.3]$$

where r_c = the radius of curvature of a cylindrical meniscus (the Cohan radius).

The Wheeler equation (2.3.2) can be now generalized into the form:

$$R = r + t \qquad [2.3.4]$$

where $r = r_c$ for adsorption; and $r = r_k$ for desorption.
Having already defined r in terms of the variable, P/P_o, the thickness t needs to be similarly defined in order to complete the characterization of R.

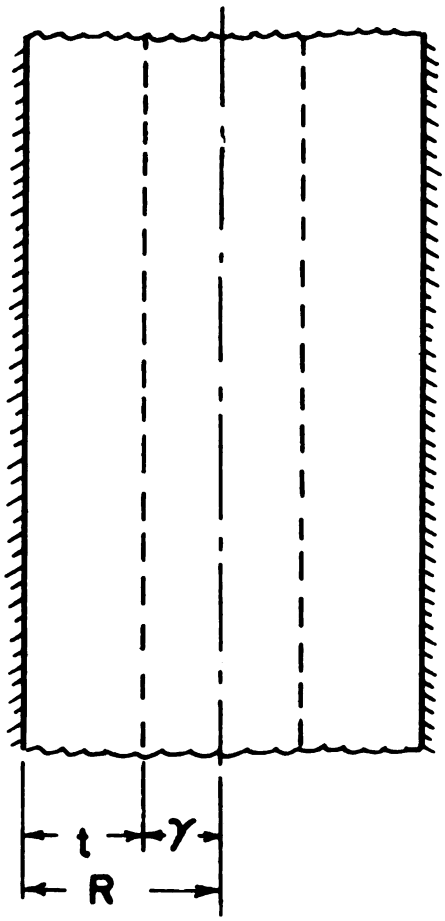

Figure 2.2. Cylindrical capillary of radius R, showing the "inside annular tube" r which may be given either by the Cohan or Kelvin equation.

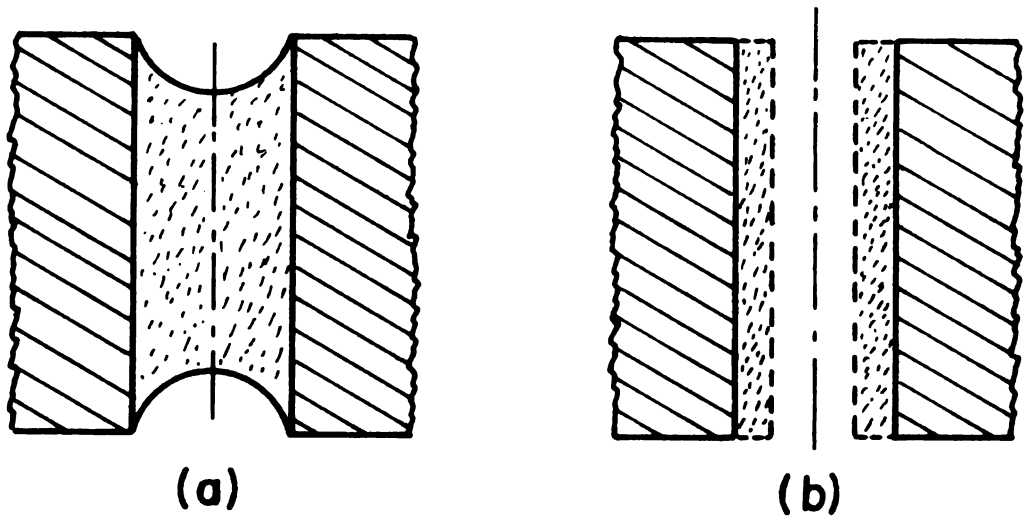

Figure 2.3. Capillary menisci: (a) Hemispherical (Kelvin) meniscus. (b) Cylindrical (Cohan) meniscus.

2.3 b. The thickness of the adsorbed multi-layer:

Halsey (1948) employed the concept of cooperative adsorption to refine the B-E-T theory. This concept implies that adsorbate molecules influence each other by horizontal interaction during the adsorption process. He derived the following semi-empirical relation for the adsorbed multi-layer thickness:

$$t(A^\circ) = \tau \left[\frac{Q_{st}}{R_g T \ln(P_o/P)} \right]^{\Omega} \qquad [2.3.5]$$

where τ = average thickness of a single layer of adsorbed molecules

Q_{st} = the isosteric heat of adsorption

Ω = an empirical constant dependent on the adsorbate, the adsorbent and possibly temperature.

The most direct empirical way of estimating t, is to determine by the standard B-E-T procedure the monolayer capacity X_m of the adsorbate. The adsorption X at any pressure can then be converted into the thickness of the film, by employing the relation.

$$t(A^\circ) = \left(\frac{X}{X_m}\right) . \tau \qquad [2.3.6]$$

$$\text{or } t(A^\circ) = n\tau \qquad [2.3.7]$$

where n is the number of molecular layers adsorbed. It needs to be emphasized that the value of τ is not necessarily the same as the molecular diameter, d of the molecules. The relationship between the two depends on (a) the mode of stacking of successive molecular layers in the adsorbed film as illustrated by the variable configurations postulated in Figure 2.4, and (b) the degree of adsorbate compression

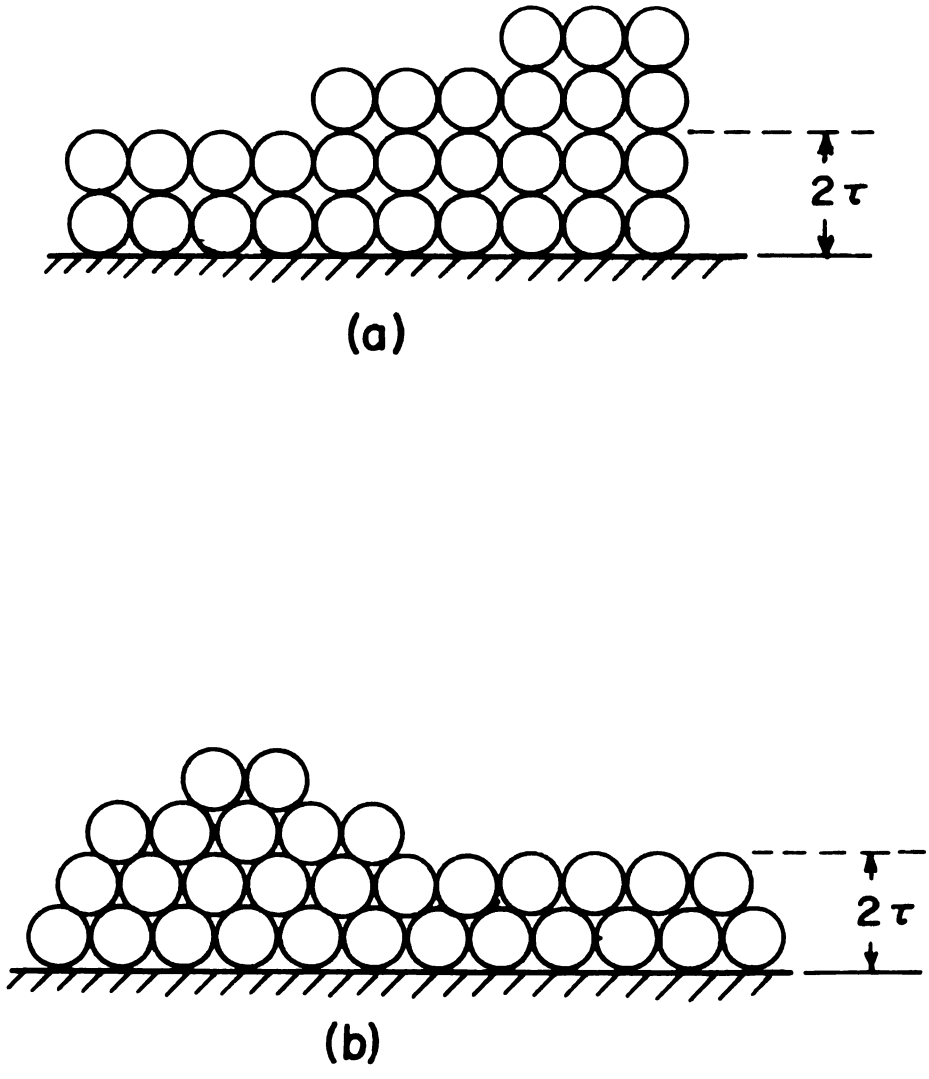

Figure 2.4. Packing of adsorbed molecules in successive molecular layers, to illustrate variable stacking configurations.

within the adsorbed film. Two different values for nitrogen of 3.5(A°) (proposed by Lippens, Linsen and deBoer, 1964) and 4.3(A°) (proposed by Shull, 1948) are clearly illustrative of the state of controversy existing on the subject. For the adsorbed water molecule, an even greater degree of uncertainty must be entertained with regard to the value of τ because of the high degree of compression associated with water adsorption (see Babbitt, 1942; Stamm, 1938).

In Figure 2.5, X/X_m is plotted against P/P_o for a number of biological products. Superposed on this plot is a curve described by the modified Halsey equation:

$$X/X_m = \left[\frac{1.75}{\ln P_o/P} \right]^{\frac{1}{2}} \qquad [2.3.8]$$

where the quantity $(\frac{Q_{st}}{R_g T})$ in the Halsey relationship is approximated by the constant 1.75. This theoretical curve fits the empirical X/X_m values fairly well. The individual points are however, scattered around the composite curve. This means that some amount of uncertainty exists in the value of X/X_m defined by equation (2.3.8) for a given sample. If this degree of uncertainty is considered within limits of acceptable error, then t is defined by the Halsey equation in the form:

$$t(A°) = 3.2 \left[\frac{1.75}{\ln P_o/P} \right]^{\frac{1}{2}} \qquad [2.3.9]$$

where for the water molecule, τ is taken to be approximately equal to d for lack of a better approximation.

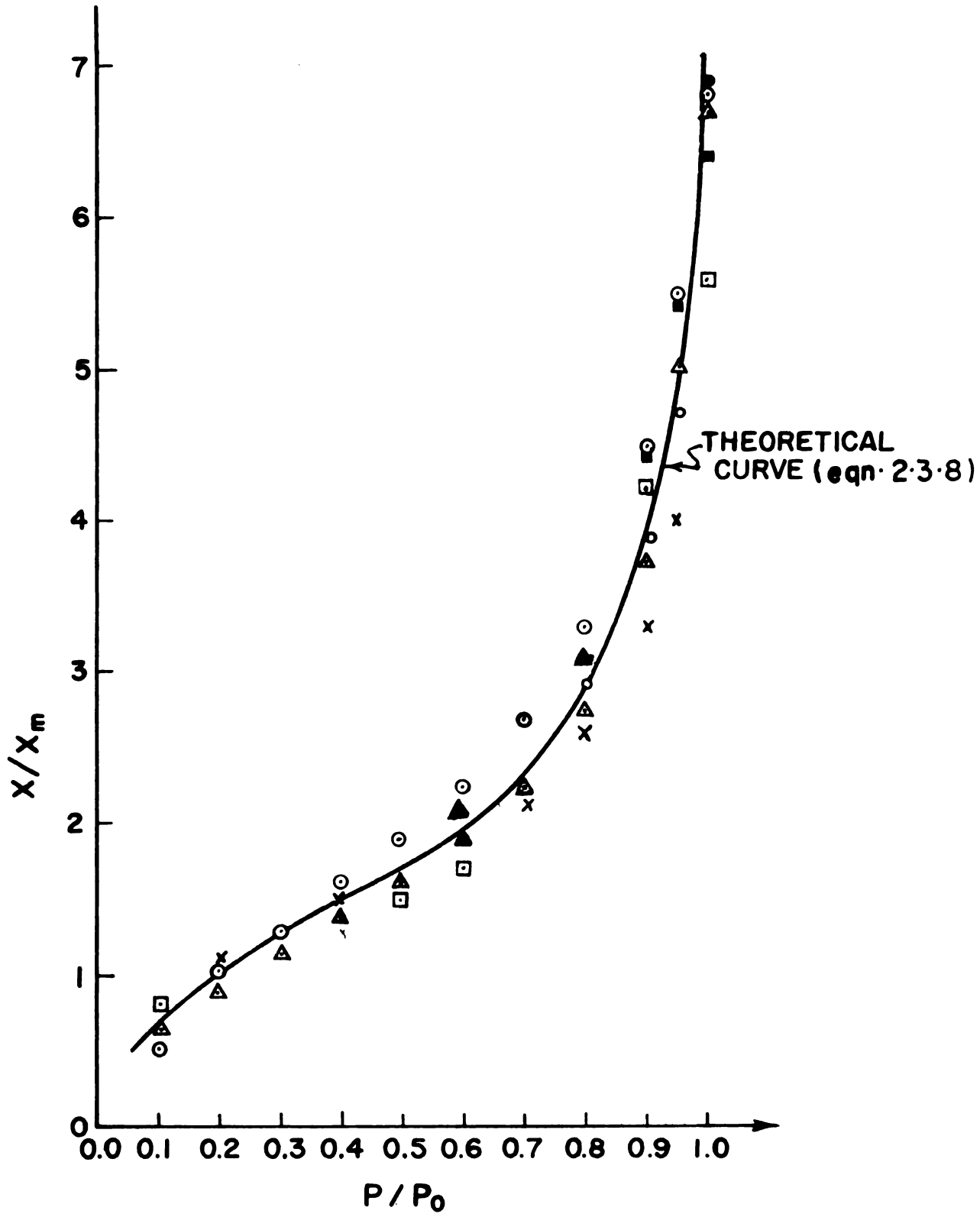

Figure 2.5. Plot of X/X_m against P/P_o.

●, wood 20°C isotherm. △, cotton 10°C isotherm. ○, cotton 20°C isotherm. ▲, cotton 30°C isotherm. ×, corn 4°C isotherm. ⊡, Ground freeze-dried beef 10°C isotherm. ■, Ground freeze-dried beef 22.2°C isotherm.

Equation (2.3.9) in a slightly different form was used by Shull (1948), Wheeler (1955), Dollimore and Heal (1964), and Viswanathan and Sastri (1967) for the calculation of the adsorbed multi-layer. It is adopted in the present study in preference to the B-E-T 3-parameters equation from which $n = X/X_m$ is derivable, for a number of reasons. It is consistent with the concept of mobile adsorbed film. It allows for the variation of heats of adsorbtion with amount adsorbed. It has a form convenient for usage in a larger context.

2.3 c. The Isotherm Equation:

With R fully defined as a function of relative vapor pressure, the equation for the adsorption isotherm is developed as follows:

The Wheeler equation (2.3.4) specifies the relative vapor pressure at which condensation will occur in a capillary of a given size. Such condensation will also occur on the adsorbed layers of water molecules already covering the concave surfaces of a porous system. If such condensation leads to a significant reduction in the radius of curvature of a concave surface or open ended capillary, condensation will continue on this surface as long as the radius of curvature continues to reduce. In this discussion, a pore will be defined as any void region in a porous material which is partially or completely filled by the combined consequence of molecular and capillary adsorbed moisture. Also the pore radius will be considered to mean the radius of curvature of the surface on which the above described filling-process started to occur. This radius is defined by the generalized Wheeler equation (2.3.4).

If a porous system of organic tissue has a given distribution or pore radii, one can say that at a specified vapor pressure, pores of radius equal to or less than the value determined by the Wheeler equation (2.3.4) will be completely filled. That is, if the volume of a pore in a porous system is expressed by the function

$$v_R = \varphi_1(R) \qquad [2.3.10]$$

and if the number of pores of radii between R and R + dr is given by

$$dN = \varphi_2(R)dR \qquad [2.3.11]$$

then, the volumes of all pores with radii between R and R + dR is:

$$d\ v_R = v_R dN = \varphi_1(R)\ X\ \varphi_2(R)\ dR \qquad [2.3.12]$$

Thus, the sum of the volumes of all pores whose radii are equal to or less than R is given by the integral:

$$V_a = \int_{R_m}^{R} [\ \varphi_1(R)\ X\ \varphi_2(R)\ ]\ dR \qquad [2.3.13]$$

where R_m, the lower limit of integration is used in recognition of the so-called "molecular sieves" effect which assumes that adsorbed molecules in the first approximation, cannot penetrate into pores smaller than their own diameter, $2R_m$.

Equation (2.3.13) is essentially an integral isotherm equation defining the adsorptive volume of the porous adsorbent. In order to solve this integral equation explicitly, it is necessary to obtain explicit analytic functions for (a) the pore geometry, $\varphi_1(R)$ and (b) the pore size distribution, $\varphi_2(R)$.

de Boer (1958) has shown that a wide variety of geometric models are possible. However, only two broad classes of these geometric shapes are consistent with the assumptions of the present development. These geometric forms represented diagrammatically in Figure 2.6 are:

(i) The Cylindrical type pore model for which:

$$\varphi_1(R) = \pi L(R) R^2 \qquad [2.3.14]$$

where L(R) = variable length of pore.

(ii) The Interconnected Spheroidal "Ink Bottle" pore model for which:

$$\varphi_1(R) = \frac{4}{3} \pi R^3 \qquad [2.3.15]$$

Wheeler (1945) suggested and Shull (1948) demonstrated that pore size distributions may be represented by simple analytical relationships of:

(i) The Maxwellian type for which:

$$\varphi_2(R) = A \frac{R}{R_o} \exp [-R/R_o]$$

(ii) The Gaussian type for which:

$$\varphi_2(R) = A \exp [- \beta^2 (\frac{R}{R_o} - 1)^2]$$

where A, β and R_o are constants. Gregg and Sing (1967) have further suggested the possible utilization of:

(iii) The Log-Normal distribution for which:

$$\varphi_2(R) = A \exp [- \beta^2 (\ln R/R_o - 1)^2]$$

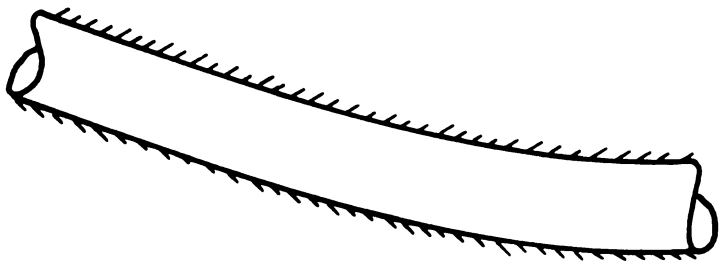

(a)

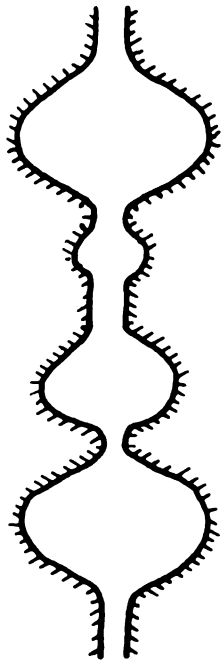

(b)

Figure 2.6. Shapes of capillaries.

(a) Cylindrical capillary

(b) Interconnected spheroidal "Ink Bottles".

No closed form solution to equation (2.3.13) is possible when any one of the above analytical functions is used to define $\varphi_2(R)$, the worst of them is mathematically intractable, the best leads to unwieldy end results. In the attempt to overcome this difficulty, Foster (1948) and Kuhn (1964) recommended a power function distribution of pore radii for which:

$$\varphi_2(R) = K_1 R^{\gamma} \qquad [2.3.16]$$

where the symbol γ is an exponent dependent on the product. Equation (2.3.16) is essentially of an exponential character, and for the most simple cases, it reduces to a simple power function in which γ can assume constant values, being positive or negative, integral or fractional.

A detailed computation of the pore-size distribution of several biological products was undertaken using a modified Cranston and Inkley (1957) scheme. The results - to be presented in chapter 4 - show that if the spheroidal "ink bottle" geometric model is assumed, $\varphi_2(R)$ [as defined in equation (2.3.11)] is well described by the power law equation (2.3.16). In view of its central importance to the development presented, the above mentioned computational scheme together with the results need to be considered here in detail. However, in order to maintain continuity in the line of thought, it is desirable to postpone this side detail for consideration in a later section.

Combining the "ink bottle" pore geometry with the power function distribution of pore radii in equation (2.3.13) yields:

$$V_a = \frac{4}{3} \pi K_1 \int_{R_m}^{R} R^{3+\gamma} \, dR \qquad [2.3.17]$$

Equation (2.3.17) integrates to:

$$V_a = \frac{\xi}{\eta} (R^{\eta} - R_m^{\eta}) \qquad [2.3.18]$$

where

$$\xi = \frac{4}{3} \pi K_1 \qquad [2.3.19]$$

and

$$\eta = 4 + \gamma \qquad [2.3.20]$$

Equation (2.3.18) is a simplified geometric expression of the adsorptively utilizable volume of a porous adsorbent. The exponent η can have positive or negative, integral or fractional values.

Substitution of the generalized Wheeler equation (2.3.4) into equation (2.3.18) and using the Cohan equation (2.3.3) together with the specialized Halsey equation (2.3.9) yields:

$$V_a = \frac{\xi}{\eta} \left\{ \left[3.2 \left(\frac{1.75}{\ln P_o/P} \right)^{\frac{1}{3}} + \frac{\sigma \bar{V}}{R_g T \ln(P_o/P_m)} \right]^{\eta} - \left[3.2 \left(\frac{1.75}{\ln P_o/P} \right)^{\frac{1}{3}} + \frac{\sigma \bar{V}}{R_g T \ln(P_o/P_m)} \right]^{\eta} \right\} \qquad [2.3.21]$$

where P_m is the vapor pressure corresponding to the adsorbed monolayer or point "B" of the isotherm.

Equation (2.3.21) is an isotherm equation relating the specific adsorbed volume of the adsorbent, V_a, with relative vapor pressure. It shows strange deviations from experience in that it gives zero adsorption, $V_a = 0$ at $P = P_m$, and negative values of V_a at pressures, $P < P_m$. This means that isotherms calculated with equation (2.3.21)

must start not at $P/P_o = 0$, but at a low relative vapor pressure $P_m/P_o > 0$. This irregularity stems from the fact that the choice of the lower limit of integration, R_m, in equation (2.3.13) while conforming with the specifications of the "molecular sieves" effect, overlooks the contribution to V_a due to the partial filling of the first mono-layer in the vapor pressure range $0 \leq P \leq P_m$. Yet, the choice of R_m is substantiated in the now accepted argument (Wheeler, 1955) that the Kelvin or Cohan radius is inapplicable in the low pressure range $0 \leq P < P_m$. In order to correct for this irregularity, a shift of the reference axes of the isotherm plot was performed, thereby reducing equation (2.3.21) to the form:

$$V_a = \frac{\xi}{\eta} (Z^{\eta} - \lambda^{\eta}) \qquad [2.3.22]$$

where

$$Z = 3.2 \left(\frac{1.75}{\ln \chi_1}\right)^{\frac{1}{2}} + \frac{\sigma \bar{V}}{R_g T \ln \chi_1} \qquad [2.3.23]$$

$$\lambda = 3.2 \left(\frac{1.75}{\ln \chi_2}\right)^{\frac{1}{2}} + \frac{\sigma \bar{V}}{R_g T \ln \chi_2} \qquad [2.3.24]$$

$$\chi_1 = (P_o + P_m)/(P + P_m) \qquad [2.3.25]$$

$$\chi_2 = (P_o + P_m)/P_m \qquad [2.3.26]$$

Equation (2.3.22) is a volumetric isotherm equation defining the specific adsorbed volume due to molecular and capillary phenomena within the intermicellular capillaries of the tissue. It is reduceable to its gravimetric equivalent by a process which converts the specific adsorbed volume to specific adsorbed mass. This can be accomplished by introducing the appropriate density term into equation (2.3.22)

to obtain the terminal relation:

$$M_a = \rho \frac{\xi}{\eta} (Z^{\eta} - \lambda^{\eta}) \qquad [2.3.26]$$

where, in view of the demonstrated variable compressibility of the adsorbed water "film" (Katz, 1933; Stamm and Seborg, 1935; and Stamm, 1938), ρ is an undefined function which is dependent on the magnitude of the intermolecular forces, the surface-impressed pressure and possibly the isotherm temperature. Polanyi's Adsorption Potential theory describes the adsorbed multi-layer as resembling the atmosphere of a planet with the highest compression at the surface of the solid and the density falling off outwards (see Figure 2.7). Babbitt (1942) insisted that any theory of adsorption must account for this adsorption compression. Stamm and Seborg (1935) demonstrated that actual adsorption compression values can be obtained, and that adsorption compression extends to the fiber saturation point. A density function for the adsorbed water film reflecting these points of view needs now be formulated to augment the derived isotherm relation (2.3.26).

2.4 Adsorption Compression on Adsorbing Bio-Materials

Even before Polanyi (1914) first expounded his now famous theory of isopotential contours within the adsorbed film, a large number of investigators had preoccupied themselves with detailed theoretical and experimental study of the adsorbed phase. Among such early investigators are Rose (1849), Jungh (1865) and Parks (1902) who speculated that adsorbed water molecules on the surface of a

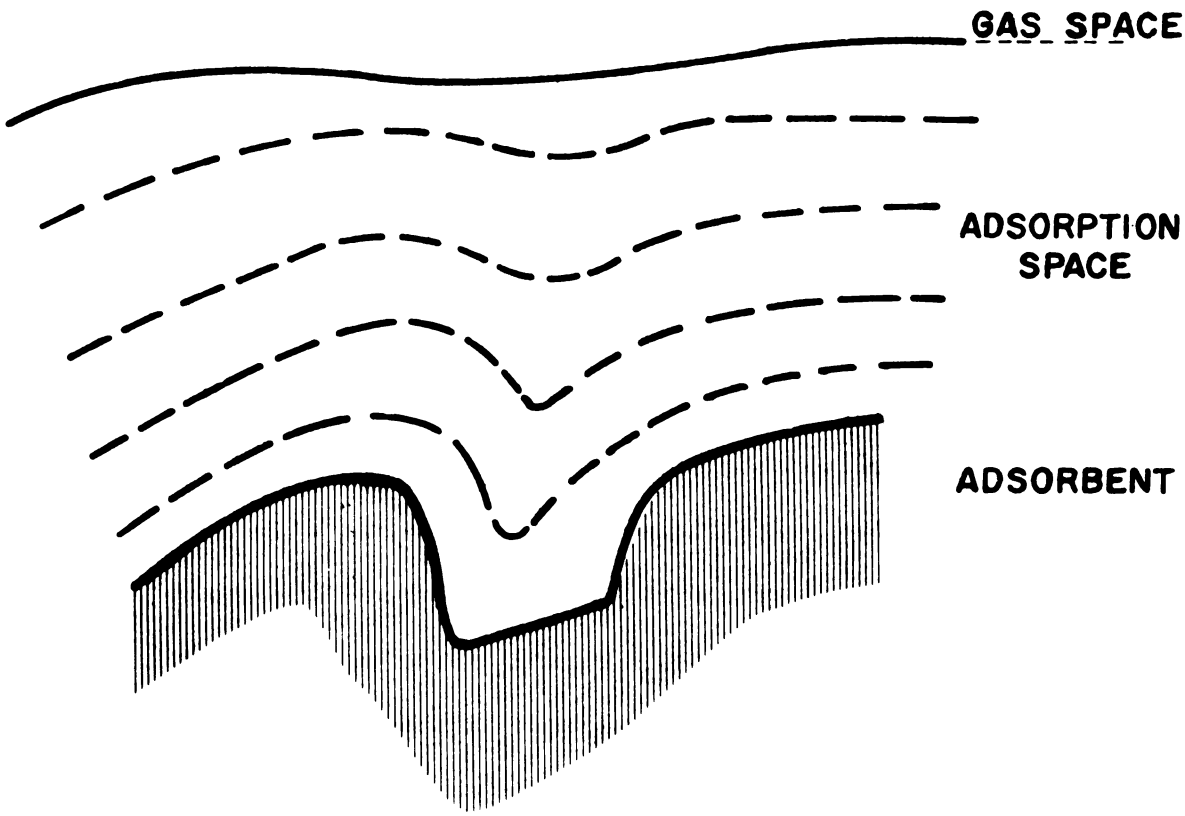

Figure 2.7. Polanyi's isopotential contours. The space between each pair of equipotential surfaces corresponds to a different degree of adsorbate compression.

solid have undergone a definite thermodynamic change in state and are held against the surface by a force which is expressible in terms of pressure and compressibility. Calorimetric measurements of the heats of adsorption undertaken by Lamb and Coolidge (1920), Patrick and Grimm (1921) and later supported by the extensive thermodynamic calculations of Harkins and Ewing (1921), estimated values of the compressive force in the range of 37,000 to 100,000 atmospheres. From specific volume determinations for cotton in different liquid and gaseous media, Davidson (1927) calculated values of the average compression of sorbed water of approximately 2000 atmospheres on the basis that compression takes place entirely in the water and that the adsorbent is essentially incompressible. Katz (1933) has shown that a qualitative proportionality exists between the heat of swelling of binary aqueous systems and the corresponding volume change. Gibson (1934) gives the relationship between the specific compression of water, the internal or intrinsic pressure change, and the externally applied pressure for aqueous solutions of certain sulfates.

Measurements are available giving the contraction in volume as a function of moisture content for cellulosic materials. Thus, Stamm and Hansen (1937) employed the Gibson compressibility relationship for water to obtain specific volume contractions for wood, pulp and cotton. Filby and Maass (1932) calculated the apparent density of water adsorbed on cotton cellulose as a function of moisture content. They concluded that below the 3% moisture level an apparent density of 2.6 gm./cc. is obtained. The apparent density value falls off with increasing moisture content, until above the 9% moisture level

where the adsorbed water appears to have its normal bulk liquid density. This result was contradicted by the work of Stamm and Seborg (1935) who found that the density of water originally adsorbed is 1.3, and demonstrated that adsorption compression extends to the fiber saturation point. Ewing and Spurway (1930) obtained apparent density values for water adsorbed on silica gel. Their values extend all the way from 1.03 at 1% moisture content to 0.54 at 7% moisture level. Morrison and McIntosh (1945) obtained the apparent density of water adsorbed on four different charcoals using the helium displacement method. Their results which exhibited considerable inconsistency, showed a notable difference in apparent density values of water between the adsorption and desorption branches. In another study, Tuck, McIntosh and Maass (1947) investigating the density of various adsorbates on charcoal, concluded that in view of the uncertainties which they observed, the utility of apparent density values of adsorbates in checking concepts in physical adsorption is limited.

From the foregoing review, it is apparent that while the broad concept of adsorption compression seems to be well established among investigators, considerable uncertainty exists regarding compressibility and apparent density values of adsorbates. This uncertainty must account, at least in part, for the seeming lack of interest on the part of investigators to come up with a descriptive density function for the adsorbed phase. The compressibility relation of Gibson notwithstanding, there exists, to the knowledge of the author, only two such equations. The first is the density

relation of Stamm (1938), which expresses adsorbate density in terms of the "true" and "apparent" specific gravities of the sorbent. The second is a computational scheme using the Lowry and Olmsted (1927) modification of Polanyi's theory to generate the so-called characteristic curves from empirical isotherm data (see Brunauer, 1945, pp. 101-104). The characteristic curves are then integrated numerically to obtain the density values. Because of the difficulty of obtaining accurate specific gravity values for porous substances, the Stamm relation does not lend itself for usage here. The Polanyi characteristic curves scheme on the other hand, is only as good as the simplified equation of state which must be assumed for the adsorbed phase. For their work, Lowry and Olmsted used a modified form of the van der Waals two-dimensional equation of state given by van Laar (1924). Even though Lowry and Olmsted (1927) and De Vries (1935) appear to have successfully used the method to obtain reasonable density values for CO_2 adsorbed on charcoal, its direct application to H_2O systems does not seem to be as yet possible since the van Laar constants for the water molecule have not been determined.

Because of the urgent need for an easily applied adsorbate density relation, a derivation of such a function will now be presented.

2.4 a. A Density Function for Sorbed Water:

Consider a closed vessel (Figure 2.8) of volume V containing the sorbent and a fixed number of molecules, n, of the sorbate at the temperature T and pressure P. If V_m denotes the molar volume

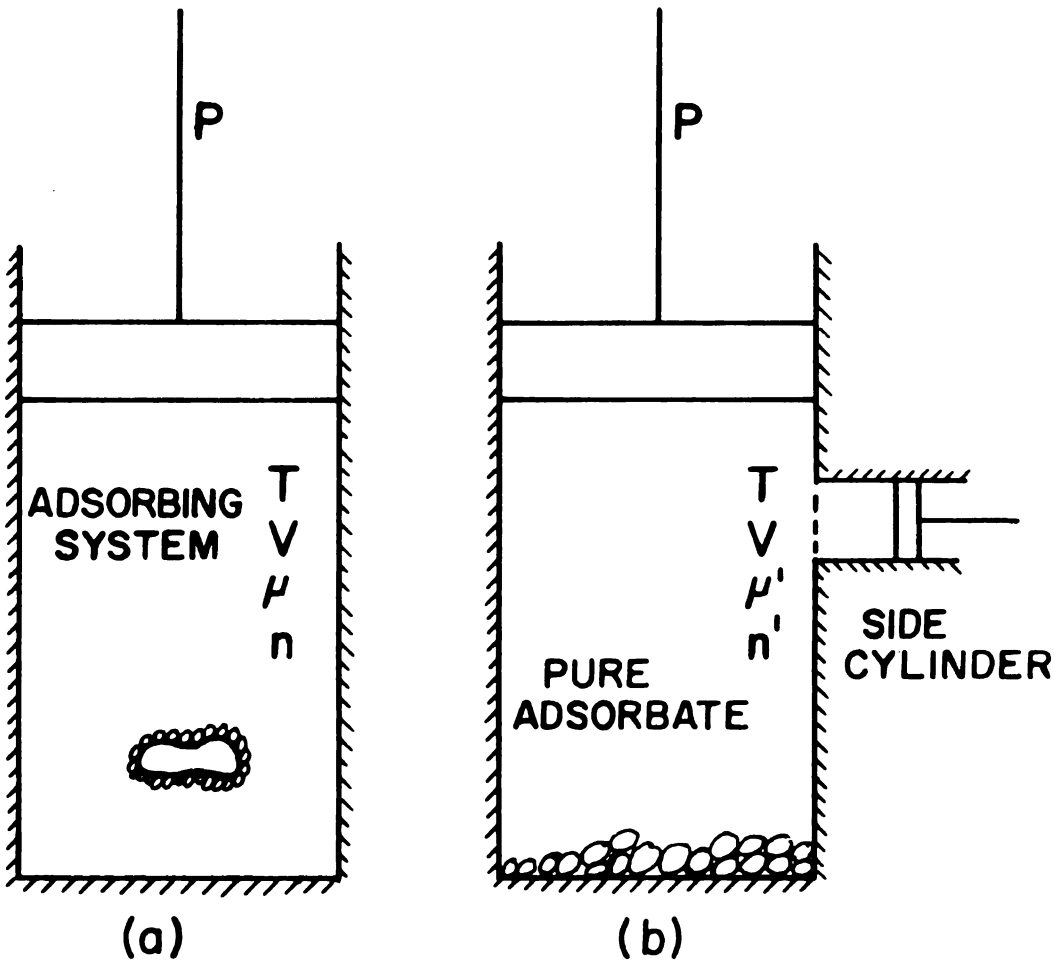

Figure 2.8. Diagram showing two thermodynamically identical systems.

(a) Contains an active sorbent

(b) Contains the pure sorbate

of the gaseous sorbate and the volume of the sorbent is assumed to be negligible, then:

$$V = (n - n^a)\, V_m \qquad [2.4.1]$$

where n^a is the adsorbed excess due to sorption over and above the amount of gas which would be contained in the same volume, at the same pressure and temperature, in the absence of the sorbent. From Maxwell's relation:

$$(\partial S/\partial P)_T = -(\partial V/\partial T)_P \qquad [2.4.2]$$

combining equations (2.4.1) with (2.4.2) gives:

$$-(\partial S/\partial P)_T = (\partial V/\partial T)_P$$

$$= (n-n^a)(\partial V_m/\partial T)_P - (\partial n^a/\partial T)_P V_m \qquad [2.4.3]$$

also

$$(\partial S/\partial P)_T = -(\partial S/\partial n^a)_T \left(\frac{\partial P}{\partial n^a}\right)_T$$

consequently

$$(\partial S/\partial n^a)_T = (\partial S/\partial P)_T\, (\partial P/\partial n^a)_T$$

$$= (n-n^a)(\partial V_m/\partial T)_P (\partial P/\partial n^a)_T - V_m (\partial n^a/\partial T)_P (\partial P/\partial n^a)_T$$

$$= (n-n^a)(\partial V_m/\partial T)_P (\partial P/\partial n^a)_T + V_m (\partial P/\partial T)_{n^a} \qquad [2.4.4]$$

Now compare the system described above with another system (shown in Figure 2.8.b) consisting of a vessel of the same volume V containing the same gas at the same temperature and pressure, but without any sorbent. If primed symbols are adopted to represent quantities relating to this second system when they may differ from those relating to the first system, then:

$$n' = n - n^a \qquad [2.4.5]$$

where n' denotes the number of molecules of pure gaseous sorbate remaining in the vessel after the amount n^a has been lost isothermally through the lateral cylinder. Moreover, since both systems are in equilibrium and the gas is in identical condition, the chemical potentials are the same, i.e.

$$\mu' = \mu \qquad [2.4.6]$$

If the molar entropy change in the first system per unit change in n^a resulting from a decrease in the pressure, is denoted by ΔS_m, then

$$\Delta S_m = (\partial S/\partial n^a)_T$$

$$= (n-n^a)(\partial V_m/\partial T)_P(\partial n^a)_T + V_m(\partial P/\partial T)_{n^a} \qquad [2.4.7]$$

If the molar entropy change in the second system corresponding to the same decrease in pressure is further denoted by $\Delta' S_m$, then,

$$\Delta' S_m = n'(\partial V_m/\partial T)_P(\partial P/\partial n^a)_T \qquad [2.4.8]$$

Subtracting equation (2.4.8) from equation (2.4.7) and using equation (2.4.5) gives:

$$\Delta S_m - \Delta' S_m = (\partial S/\partial n^a)_T - (\partial S/\partial n^a)_T = V_m(\partial P/\partial T)_{n^a} \qquad [2.4.9]$$

Multiplying equation (2.4.9) by T gives:

$$T\,\Delta S_m - T\,\Delta' S_m = T(\partial P/\partial T)_{n^a} V_m \qquad [2.4.10]$$

It follows immediately from equation (2.4.6) that:

$$\Delta \mu = \Delta' \mu \qquad [2.4.11]$$

From the fundamental equations of thermodynamics (see Guggenheim, 1967, p. 24),

$$\frac{\partial}{\partial T} (\mu^{\alpha}/T) = - \frac{S^{\alpha}}{T} - \frac{\mu^{\alpha}}{T^2} = - \frac{H^{\alpha}}{T^2} \qquad [2.4.12]$$

It follows immediately from equation (2.4.12) that:

$$T \Delta S^{\alpha} + \Delta \mu^{\alpha} = \Delta H^{\alpha} \qquad [2.4.13]$$

Subtracting equation (2.4.11) from equation (2.4.10) and using equation (2.4.13) yields:

$$\Delta H_m - \Delta' H_m = T(\partial P/\partial T)_{n^a} V_m \qquad [2.4.14]$$

The left hand side of equation (2.4.14) may be taken to represent the equilibrium molar enthalpy (heat) of sorption. It is the heat which must be supplied per unit change in n^a resulting from decrease of pressure under isothermal quasi-equilibrium conditions, minus the heat that must be supplied to the second system when the pressure is identically reduced by the same amount. It needs to be emphasized that every quantity occuring in equation (2.4.14) is experimentally determinable without the use of approximations or extraneous assumptions. Thus the quantity $\Delta' H_m$ is a molar work function for a real gas, and ΔH_m and $(\partial P/\partial T)_{n^a}$ are obtainable from sorption isosteres.

If the sorbed mass in the sorbent-sorbate system is denoted by M_a and the corresponding volume by V_a then,

$$V_a = n^a V_m = (M_a/M) V_m \qquad [2.4.15]$$

also $$\rho = M_a/V_a = M/V_m \qquad [2.4.16]$$

where ρ is the density of the sorbate and M is its gram molecular weight. Multiplying equation (2.4.14) by n^a and using equations (2.4.15) and (2.4.16) gives:

$$\frac{M_a}{M} (\Delta H_m - \Delta' H_m) = T(\partial P/\partial T)_{n^a} V_a \qquad [2.4.17]$$

so that:

$$\rho = \frac{T(\partial P/\partial T)_{n^a}}{(\Delta H - \Delta' H)} \qquad [2.4.18]$$

Equation (2.4.18) can be expressed in terms of a standard density, ρ_o, such that:

$$\rho/\rho_o = \left(\frac{\Delta H^\circ - \Delta' H^\circ}{\Delta H - \Delta' H}\right) \left(\frac{(\partial P/\partial T)_{n^a}}{(\partial P/\partial T)_{n^o}}\right) \qquad [2.4.19]$$

where the superscript "o" denotes saturation values, and ρ_o is the density of the sorbate at saturation pressure.

The differential terms of equation (2.4.19) can be defined by invoking the Clausius-Clapeyron equation without any loss of accuracy. Thus:

$$\left(\frac{\partial P}{\partial T}\right)_{n^a} = \frac{\Delta H\ P}{R_g T^2} \qquad [2.4.20]$$

$$\left(\frac{\partial P}{\partial T}\right)_{n_o} = \frac{\Delta H^\circ P_o}{R_g T^2} \qquad [2.4.21]$$

combining equations (2.4.20) and (2.4.21) yields:

$$\frac{(\partial P/\partial T)_{n_a}}{(\partial P/\partial T)_{n_o}} = \frac{\Delta H}{\Delta H^\circ}(P/P_o) \qquad [2.4.22]$$

Substituting equation (2.4.22) in equation (2.4.19) gives:

$$\rho/\rho_o = \frac{P}{P_o}\left(\frac{\Delta H^\circ - \Delta' H^\circ}{\Delta H - \Delta' H}\right) \cdot \frac{\Delta H}{\Delta H^\circ} \qquad [2.4.23]$$

or

$$\rho/\rho_o = \mu^* \, (\Delta H/\Delta H^\circ) \qquad [2.4.24]$$

where $$\mu^* = (P/P_o)\left(\frac{\Delta H^\circ - \Delta' H^\circ}{\Delta H - \Delta' H}\right) \qquad [2.4.25]$$

for pure water vapor $\Delta' H^\circ \simeq 0$

consequently

$$\mu^* = \frac{P}{P_o}\left(\frac{\Delta H^\circ}{\Delta H - \Delta' H}\right) \qquad [2.4.26]$$

Equation (2.4.24) states that the adsorbate density is a direct function of the isosteric heat of sorption which in turn is a measure of the intermolecular force of attraction. This result appears to support the earlier qualitative observation of Katz (1933), that a proportionality exists between the heat of swelling of a binary aqueous system and the corresponding volume change. Since a purely theoretical determination of the function μ^* is not possible without simplification of the work function $\Delta' H$, the decision was made to obtain an estimate of μ^* using the

empirical data of Stamm (1938). It seems reasonable, judging from the nature of the terms present in equation (2.4.26), that μ^* will not vary appreciably from one biological material to another. Thus, while the quantity ($\Delta H/\Delta H°$) - the ratio of the heat of adsorption at any P/P_o value to that at saturation - characterizes the specific character of the individual substance, the deterministic function μ^* classifies it as a class or sub-class.

The work sheet used for the calculation of μ^* from the empirical data of Stamm (1938) is shown in Table 2.1. Column 1 shows the standard relative vapor pressure and column 2 gives the corresponding specific adsorbed mass read from the isotherm. The figures given in column 3 are the mono-layer capacities determined by the standard B-E-T procedure. Columns 4 and 5 show the numbers of adsorbed layers of water molecules. Column 6 is simply a reduced form of column 5, obtained by dividing each value of column 5 by the number of adsorbed molecular layers at saturation. Column 7 contains the isosteric heat values for spruce wood taken from Figure A.1 of the appendix. Column 8 shows the average ΔH values in terms of molecular layers, obtained by careful averaging of the relevant values of column 7. Column 9 expresses the average isosteric heat values as a ratio of the isosteric heat value at saturation. Column 10 is a tabulation of the density values obtained from Stamm (1938), and columns 11 and 12 are reduced forms of column 10. Column 13 is obtained by dividing terms in column 12 by the corresponding terms of column 9 in accordance with equation (2.4.24).

Table 2.1. The function μ^* as determined from the empirical data of Stamm (1938) for spruce wood at 25°C.

1	2	3	4	5	6	7	8	9	10	11	12	13
P/P_o	X	X_m	X/X_m	# Layers	$\frac{X/X_m}{X_L/X_m}$	ΔH	$\overline{\Delta H}$	$\frac{\overline{\Delta H}}{\Delta H^\circ}$	ρ	ρ/ρ_o	ρ/ρ_o	μ^*
		.050										
0.00		"							1.300	1.180		
0.05	.0130	"	.26			770			1.286	1.170		
0.10	.025	"	.50			710			1.274	1.160		
0.20	.050	"	1.00	# 1	.142	644	688	1.180	1.248	1.134	1.153	0.98
0.30	.063	"	1.26			630			1.234	1.120		
0.40	.080	"	1.60			616			1.218	1.110		
0.50	.095	"	1.90			610			1.204	1.094		
				# 2	.285		615	1.053			1.101	1.045
0.60	.113	"	2.26			604			1.19	1.080		
0.70	.135	"	2.70			595			1.174	1.070		
				# 3	.428		596	1.020			1.067	1.045
0.80	.165	"	3.30			590			1.157	1.050		
				# 4	.571		587	1.008			1.042	1.035
0.90	.225	"	4.50			584			1.138	1.034		
				# 5	.714		584	1.000			1.024	1.024
0.95	.275	"	5.50			584			1.116	1.013		
				# 6	.857		584	1.000			1.007	1.007
1.00	.340	"	6.80			584			1.100	1.000		
				# 7	1.000		584	1.000			1.000	1.000

Table 2.2. The reduced function $\rho/\rho_o = u^*$ ($\Delta H \; \Delta H^\circ$) for corn. Based on the desorption isotherm (4°C) data of Rodriguez Arias (1956).

1	2	3	4	5	6	7	8	9	10	11
P/P_o	X	X_m	X/X_m	# Layers	$\frac{X/X_m}{X_L/X_m}$	ΔH	$\overline{\Delta H}$	$\frac{\overline{\Delta H}}{\Delta H^\circ}$	u^*	ρ/ρ_o
		.087								
0.10	.065	"	.751			812				
				# 1	0.25		784	1.322	.98	1.295
0.20	.093	"	1.070			756				
0.30	.110	"	1.271			704				
0.40	.128	"	1.473			666				
0.50	.148	"	1.647			644				
0.60	.163	"	1.878			626				
				# 2	0.50		650	1.096	1.045	1.145
0.70	.183	"	2.109			614				
0.80	.213	"	2.456			603				
				# 3	0.75		593	1.008	1.035	1.043
0.90	.270	"	3.121			593				
0.95	.300	"	3.468			593				
				# 4	1.00		593	1.000	1.00	1.000
1.00	.350	"	4.046			593				

Table 2.3. The reduced function $c/c_o = \mu^* (\Delta H/\Delta H^\circ)$ for cotton. Based on the adsorption isotherm (10°C) data of Urquhart and Williams (1924).

1 P/P_o	2 X	3 X_m	4 X/X_m	5 # Layers	6 $\frac{X/X_m}{X_L/X_m}$	7 ΔH	8 $\overline{\Delta H}$	9 $\frac{\overline{\Delta H}}{\Delta H^\circ}$	10 μ^*	11 ρ/ρ_o
		.0357								
0.05	.017	"	.48			750				
0.10	.023	"	.644			716				
0.20	.032	"	.896			680				
				# 1	.142		700	1.190	.98	1.166
0.30	.041	"	1.15			656				
0.40	.049	"	1.372			642				
0.50	.058	"	1.624			634				
0.60	.068	"	1.904			628				
				# 2	.285		633	1.072	1.045	1.121
0.70	.080	"	2.24			630				
0.80	.099	"	2.77			629				
				# 3	.428		617	1.045	1.045	1.092
0.90	.132	"	3.697			604				
				# 4	.571		598	1.013	1.035	1.048
0.95	.164	"	4.593	# 5	.714	592	591	1.001	1.024	1.025
				# 6	.857		590	1.00	1.007	1.007
1.00	.24	"	6.722			590				
				# 7	1.000		590	1.00	1.000	1.000

Table 2.4. The reduced function $\sigma/\sigma_o = \mu^* (\angle H/\angle H°)$ for pre-cooked freeze dried Beef Powder. Based on adsorption isotherm (10°C) data obtained in the experimental part of this study.

1 P/P_o	2 X	3 X_m	4 X/X_m	5 # Layers	6 $\frac{X/X_m}{X_L/X_m}$	7 ΔH	8 $\overline{\Delta H}$	9 $\frac{\overline{\Delta H}}{\Delta H°}$	10 μ^*	11 ρ/ρ_o
		.091								
0.05	.047	"	.52			850				
0.10	.070	"	.769			835				
				# 1	.167		825	1.380	.99	1.360
0.20	.095	"	1.044			820				
0.30	.110	"	1.210			795				
0.40	.122	"	1.341			764				
0.50	.135	"	1.484			760				
0.60	.155	"	1.703			733				
				# 2	.333		749	1.260	1.045	1.316
0.70	.191	"	2.100			695				
0.80	.260	"	2.860			658				
				# 3	.500		664	1.116	1.043	1.164
0.90	.380	"	4.180	# 4	.667	640	652	1.096	1.028	1.126
0.95	.450	"	4.950			617				
				# 5	.833		627	1.054	1.008	1.062
1.00	.505	"	5.550			600				
				# 6	1.00		595	1.000	1.000	1.000

Superposed plots of ρ/ρ_o (column 12, Table 2.1), and $\Delta H/\Delta H^\circ$ (column 9, Table 2.1), against the number of adsorbed molecular layers (column 5, Table 2.1), are shown in Figure 2.9. The function, μ^*, as generated from Table 1 (column 13) is plotted in Figure 2.10 as a function of the number of adsorbed molecular layers. In anticipation of its wider usage in this work, the modifying function μ^* is plotted in a more generalized form in Figure 2.11. Using Figure 2.11 as the invariant function μ^* for the class of biological products of interest, Tables 2.2, 2.3 and 2.4 are developed as typical work sheets for the calculation of the reduced density function, ρ/ρ_o. In view of their close identity to Table 2.1, the detailed description of these tables is not given. Density curves for water adsorbed on spruce wood, freeze-dried beef powder, corn kernels and cotton based on these tables are plotted in Figure 2.12. The plots represent a wide variety of biological species - cellulosic materials, animal tissue, seeds and textile fibres.

In conclusion, it may be noted that the nature and composition of equation (2.4.23) can be derived from purely dimensional considerations. While the present definition of μ^* may appear suspect because it is based on just one set of empirical data, it will be shown later - from independent calculations in chapter four - that the density values are acceptable first estimates. It will be desirable, however, to revise the function μ^* to reflect a broader spectrum of empirical data as more experimental density values for water sorbed on biological products become available.

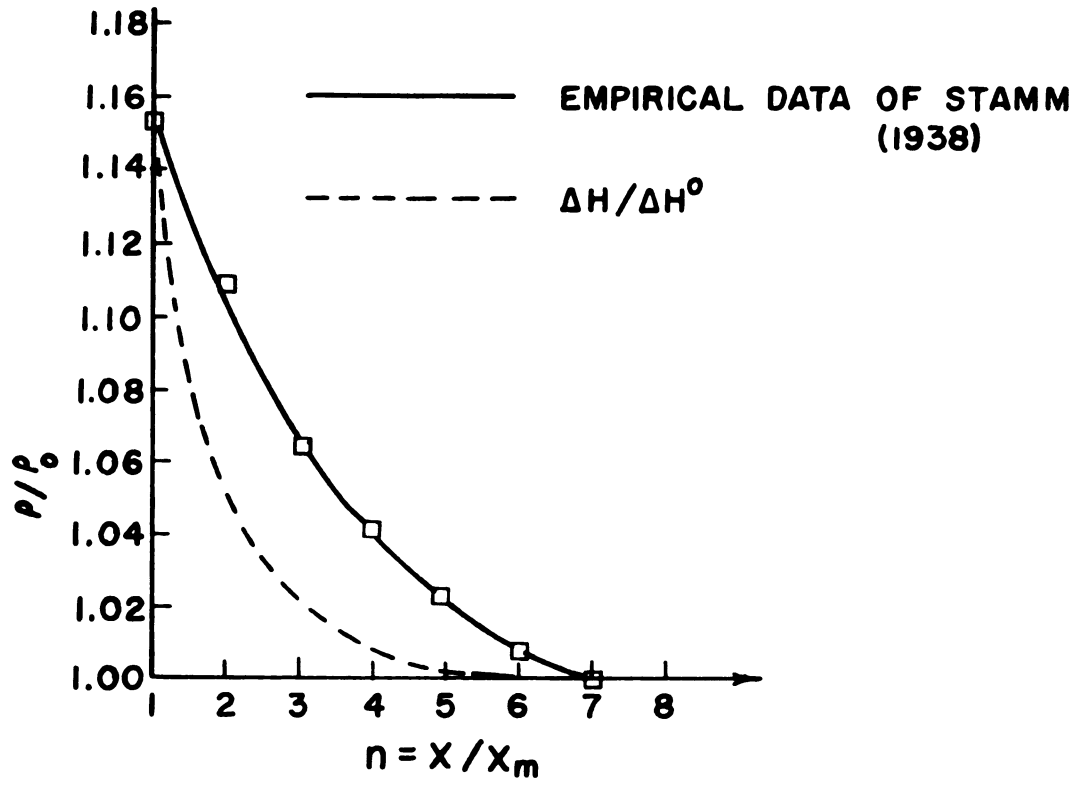

Figure 2.9. (——), reduced density of water, adsorbed on wood as a function of adsorbed layers of water molecules. (---), isosteric heat ratio, $\Delta H/\Delta H^{\circ}$ as a function adsorbed layers of water molecules.

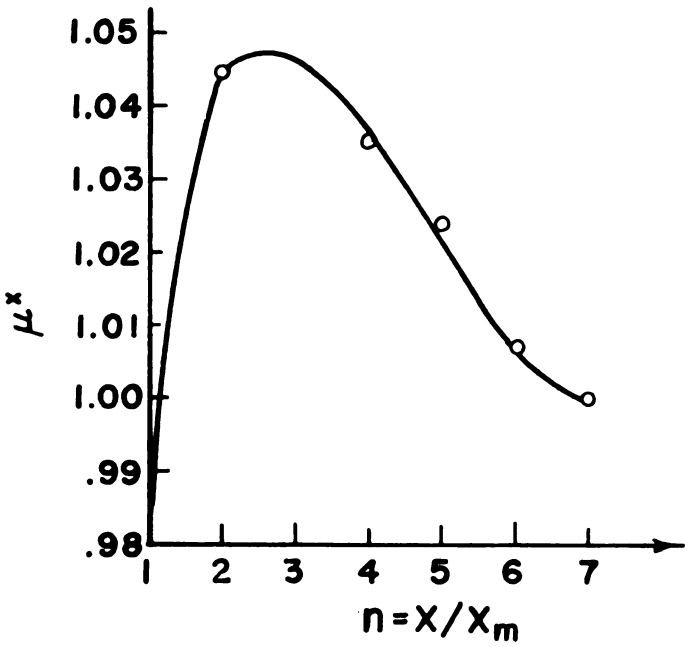

Figure 2.10. Plot of the function μ^* as obtained from the empirical data of Stamm (1938).

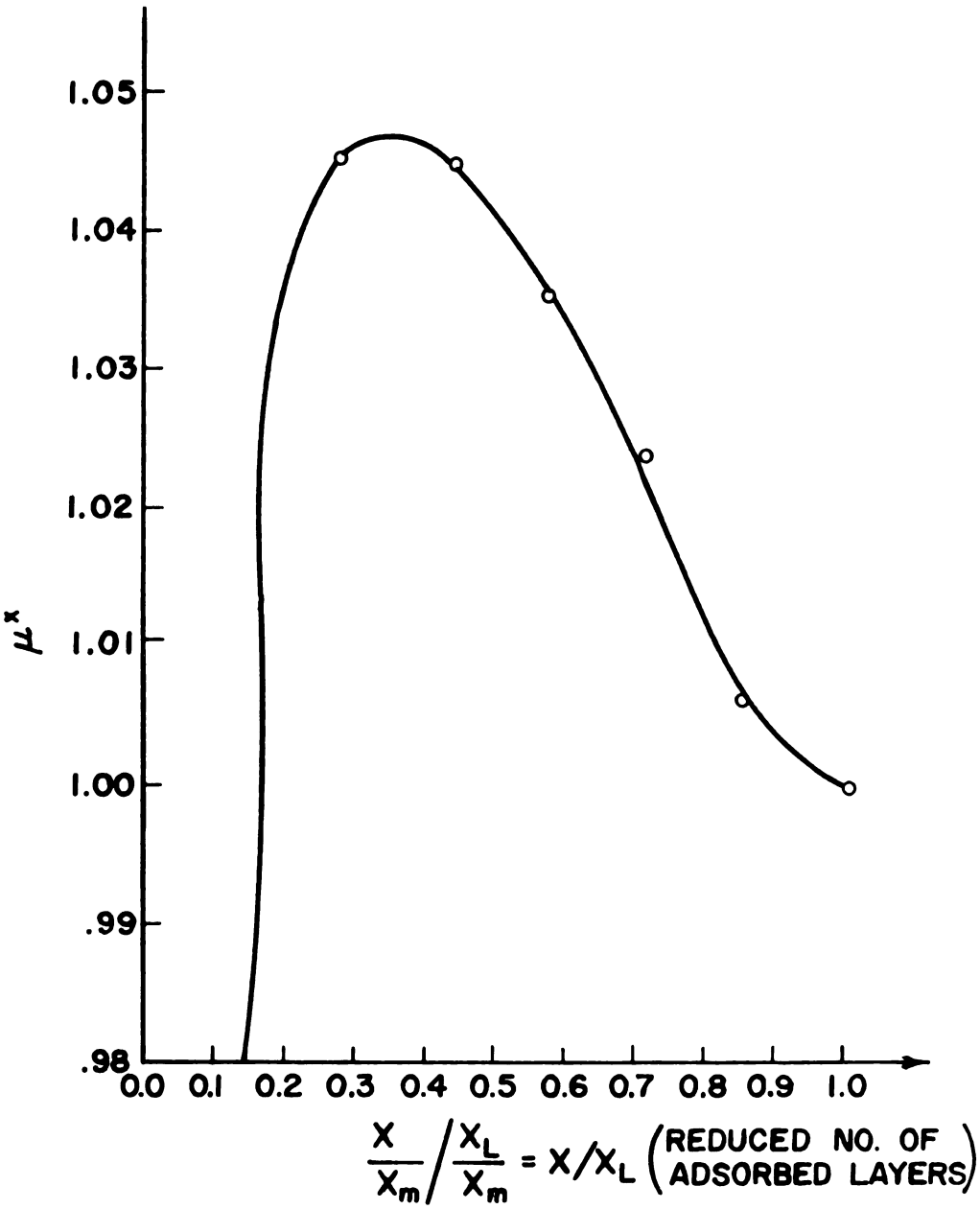

Figure 2.11. Generalized plot of the function, μ* as obtained from the empirical data of Stamm (1938) for Spruce wood.

X_L = Moisture content at hygroscopic point.

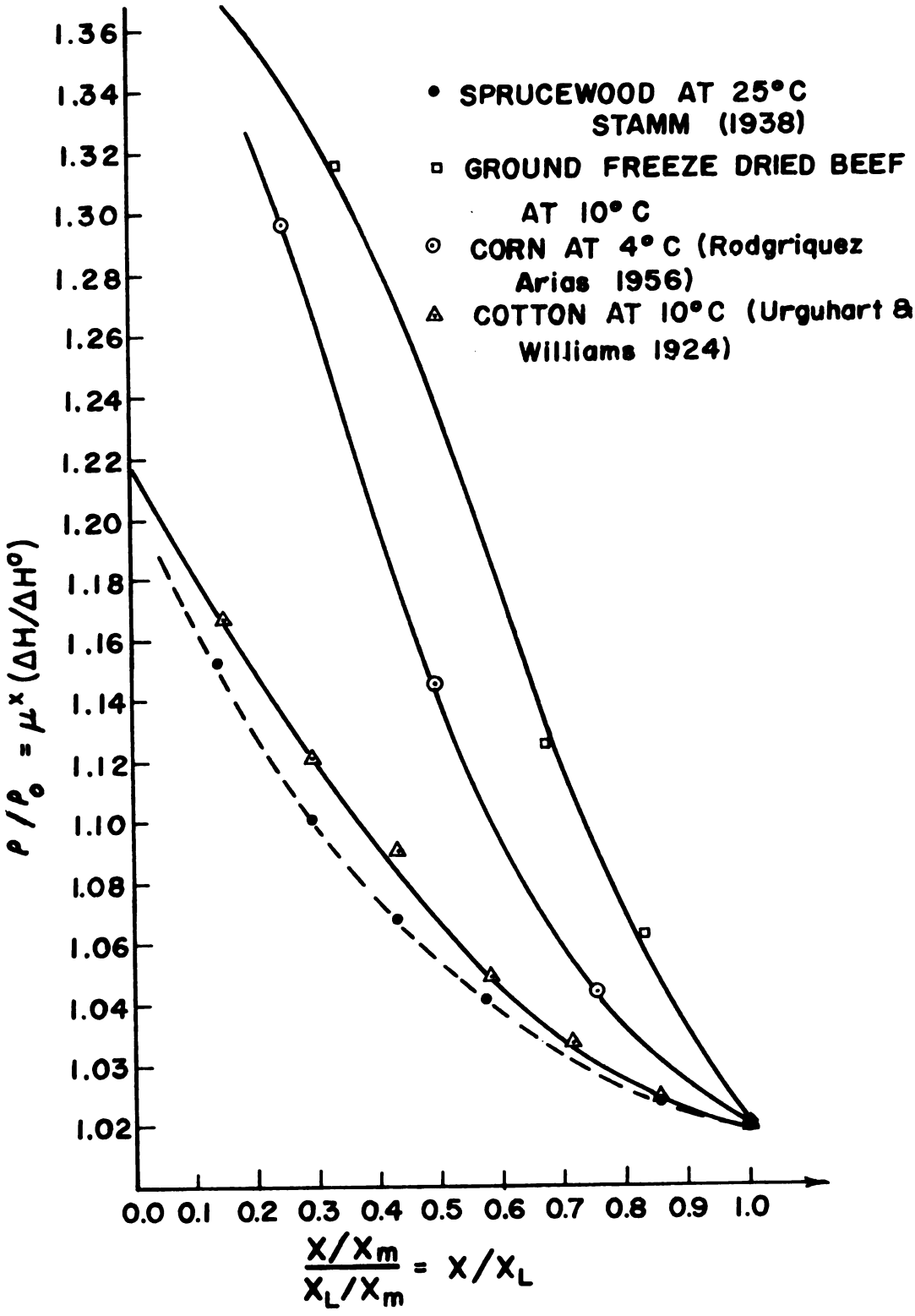

Figure 2.12. Plot of reduced density function against dimensionless number of adsorbed layers.

X_L = Moisture content at hygroscopic point.

2.5 Sorption Hysteresis in Biological Materials

A fundamental characteristic of sorption isotherms of biological materials is their dependence on the previous sorption history. Thus, the adsorption isotherm obtained by placing a dry biological material in atmospheres of increasing relative vapor pressures of water in the words of Ewing (1881) "lags behind" the desorption isotherm obtained by placing the wet product in atmospheres of decreasing relative humidity. This phenomenon, of general occurence for biological materials, is called hysteresis. It executes a closed loop - the hysteresis loop - between the upper and lower bounds of relative humidity, $0 \leq P/P_o \leq 1$. In some systems the size of the hysteresis loop depends upon the speed and frequency with which the loop is traversed. When experiments are carried out very slowly, or are repeated a sufficient number of times, hysteresis may disappear. Time-dependent hysteresis which has been attributed to relaxation phenomena (Alfrey and Doty, 1945; ter Haar, 1950), raised some serious doubts among investigators as to the reality of the phenomenon (McGavack and Patrick, 1920; Patrick 1929). However, the excruciating and extensive work of Allmand and collaborators (1929), Urquhart (1929), Urquhart and Eckersall (1930), Lambert and Foster (1932), Foster (1934), Burrage (1934) and Rao (1941) appear to have established the phenomenon as real and fundamental. In consequence, it has long become an important self-consistency rule for any given theory of adsorption that sorption hysteresis be inherently explicable within its governing framework.

In pursuing this practice in this section from posterior considerations, it seems possible, taking the facts as a whole, to think of the sorptive behavior of biological materials as a double superposition effect. On the one hand, adsorption hysteresis in bio-materials must be linked with condensation and evaporation processes in irregular voids - leading logically to the so-called capillary condensation theories (Everett, 1967). On the other hand, as "organogels" (Urquhart, 1929; Katz, 1933; Rao, 1941), adsorbed water molecules influence such physical properties of biological products as strength, elasticity, rigidity, swelling and evolution of heat. This water-induced change leads to what will be called for lack of a better term - "swelling fatigue" hysteresis.

2.5 a. Capillary Condensation Hysteresis:

While Zsigmondy's earliest "impurity - contact - angle" hysteresis theory is inadmissible as a general explanation of "permanent hysteresis" in bio-materials, it does give a creditable qualitative account of time - dependent hysteresis in these systems.

If the soluble components of adsorbing biological products are considered to be "impurities" present on the adsorbing insoluble surfaces, then the alternate desolving and deposition of such soluble matter with adsorption and desorption, respectively, can conceivably lead to varying wetting patterns in both processes. Suppose now that each desolving-deposition cycle is associated with a measurable translocation of the solute particles, then the contact-angle hysteresis induced by such translocatable impurity can conceivably be even more pronounced.

Foster's (1932) "open-pore" or "delayed meniscus" theory of adsorption hysteresis is based on a consideration of the mechanism of meniscus formation in the adsorption process and of meniscus disappearance in desorption. These mechanisms are supposed to differ. On the other hand, the so-called "ink bottle" or "bottle neck" theory of hysteresis advanced separately by Kraemer (1931) and McBain (1935) depends on the geometrical irregularity of the pores. In essence, both theories attribute capillary condensation hysteresis in physical adsorption by rigid non-swelling adsorbents to topographical factors. On qualitative grounds, both theories are compatible with the general physical model which has been proposed. They are consequently each capable of making a possible contribution to adsorption hysteresis in biological materials. It appears necessary, as a realistic approach to capillary condensation hysteresis in these products, to combine the essential features of Foster's theory and of the ink bottle theory. Katz (1949), in a detailed theoretical discussion of permanent hysteresis seems to have been the first to propose this point.

The open-pore theory was applied to the simple case of an open-ended cylindrical capillary by Cohan (1938). This development is often regarded as a limited quantitative expression of Foster's ideas. However, in a later paper, Cohan (1944) showed conclusively that his considerations are also applicable to closed capillaries possessing constrictions. For the present discussion therefore, the Cohan theory of capillary condensation is adopted with modifications as an essential combination of the open-pore and ink bottle theories in the first approximation.

This theory, simultaneously developed independently by Cohan (1938) and Coelingh (1938), explained hysteresis in terms of the different shape of the meniscus during adsorption and desorption. Along the adsorption path, the meniscus assumes a cylindrical shape with a radius of curvature defined by the equation:

$$R_a = t + \sigma \bar{V}/R_g T \ln(P_o/P_a) \qquad [2.5.1]$$

Along the desorption branch on the other hand, the Kelvin mechanism is assumed - the meniscus being hemispherical with a radius of curvature:

$$R_d = t + 2\ \sigma \bar{V}/R_g T \ln(P_o/P_d) \qquad [2.5.2]$$

Comparing equations (2.5.1) and (2.5.2) under conditions of perfect wetting, yields the well known Cohan relation for open ended tubular capillaries:

$$(P_a/P_o)^2 = (P_d/P_o) \qquad [2.5.3]$$

From the detailed consideration of the shapes of capillaries by de Boer (1958), equation (2.5.3) is easily generalized to the form:

$$(P_a/P_o)^{\omega} = (P_d/P_o) \qquad [2.5.4]$$

where the exponent, ω, is a parameter specifying the pore geometry. Considering the different shapes of interconnected "ink bottles" possible in the porous structure under consideration, ω lies in the range $\omega \geq 1$ (de Boer, 1958; Linsen and van den Heuvel, 1967). While the exact value of ω must depend on the particular product, it suffices to point out that its predicted domain in the range above 1 ensures that the adsorption path consistently lags behind the desorption branch.

2.5 b. "Swelling Fatigue" Hysteresis

Since biological materials are elastic organogels which swell and contract with adsorption and desorption of water vapor, respectively, the purely topographical explanation of hysteresis given above is necessarily incomplete. In addition to the geometrical factors discussed, there exists a contribution to hysteresis due to water-induced changes in the properties of the swelling adsorbent.

Urquhart (1929), Katz (1933), White and Eyring (1947) recognizing the importance of these water-induced changes attributed hysteresis in elastic gels such as celluloses to the free secondary-valence bonds of the hydroxyl groups of the cellulose molecules. In the original water-soaked condition, the free hydroxyl groups are practically all satisfied by water. When the cellulose is dried, these hydroxyl groups are freed and, as a result of the shrinking, pairs are drawn together so that the individual groups mutually satisfy each other. Upon adsorption, part of the hydroxyl groups that have mutually satisfied each other are not free for water adsorption, thus giving reduced adsorption. Rao (1941) explained hysteresis in some cereal grains in terms of the water-induced changes in their elastic properties. Chung and Pfost (1967) acknowledged these changes in their molecular shrinkage-crack concept of hysteresis in cereal grains. Henderson (1969) in a recent paper on the subject, stressed the importance of unique changes associated with moisture adsorption by biological materials.

All these accounts attributing hysteresis in biological products to water-induced physico-chemical changes are basically qualitative descriptions of the phenomenon. In order to make them expressible quantitatively certain approximations are mandatory. Thus it appears logical to consider that, in spite of their separate physical and chemical origins, adsorbed moisture-induced changes are ultimately mirrored in such physical properties as elasticity, strength and swelling. Such generally irreversible changes can be collectively classified as fatigue - hence the term "swelling fatigue" hysteresis.

An approximate thermodynamic relationship exists between the pressure of swelling and the vapor pressure of a partially swollen substance. This relationship has been given by Katz (1933) and White and Eyring (1947) as:

$$P_s = \frac{R_g T}{M V_a} \ln (P_o/P) \qquad [2.5.5]$$

where V_a is the specific adsorbed volume corresponding to the relative vapor pressure P/P_o. The pressure, P_s, is responsible for the so-called hydro-stress in biological materials (Hammerle, 1968). To correlate dimensional changes with the changes in stress resulting from adsorption the relation:

$$\sigma_H = \beta_o E (M_a - M_o) \qquad [2.5.6]$$

was proposed by Hammerle (1968) by assuming Hooke's law and isotropic propagation of stress within the adsorbing bio-material. If it is further assumed that the deviatoric stress is negligible and the the swelling pressure, P_s, is a mean normal stress, then equations

(2.5.5) and (2.5.6) can be combined to yield:

$$E = \frac{R_g T \ln (P_o/P)}{M V_a \beta_o (M_a - M_o)} \qquad [2.5.7]$$

The well known relationship (Jastrzebski, 1959) between the modulus of elasticity E, and K, the bulk modulus is:

$$K = E/3(1-2\nu) \qquad [2.5.8]$$

Substituting equation (2.5.8) in equation (2.5.7) gives:

$$K = \frac{R_g T \ln (P_o/P)}{3(1-2\nu) M V_a \beta_o (M_a - M_o)} \qquad [2.5.9]$$

Using the definition of K as:

$$K = P_s / \frac{\Delta v}{V_s} \qquad [2.5.10]$$

in equation (2.5.9) and rearranging terms yields:

$$\Delta v = \frac{3(1-2\nu) P_s M V_s V_a \beta_o (M_a - M_o)}{R_g T \ln (P_o/P)} \qquad [2.5.11]$$

Substituting equation (2.5.5) in (2.5.11) yields:

$$\Delta v = 3(1-2\nu) V_s \beta_o (M_a - M_o) \qquad [2.5.12]$$

Equation (2.5.12) gives the volumetric hydro-expansion of an adsorbing bio-material as a function of moisture content. The volume V_s, is defined not as the bulk volume of the sorbent, but instead as the effective volume filled in a finite adsorption step from the relative vapor pressure P_1/P_o to P_2/P_o, where P_1 corresponds to the Wheeler radius R_1 and P_2 to the radius R_2 ($R_2 > R_1$). The total volume adsorptively filled during this step is:

$$v_{12} = \int_{R_1}^{R_2} v_r \, dR \qquad [2.5.13]$$

It is the implication of the capillary condensation theory that:

$$v_{12} = \pi \bar{R} L(\bar{R}) \qquad [2.5.14]$$

where the capillary is assumed to be cylindrical with mean radius $\bar{R} = \frac{1}{2} (R_1 + R_2)$, and length, $L(\bar{R})$.

Making the simplified assumption that for each finite adsorption step the associated hydro-expansion Δv is restricted within the corresponding volume v_{12}, it is justifiable to consider for suitably small steps that:

$$V_s = v_{12} \qquad [2.5.15]$$

Thus, equation (2.5.12) can now be rewritten as:

$$\Delta v = 3(1-2\nu)\ v_{12}\ \beta_o\ (M_a - M_o) \qquad [2.5.16]$$

This volumetric expansion means, in effect, that a pore of mean radius $\bar{R}$ changes its volumetric capacity from v_{12} in adsorption to $v_{12} + \Delta v$ in desorption. The volumetric hydro-expansion, as defined above, depends on the mechanical properties of the product. Since these properties exhibit water-induced changes of physico-chemical origins, their collective contribution to permanent hysteresis is well represented in Δv. For purposes of usage, Δv is converted to its gravimetric equivalent by introducing the appropriate density term, ρ, so that:

$$\Delta M_d = \frac{\Delta v}{\rho} = 3(1-2\nu)\ v_{12}\ \beta_o\ (M_a - M_o)/\rho \qquad [2.5.17]$$

If the bulk modulus, K of a substance is known as a function of moisture content, it can be readily shown that equation (2.5.17) can be written in the form:

$$\Delta M_d = \frac{R_g T \ln(P_o/P)\, v_{12}}{V_a M K \rho} \qquad [2.5.17a]$$

2.5 c. Double Superposition of "Capillary Condensation" - and - "Swelling Fatigue" - Hysteresis

Using the Boltzman superposition principle that the effect of the sum of causes equals the sum of effects of each of the causes, total hysteresis may now be approximated by the following additive procedure:

(i) Compute for each P_a/P_o value, the specific desorbed mass, M_d, using the relationship:

$$M_d = M_a + \Delta M_d \qquad [2.5.18]$$

(ii) Compute, using the Cohan relationship, the desorption relative vapor pressure, P_d/P_o, corresponding to each M_d value, such that:

$$P_d/P_o = (P_a/P_o)^{\omega}$$

where ω is empirically determined for each product.

(iii) Plot M_d obtained in accordance with equation (2.5.18) against the corresponding P_d/P_o value to obtain the desorption isotherm.

This scheme will be tested in chapter four for biological products whose bulk moduli have been empirically determined as a function of moisture content.

III EXPERIMENTAL

The adsorption and desorption equilibrium moisture isotherms of pre-cooked freeze-dehydrated beef were determined gravimetrically by exposing the product to a temperature-controlled free water surface under vacuum. The sorptive weight change was automatically and continuously recorded by a Cahn electrobalance.

3.1 Product Preparation

Low fat commercial grade beef was secured in the form of approximately one-inch cubes. The initial fat content was approximately 9%. The product was cooked in a forced-convection-air oven at 300°F for a period of 30 minutes. The product cubes were placed in aluminum trays and covered during the cooking process.

The cooked beef cubes were subsequently frozen in aluminum foil trays at 20°F prior to freeze-drying. The freeze-drying was done in a commercial freeze-drier at a platen temperature of 105°F with a pressure of less than 1 mm of mercury. Both the platen temperature and pressure were held constant during the freeze-drying operation. Approximately 15 to 20 hours were required to dry the product to less than 2% moisture content on the dry basis (d.b.).

After drying, the product was ground in a Fritz-Patrick mill using a 0.063-inch screen. The resulting powder was immediately placed in sealed bottles which were stored in a desiccator at -20°F. Portions of the product to be used for equilibrium moisture content determinations were equilibrated to the isotherm temperature prior to the run.

The moisture content of the freeze-dried beef following the freeze-drying operation and prior to preserve-storage was determined in a heated-air oven in accordance with a procedure prescribed by Triebold and Aurand (1963). In this method an oven temperature of 80°C was used for a time duration of 16 hours.

3.2 Determination of Equilibrium Moisture Content

3.2 a. The Adsorption System:

Equilibrium moisture content of the pre-cooked freeze-dried beef powder was determined by observing the weight change of the product sample when exposed to a constant water vapor pressure under vacuum. Following the attainment of equilibrium at a specified condition, the vapor pressure was adjusted to a different value and the new equilibrium point determined. In this way it was possible to obtain adsorption and desorption isotherms in one continuous experimental process on the same product sample.

The basic component of the system was a Cahn RG automatic electrobalance. This highly sensitive instrument (effective sensitivity of 0.2% of full scale) was enclosed in a Cahn glass vacuum bottle with hangdown glass tubes for product exposure; see Figures 3.1 and 3.3. The principle of operation of the balance is illustrated schematically in Figure 3.2. The instrument in essence, converts the sorptive weight change of the sample into an electrical signal by the use of a beam position sensing apparatus shown in the diagram. This signal is amplified in a 2-stage servo amplifier and then employed to drive a strip chart recorder. The electrobalance

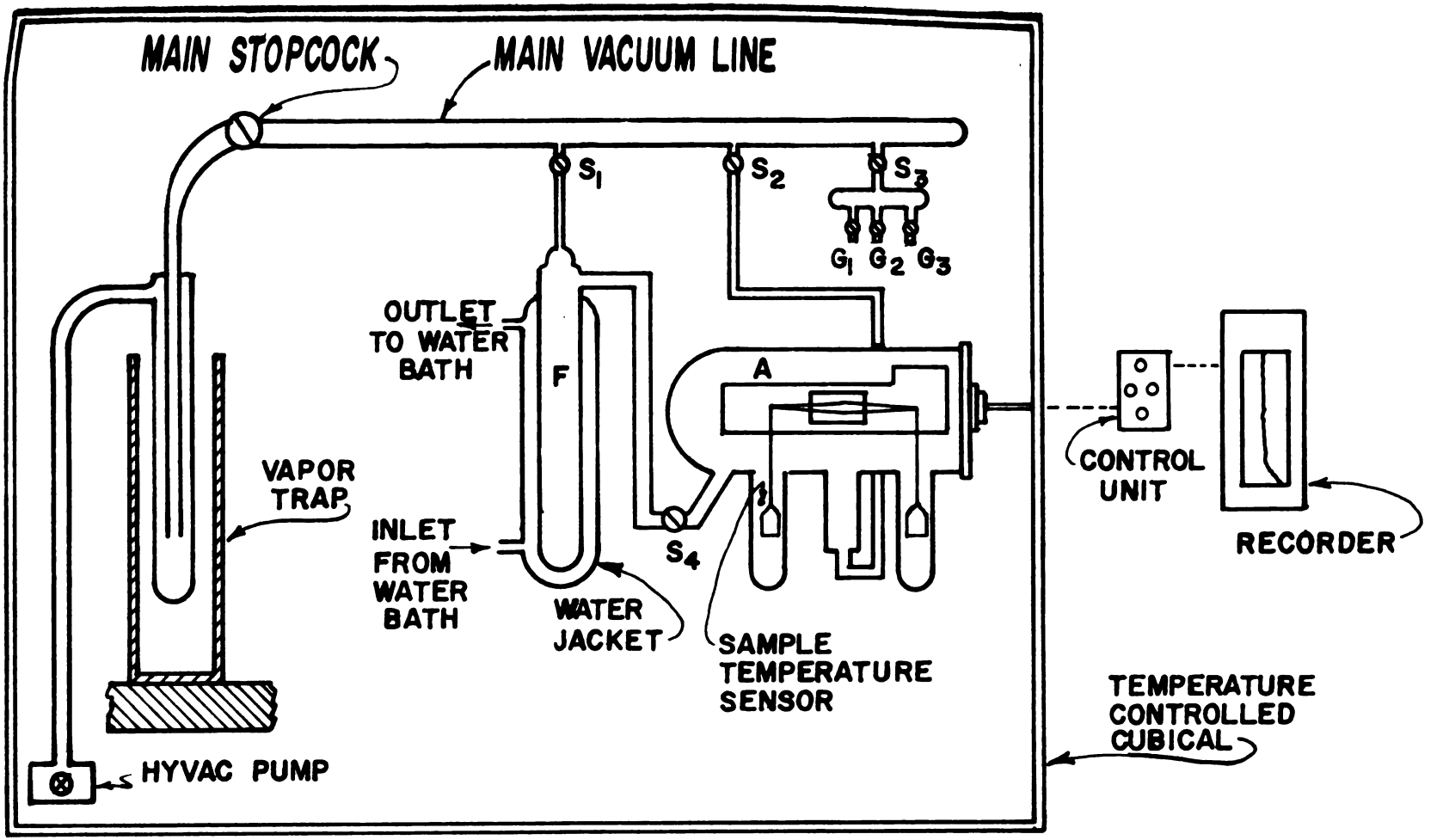

FIGURE 3.1. ADSORPTION APPARATUS

$S_{(1,2,3,4)}$ = HYVAC STOPCOCKS
$G_{(1,2,3)}$ = " " (Taps to Pressure Gages)
F = RESRVOIR
A = CAHN ELECTROBALANCE IN GLASS VACUUM CHAMBER

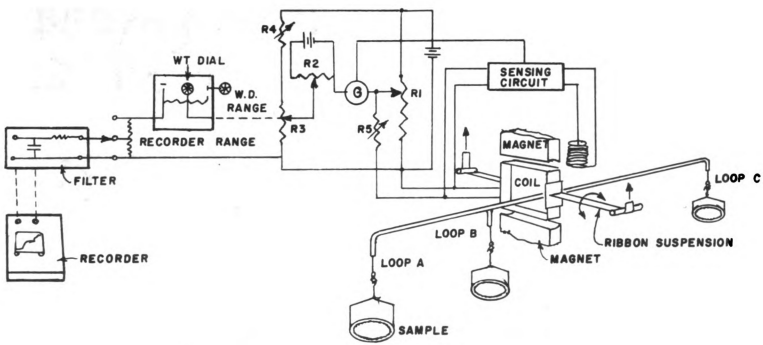

Figure 3.2. Principle of the Cahn-Electrobalance.

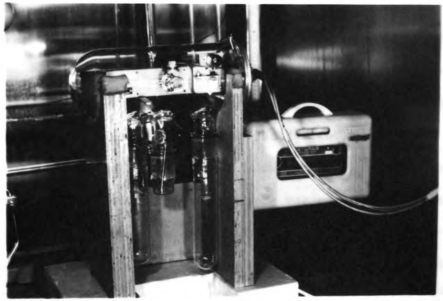

Figure 3.3a Close up view of the Cahn automatic electrobalance in the vacuum line.

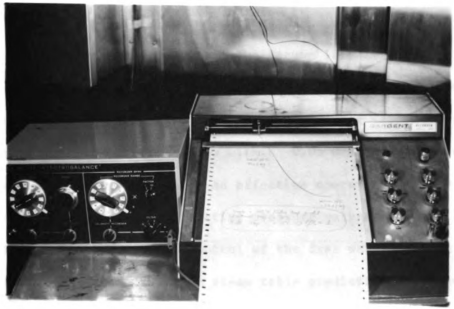

Figure 3.3b Control unit and recorder outside the experimental chamber.

works on the null-balance principle. Thus, an accurate and continuous recording of product weight change can be obtained in the entire sorptive range. The control unit (see Figure 3.1) functions as a standardization and calibration device.

Figure 3.1 is a schematic diagram of the vacuum line. The glass chamber containing the balance was connected at one end to a 13 mm inside diameter main vacuum line, and at the other end to a pure water vapor source. The main line was connected through a vapor trap to a mechanical-diffusion pump combination capable of pumping the system down to a pressure of 1×10^{-3} torr in fifteen minutes. The vapor trap was a glass trap with external reservoir. In its position at the inlet to the pump, the trap served two purposes: first, it acted as a baffle to the molecules of the pumping fluid back-streaming from the diffusion pump, and secondly, it prevented the possible contamination of the pumping fluid by condensable vapors emanating from within the vacuum line itself.

The vapor source consisted of a temperature-controlled distilled water reservoir; F of Figure 3.1. The temperature of the reservoir was controlled to within 0.05°C using a constant temperature laboratory bath with an effective operating range of -30°C to +71°C. Thus, desired relative pressure values were easily attained by precise temperature control of the free water surface in the reservoir. As a check on steam table predictions, pressure measurements were made in the system by means of three over-lapping and independent vacuum guages, namely: (i) a mercury u-tube manometer

for measurements in the pressure range from 5 to 760 torr, (ii) a Virtis McLeod guage for the range 0.5 to 10 torr, and (iii) a standard type McLeod guage for the pressure range from 1×10^{-3} to 0.5 torr.

All connections in the vacuum line incorporated hyvac stopcocks in such a manner that the isolation of any desired component of the system was easily achieved. The entire apparatus, with the exception of the control unit and the recorder, was enclosed in a 5 ft. x 4 ft. x 9 ft. controlled temperature cubical. Figure 3.3(a) is a close-up view of the balance in the vacuum line, and Figure 3.3(b) shows the control unit and recorder outside the experimental chamber. A continuous record of temperature was monitored by copper-constantan thermocouples from (a) the immediate vacuum around the test sample, (b) several locations in the cubical, and (c) the vapor-regulating bath.

3.2 b. Procedure

For the adsorption test, about 100 milligrams of the sample were placed in the aluminum sample container, and the entire system evacuated to 1×10^{-3} torr in order to establish the 0% relative humidity reference with which the sample was allowed to attain initial equilibrium. After the sample had attained the isotherm (cubical) temperature, the stopcock S_4 of Figure 3.1 was opened to expose the sample to a pre-conditioned free water surface in the reservoir, F. The adsorption isotherm was established by adjusting the vapor pressure of the free water surface to pregressively higher

values corresponding to higher relative humidities and allowing time for equilibration at each level. A minimum of ten experimental moisture equilibrium points were employed to establish an isotherm. Following the establishment of equilibrium at 100% relative humidity the vapor pressure was progressively reduced - step by step - to determine the desorption isotherm of the same sample.

IV RESULTS AND DISCUSSION

4.1. The Determination of Pore Structure from Water Sorption Isotherms - Verification of a Pore-Size Distribution Function of the Power Law Type for Bio-materials

The crux of the isotherm equation developed in chapter II, is the power law type distribution of pore radii which was postulated. It is therefore of central importance to the considerations to be undertaken in the present chapter, that the basis of this hypothesis be explored and verified in detail.

The determination of pore-size distributions of catalysts from sorption isotherms is a well-established technique (Lester, 1967). In this technique (See for example Gregg and Sing, 1967, pp. 160-172), the Kelvin equation is applied directly to the desorption branch of the isotherm; the results so obtained give a qualitative picture of pore structure. Of the various refinements which have been proposed (Carman, 1951; Barrett, Joyner, and Halender, 1951; Harvey, 1943; Dollimore and Heal, 1964; Viswanathan and Sastri, 1967), the approach of Cranston and and Inkley (1957) is of particular interest because: (a) it is more exact than any of the other methods, (b) it may be applied either to the adsorption or desorption branch of the isotherm and (c) the total specific surface area estimated by this method can be compared with the corresponding B-E-T values and the differences used as an evaluation of the physical assumptions regarding the pore geometry.

The original scheme of Cranston and Inkley is generalized to handle pores of shape other than a cylindrical geometry as follows:

Consider a finite adsorption step from relative vapor pressure P_i/P_o to P_{i+1}/P_o with condensation occuring in pores with radius varying between R_i and R_{i+1} ($P_{i+1} > P_i$, $R_{i+1} > R_i$). If the step in relative vapor pressure is kept small, the above described pores have an average radius of $\overline{R_i} = \frac{R_i + R_{i+1}}{2}$. At the same time, smaller pores are already filled, while in larger pores the thickness of adsorbed layers on their walls increases from t_i to t_{i+1}. The total volume of water adsorbed in the step, i = 1 is shown in appendix B to be:

$$v_{12} = \int_{R_1}^{R_2} v_R \, dR$$

$$= \int_{R_1}^{R_2} \frac{(R-t_1)^{\varkappa}}{R^{\varkappa}} \cdot f_1 \cdot V_R \, dR$$

$$+ (t_2-t_1) \int_{R_2}^{\infty} \frac{R-t_{12}}{R} \cdot f_2 \cdot \frac{V_R}{R} \, dR \qquad [4.1.1]$$

where $t_{12} = (t_1 + t_2)/2$

V_R = total volume of pores in the range dR

$\varkappa$, f_1 and f_2 are shape factors such that:

$\varkappa = 2$, $f_1 = 1$, $f_2 = 2$ for a cylindrical geometry

$\varkappa = 3$, $f_1 = 3/4$, $f_2 = 3$ for a spheroidal geometry

and the quantity $(\frac{R-t_1}{R})$ is a correction factor for the curvature of the meniscus.

Assuming that V_R is suitably constant over the range R_1 to R_2 and letting this value of V_R be specified as V_{12}, equation (4.1.1) becomes:

$$v_{12} = \frac{V_{12}}{R_2-R_1} \cdot f_1 \cdot \int_{R_1}^{R_2} \frac{(R-t_1)^{\kappa}}{R^{\kappa}} \cdot dR$$

$$+ (t_2 - t_1) \cdot f_2 \cdot \int_{R_2}^{\infty} \frac{V_R(2R-t_1-t_2)}{2R^2} \, dR \qquad [4.1.2]$$

Rearranging equation (4.1.2) gives:

$$V_{12} = r_{12}(v_{12}-k_{12} \int_{R_2}^{\infty} \frac{R-t_{12}}{2R^2} \cdot V_R \cdot dR) \qquad [4.1.3]$$

where $r_{12} = (R_2-R_1)/f_1 \cdot \int_{R_1}^{R_2} [(R-t_1)^{\kappa}/R^{\kappa}] \, dR$

$$\simeq \frac{1/f_1}{[(\bar{R}-t_1)/\bar{R}]^{\kappa}} \qquad [4.1.4]$$

for a suitably small difference, $dR = (R_2-R_1)$

and $k_{12} = 2f_2(t_2-t_1)$ [4.1.5]

For computational purposes, the integral term of equation (4.1.3) is replaced by a summation term of all increaments of radii from R_2 to the largest possible pore radius, so that:

$$V_{12} = r_{12} \{ v_{12} - k_{12} \sum_{R_2}^{R_{max}} (\frac{R-t_{12}}{2R^2} \cdot V_R \cdot \Delta R) \} \qquad [4.1.6]$$

Pore-size distribution is defined in terms of:

(a) <u>Pore-Length</u> L(R) in the case of a cylindrical geometry where:

$$L(R) = V_{12}/\pi \bar{R}^2 \qquad [4.1.7]$$

and

$$\varphi_2(R) = \frac{dL(R)}{dR} \qquad [4.1.8]$$

Also, because $V_{12} = \pi \bar{R}^2 L(R)$

and $S_{12} = 2 \pi \bar{R} L(R)$

therefore

$$S_{12} = 2 V_{12}/\bar{R} \qquad [4.1.9]$$

or (b) Pore-Number N(R) for spheroidal "ink bottles" where:

$$N(R) = V_{12}/\tfrac{4}{3} \pi \bar{R}^3 \qquad [4.1.10]$$

$$\varphi_2(R) = dN(R)/dR \qquad [4.1.11]$$

and $$S_{12} = 3 V_{12}/\bar{R} \qquad [4.1.12]$$

Cummulative specific surface areas computed using equations (4.1.9) and (4.1.12) can be compared with corresponding B-E-T surfaces - thus, affording a convenient criterion of geometrical selectivity.

The complete calculation is performed on a CDC 3600 computer using a modified Cranston and Inkley (1957) method. In this scheme only 12 to 15 experimental isotherm points are read in as shown in the illustrative input tabulation of Table 4.1.1. The 40 or more points usually needed are synthesized by the use of the Aitken-Neville modified Lagrange iterated interpolation scheme (this scheme is discussed by Moursund and Duris, 1967, p. 135). After this point, the calculation of pore-size distributions follows closely the method of Cranston and Inkley (1957). The essential differences being that the "cylindrical" formulations of Cranston and Inkley are replaced by their generalized counterparts as developed earlier in this section. This generalization makes it possible to assume any desired geometrical model for a pore. Two geometrical models - cylindrical pores and spheroidal ink-bottles - are investigated for comparative reasons.

Table 4.1.1. Illustrative input data for beef powder freeze-dried at 105°F platen temperature.

Isotherm temperature = 10°C

P/P_o	M_a = mass adsorbed (gm/gm)	v_{H_2O} adsorbed (cc/gm)	Pore Radius (R) for P/P_o (A°)
0.000		0.000	
0.100	.070	0.0515	6.742
0.200	.095	0.0699	9.635
0.300	.110	0.0825	12.463
0.400	.122	0.0927	15.617
0.500	.135	0.1026	19.680
0.600	.155	0.1178	25.624
0.700	.191	0.1546	34.563
0.800	.260	0.2234	52.743
0.900	.380	0.3375	106.054
0.950	.450	0.4240	214.982
.963			300.000
1.000	.505	0.505	

It turns out that in all cases investigated (see Tables 4.1.2(a) and 4.1.2(b)), the cummulative specific surface areas calculated on the model of interconnected spheroidal ink-bottle geometry compares better with the B-E-T surfaces, than the surfaces bases on the cylindrical pore model. It is concluded on the basis of this finding, that the pores of biological materials are best modeled for theoretical treatments as interconnected spheroidal ink-bottles.

Figures 4.1 through 4.4 are log-log plots of pore-size distributions of several biological materials calculated on the basis of the spheroidal ink-bottle pore model. The remarkable linearity of these plots indicates that a strong tendency exists in biomaterials toward a power law type distribution function for pore-size. Thus, the power law equation (2.3.16) when expressed in its logarithmic form:

$$\ln \varphi_2 = \ln K_1 + \gamma \ln (R) \qquad [4.1.13]$$

yields an empirical straight line with a slope γ, and an intercept of magnitude $\ln K_1$.

In Table 4.1.3, the parameters γ and K_1, as determined from the pore-size distribution plots, are summarized. These values were obtained from least square straight line approximations of the data plotted in figures 4.1 through 4.4.

In spite of the elaborate refinements of the Cranston and Inkley method, there exists (as with the other methods) no generally accepted accuracy criteria for evaluating pore-size distributions so

Table 4.1.2(a) Pore-size distribution for beef powder freeze-dried at 105°F platen temperature. Calculated by a modified Cranston and Inkley scheme, and based on 10°C isotherm. A cylindrical pore geometry is assumed.

1 P/P_o (interpolated)	2 Average pore radius (A°)	3 Volume adsorbed for interpolated P/P_o v(cc/gm)	4 $v_{12} = v_i - v_{i+1}$ (cc/gm)	5 V_{12} based on EQN.(4.1.6) (cc/gm)	6 L(R) based on EQN.(4.1.7) (A°)	* 7 $\varphi_2(R) = \frac{dL(R)}{dR}$	8 S_{12} based on EQN.(4.1.9) (m^2)	9 ΣS_{12} = Cumm. Surface (m^2)
.963		.433						
	295		.003	.0034	1.230	0.000	.2278	.2278
.962		.430						
	285		.005	.0056	2.198	9.7×10^{-2}	.3934	.6212
.960		.425						
	275		.003	.0034	1.414	7.8×10^{-2}	.2443	.8655
.959		.422						
	265		.004	.0045	2.035	6.2×10^{-2}	.3387	1.204
.957		.408						
	255		.001	.0011	0.537	1.5×10^{-1}	.0860	1.290
.956		.407						
	245		.002	.0022	1.184	6.5×10^{-2}	.1821	1.472
.954		.405						
	235		.004	.0045	2.599	1.4×10^{-1}	.3836	1.856
.952		.401						
	225		.002	.0022	1.400	1.2×10^{-2}	.1978	2.054
.950		.399						
	215		.002	.0022	1.534	3.6×10^{-1}	.2071	2.261
.947		.397						
	205		.006	.0068	5.173	1.5×10^{-1}	.6660	2.927
.945		.391						
	195		.007	.0080	6.687	3.3×10^{-2}	.8189	3.746
.942		.384						
	185		.006	.0068	6.355	2.0×10^{-1}	.7383	4.484
.939		.378						
	175		.007	.0080	8.318	1.7×10^{-1}	.9141	5.398
.935		.377						
	165		.005	.0057	6.620	8.7×10^{-1}	.6859	6.084

Table 4.1.2(a) (Cont'd) -

1	2	3	4	5	6	7	8	9
.927		.372						
	155		.010	.0120	15.320	$8.6x10^{-1}$	1.491	7.575
.922		.362						
	145		.004	.0044	6.729	1.774	..6128	8.188
.916		.358						
	135		.012	.0140	24.470	1.310	2.0740	10.260
.910		.346						
	125		.005	.0056	11.370	3.135	.8923	11.150
.902		.341						
	115		.015	.0177	42.720	1.273	3.085	14.240
.893		.326						
	105		.009	.0104	29.980	4.173	1.977	16.220
.881		.317						
	95		.017	.0203	71.710	1.796	4.278	20.49
.868		.300						
	85		.017	.0203	89.670	4.748	4.786	25.28
.850		.283						
	75		.020	.0242	137.20	4.562	6.460	31.74
.828		.263						
	65		.020	.0243	182.80	2.2x10	7.461	39.20
.797		.240						
	55		.030	.0379	398.70	7.573	13.770	52.97
.777		.210						
	47.5		.019	.0242	341.90	3.150	10.20	63.17
.753		.191						
	42.5		.015	.0185	326.20	4.5x10	8.705	71.88
.723		.176						
	37.5		.019	.0243	549.90	1.7x10	12.95	84.83
.685		.157						
	32.5		.017	.0211	637.30	8.9x10	13.01	97.84
.635		.140						

Table 4.1.2(a) (Cont'd) -

1	2	3	4	5	6	7	8	9
	27.5		.020	.0257	1082.0	5.9x10	18.69	116.5
.567		.130						
	22.5		.018	.0219	1379.0	$2.0x10^2$	19.48	136.0
.532		.102						
	19.0		.007	.0780	688.10	3.3x10	8.210	144.2
.492		.095						
	17.0		.006	.0564	621.90	6.1x10	6.640	150.9
.444		.089						
	15.0		.006	.0526	744.00	$7.3x10^2$	7.008	157.9
.338		.083						
	13.0		.002	.0038				
.321		.081						
	11.0		.006	.0045				
.242		.075						
	9.0		.008	.0087				
.197		.067						
	7.5		.004	.0033				
.151		.063						
	6.5		.009	.0310				
.103		.054						
	5.5		.013	.0340				
.023		.041						
	4.0		.033	.1410				
		.008						

$S_{BET} = 322(m^2)$ (based on mono-layer capacity at 10°C)

$$\frac{\Sigma S_{12}}{S_{BET}} = \frac{157.9}{322} = 0.54$$

* differentiation was done numerically by a central difference scheme.

Table 4.1.2(b) Pre-size distribution for pre-cooked beef powder freeze-dried at 105°F platen temperature. Calculation by a modified Cranston and Inkley scheme, and based on 10°C isotherm. A spheroidal Ink-bottle pore model is assumed.

1 P/P_o	2 Average pore radius (A°)	3 Volume adsorbed for interpolated P/P_o, v (cc/gm)	4 v_{12} $v_i - v_{i+1}$ (cc/gm)	5 V_{12} based on EQN.(4.1.6) (cc/gm)	6 N(R) based on EQN. (4.1.10)	*7 $\omega_2(R) = \frac{dN(R)}{dR}$	8 S_{12} based on EQN. (4.1.12) (m^2)	9 ΣS_{12} = cumm. surface (m^2)
.963		.433						
	295		.003	.0047	4.4×10^{-4}	0.000	.4821	.4821
.962		.430						
	285		.005	.0079	8.2×10^{-11}	3.8×10^{-12}	.8327	1.315
.960		.425						
	275		.003	.0047	5.4×10^{-11}	2.7×10^{-12}	.5153	1.830
.959		.422						
	265		.004	.0063	8.1×10^{-11}	2.7×10^{-12}	.7152	2.545
.957		.408						
	255		.001	.0015	2.2×10^{-11}	5.9×10^{-12}	.1765	2.722
.956		.407						
	245		.002	.0031	5.1×10^{-11}	2.9×10^{-12}	.3806	3.102
.954		.405						
	235		.004	.0063	1.2×10^{-10}	6.6×10^{-12}	.8094	3.912
.952		.401						
	225		.002	.0031	6.5×10^{-11}	5.2×10^{-12}	.4107	4.322
.950		.399						
	215		.002	.0031	7.4×10^{-11}	9.3×10^{-13}	.4289	4.751
.947		.397						
	205		.006	.0096	2.7×10^{-10}	1.9×10^{-11}	1.411	6.163
.945		.391						
	195		.007	.0113	3.6×10^{-10}	9.6×10^{-12}	1.736	7.899
.942		.384						
	185		.006	.0096	3.6×10^{-10}	1.5×10^{-10}	1.557	9.455
.939		.378						

Table 4.1.2(b) (Cont'd) -

1	2	3	4	5	6	7	8	9
	175		.007	.0113	5.0×10^{-10}	1.0×10^{-10}	1.930	11.39
.935		.377						
	165		.005	.0078	4.2×10^{-10}	3.1×10^{-10}	1.427	12.81
.927		.372						
	155		.010	.0164	1.1×10^{-9}	1.0×10^{-10}	3.165	15.98
.922		.362						
	145		.004	.0060	4.7×10^{-10}	5.1×10^{-10}	1.234	17.21
.916		.358						
	135		.012	.0199	1.9×10^{-9}	3.1×10^{-10}	4.413	21.62
.910		.346						
	125		.005	.0074	9.1×10^{-10}	8.2×10^{-10}	1.784	23.41
.902		.341						
	115		.015	.0253	3.9×10^{-9}	9.8×10^{-10}	6.589	30.00
.893		.326						
	105		.009	.0142	2.9×10^{-9}	4.8×10^{-9}	4.061	34.06
.881		.317						
	95		.017	.0288	8.0×10^{-9}	1.3×10^{-10}	9.103	43.16
.868		.300						
	85		.017	.0286	1.1×10^{-8}	1.1×10^{-10}	1.008	53.24
.850		.283						
	75		.020	.0341	1.9×10^{-8}	1.5×10^{-8}	1.362	66.86
.828		.263						
	65		.020	.0335	2.9×10^{-8}	6.8×10^{-9}	1.545	82.31
.797		.240						
	55		.030	.0538	7.7×10^{-8}	3.7×10^{-8}	2.935	111.7
.777		.210						
	47.5		.019	.0342	7.6×10^{-8}	1.9×10^{-8}	2.161	133.3
.753		.191						
	42.5		.015	.0243	7.6×10^{-8}	7.6×10^{-8}	1.718	150.4
.723		.176						
	37.5		.019	.0328	1.5×10^{-7}	7.9×10^{-8}	2.626	176.7
.685		.157						
	32.5		.017	.0263	1.8×10^{-7}	5.1×10^{-8}	2.424	201.0
.635		.140						
	27.5		.020	.0321	3.7×10^{-7}	1.0×10^{-6}	3.500	236.0

Table 4.1.2(b) (Cont'd) -

1	2	3	4	5	6	7	8	9
.567		.120						
	22.5		.018	.0222	4.7×10^{-7}	8.5×10^{-7}	2.961	265.6
.532		.102						
	19.0		.007	.0576	2.0×10^{-7}	1.0×10^{-6}	9.091	274.7
.492		.095						
	17.0		.006	.0009	4.3×10^{-8}	1.5×10^{-6}	1.550	276.2
.444		.089						
	15.0		.006					
.388		.083						
	13.0		.002					
.321		.081						
	11.0		.006					
.242		.075						
	9.0		.008					
.197		.067						
	7.5		.004					
.151		.063						
	6.5		.009					
.103		.054						
	5.5		.013					
.023		.041						
	4.0		.033					
		.008						

$S_{BET} = 322\ (m^2)$ (based on mono-layer capacity at 10°C)

$$\frac{\Sigma S}{S_{BET}} = \frac{276.2}{322} = 0.86$$

* Differentiation was done numerically by a central difference scheme.

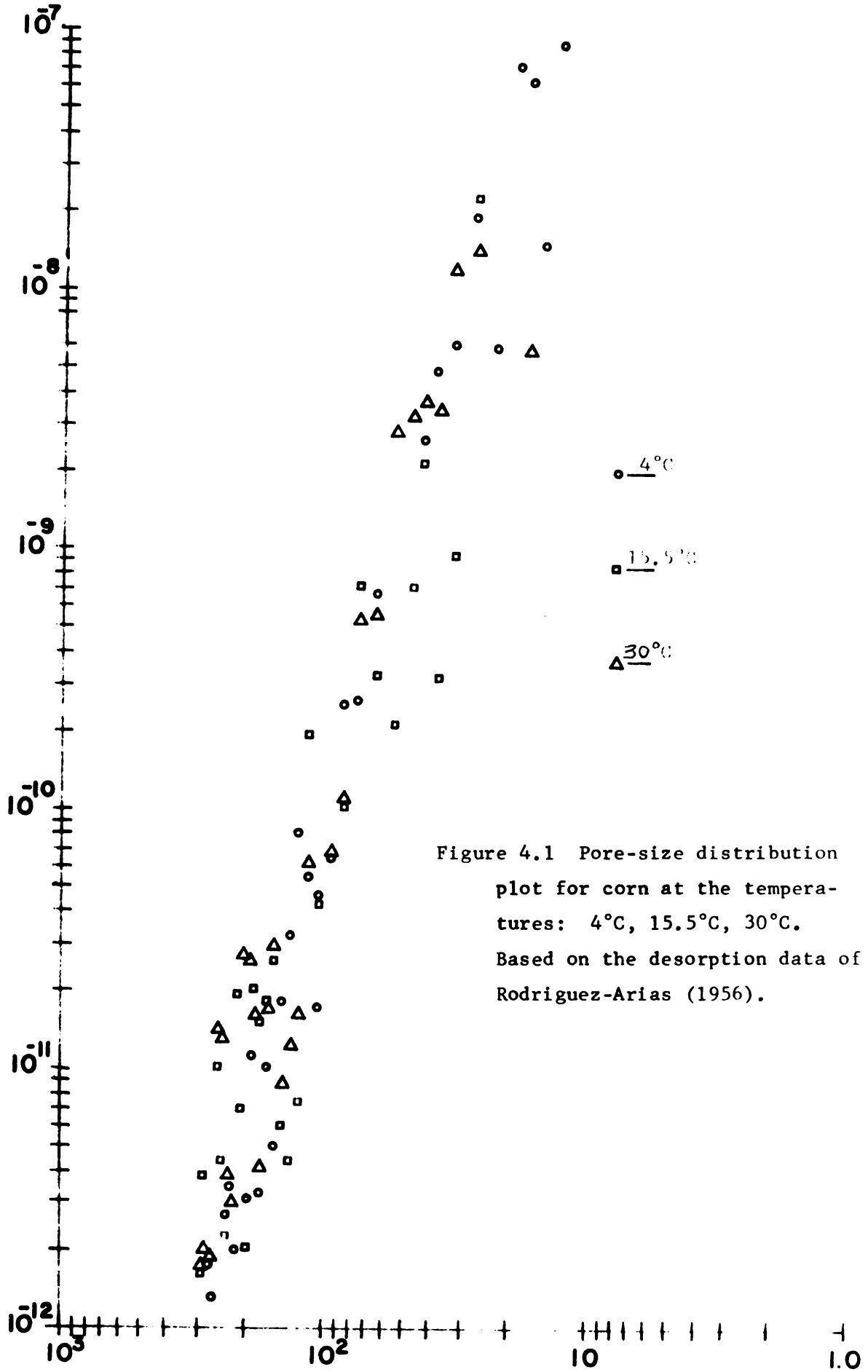

Figure 4.1 Pore-size distribution plot for corn at the temperatures: 4°C, 15.5°C, 30°C. Based on the desorption data of Rodriguez-Arias (1956).

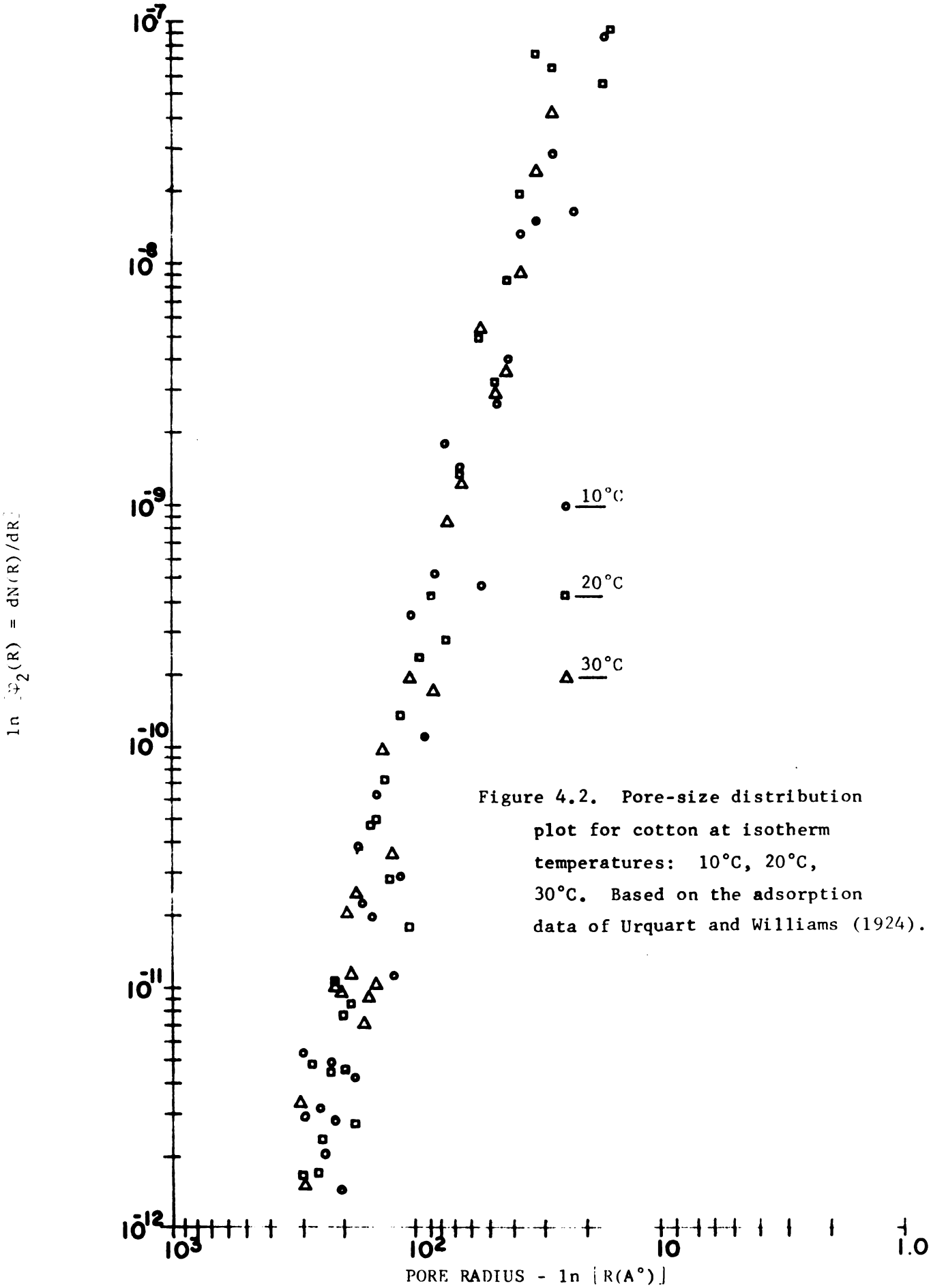

Figure 4.2. Pore-size distribution plot for cotton at isotherm temperatures: 10°C, 20°C, 30°C. Based on the adsorption data of Urquart and Williams (1924).

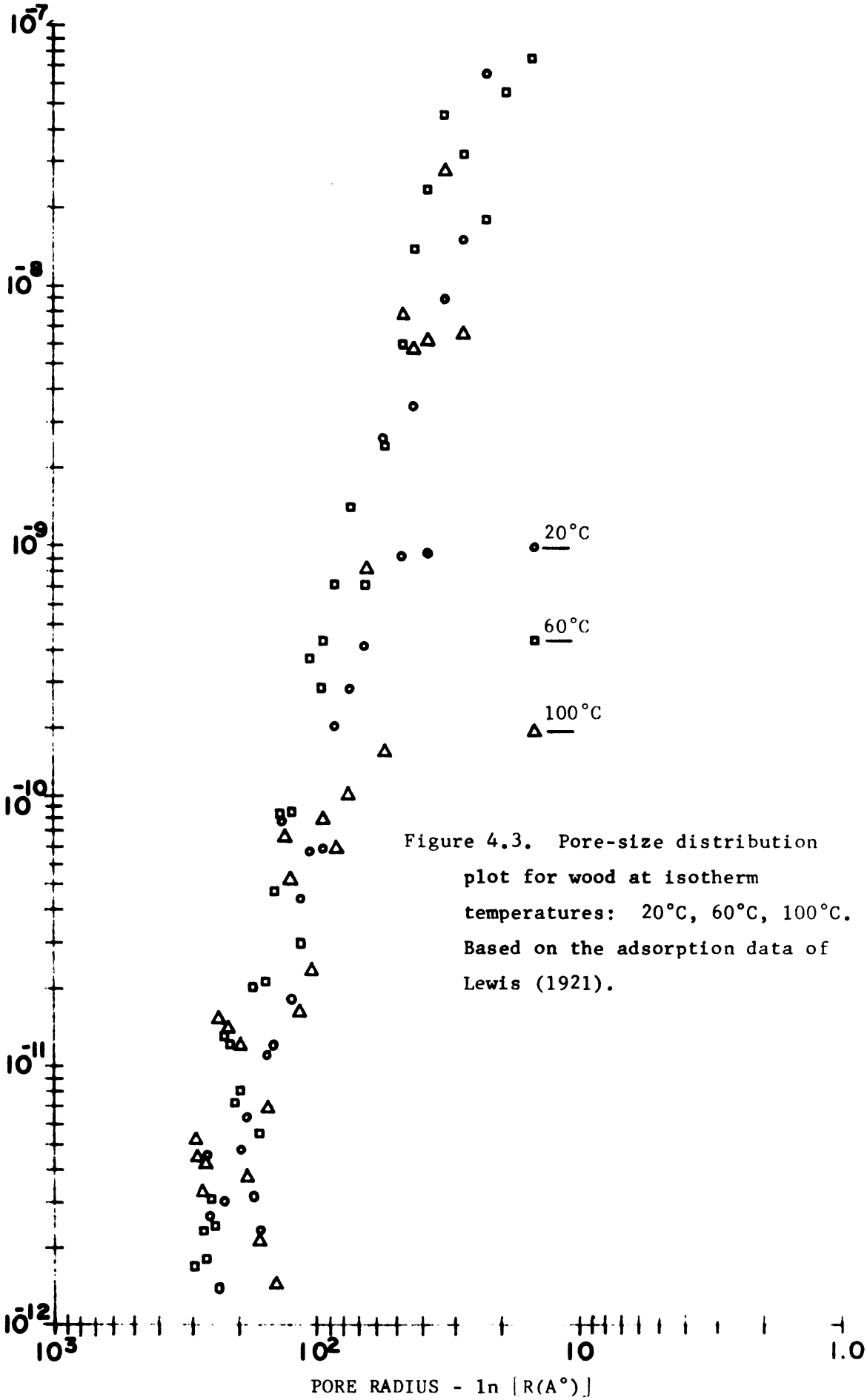

Figure 4.3. Pore-size distribution plot for wood at isotherm temperatures: 20°C, 60°C, 100°C. Based on the adsorption data of Lewis (1921).

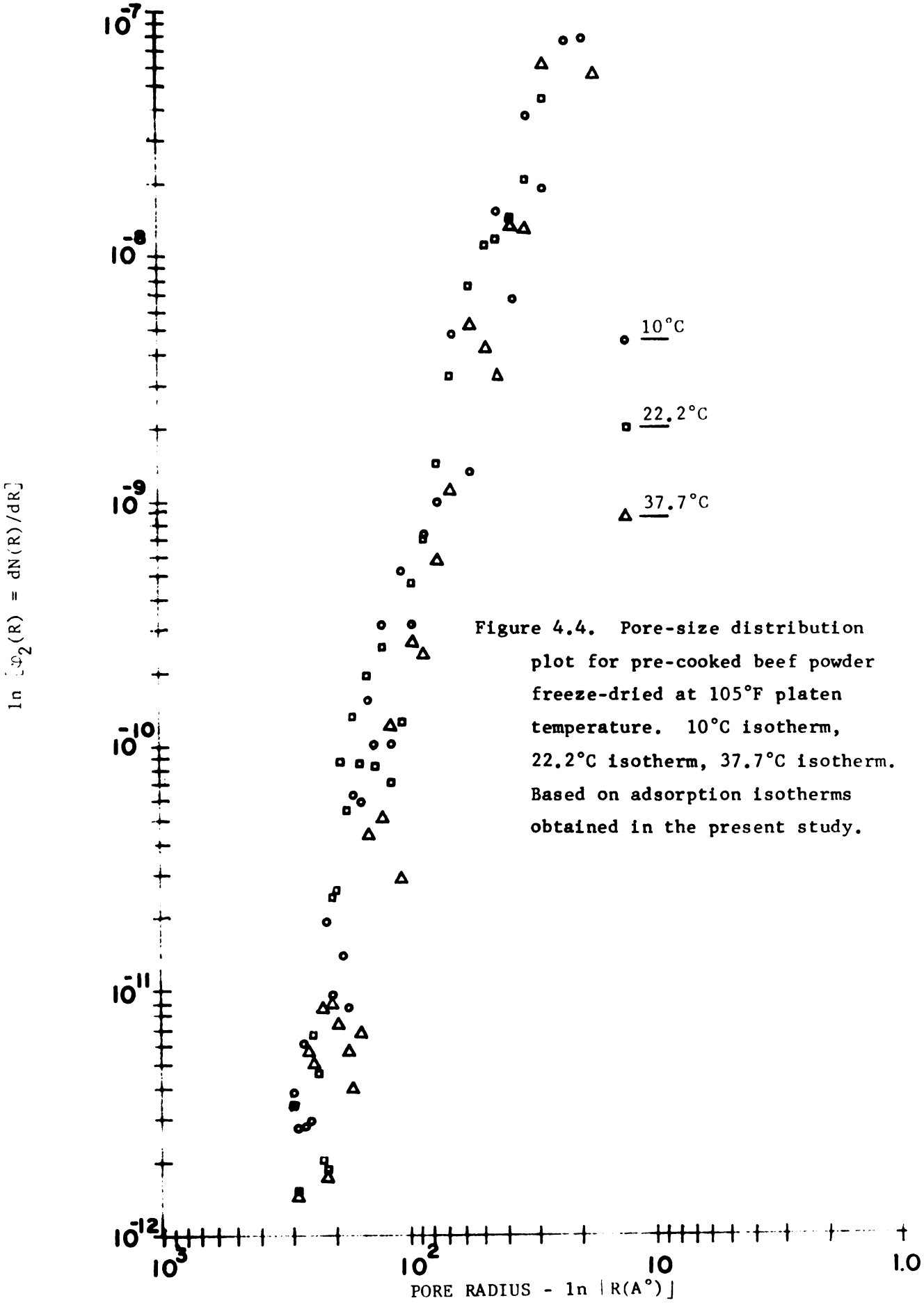

Figure 4.4. Pore-size distribution plot for pre-cooked beef powder freeze-dried at 105°F platen temperature. 10°C isotherm, 22.2°C isotherm, 37.7°C isotherm. Based on adsorption isotherms obtained in the present study.

Table 4.1.3 Summary of the characteristic parameters of pore structure as determined from pore-size distribution plots.

PRODUCT	Temp °C	γ from pore-size distribution plots	K_1 from pore-size distribution plots	n = 4 + γ EQN. (2.3.20)	ξ = 4/3 πK_1 EQN. (2.3.19)
	4.0	-4.636	0.335	-0.636	1.404
CORN	15.5	-5.015	2.237	-1.015	5.182
	30.0	-5.059	1.853	-1.059	7.763
	10.0	-4.394	0.049	-0.394	0.207
COTTON	20.0	-4.560	0.214	-0.560	0.897
	30.0	-4.603	0.238	-0.603	0.995
	20.0	-4.416	0.0934	-0.416	0.391
WOOD	60.0	-4.555	0.2053	-0.555	0.860
	100.00	-5.202	4.448	-1.202	18.634
PRE-COOKED FREEZE-DRIED BEEF POWDER	10.0	-4.344	0.119	-0.344	0.497
	22.2	-4.599	0.487	-0.599	2.039
	37.7	-4.876	0.756	-0.876	3.167

calculated (Everett, 1958). It seems appropriate that until such criteria are established so that the magnitude of the various quantities involved can be ascertained in absolute terms, pore-size distribution plots of the type represented in figures 4.1 through 4.4 should be considered as having qualitative but not absolute significance. Thus, the pore-size distribution parameters - γ and K_1 - of Table 4.1.3, cannot be expected to be quantitatively accurate. Nevertheless, the exponential nature of the pore-size distribution function, $\varphi_2(R)$, is conclusively established from a qualitative standpoint, because of the well defined linear tendency of the log-log plots. In addition, the following observations regarding the parameters γ and K_1 are qualitatively discernible from Table 4.1.3. :

1. As characteristic parameters for the pore structure of the sorbent, γ and K_1 are unique for each sorbent system.
2. Both γ and K_1 are clearly temperature sensitive. This implies that the pore structure of the sorbent changes with isotherm temperature. While it is as yet premature to determine from a priori considerations, the exact nature of this change, it appears reasonable, in view of the effects of temperature on swelling forces, that the pores could undergo a certain amount of deformation with changing isotherm temperature. Although a purely temperature-induced expansion or contraction cannot reasonably be expected to alter the pore structure appreciably,

Hammerle (1968) did show that the so-called hydro-expansion in bio-materials is considerably temperature sensitive.

In closure, it has been shown in this section that (a) the pores of biological materials are best modeled as inter-connected spheroidal ink-bottles; (b) the pore-size distributions of these products are well described by an analytical function of the power law type; (c) while the present state of the art does not allow for precise quantification of the pore-size distribution parameters, useful insights have been gained into their qualitative characters. These results have important application in the theoretical consideration of moisture transport in biological materials.

4.2 Experimental Results

Adsorption and desorption data for pre-cooked freeze-dried beef powder obtained in this investigation are summarized in Tables 4.2.1 and 4.2.2, respectively. The specific adsorbed mass is recorded on the dry basis (d.b.). Each value represents an average of three independent tests. The isotherm data are reproduced in Figures 4.5 and 4.6.

The plots show the traditional sigmoid shape expected of porous water-binding biological materials. They are temperature dependent, showing decreasing adsorption with rising isotherm temperature. A distinctively pronounced hysteretic behavior is apparent in figures 4.7(a) and (b). While the desorption curves show a

	← ADSORPTION in (d.b.) →		
P/P_o	10°C	22.2°C	37.7°C
.05	.047	.03	.0136
.10	.070	.045	.0209
.20	.095	.062	.0309
.30	.110	.075	.0391
.40	.122	.087	.0500
.50	.135	.100	.0591
.60	.155	.125	.0791
.70	.191	.163	.102
.80	.260	.230	.141
.90	.380	.33	.200
.95	.450	.405	.241
.98	.049	.465	.27
1.00	.505	.490	.286

Table 4.2.1. Equilibrium moisture content of pre-cooked freeze-dried ground beef.

platen temperature = 105°F

sample size = 100-150 milligrams

Fat content = 9.8%

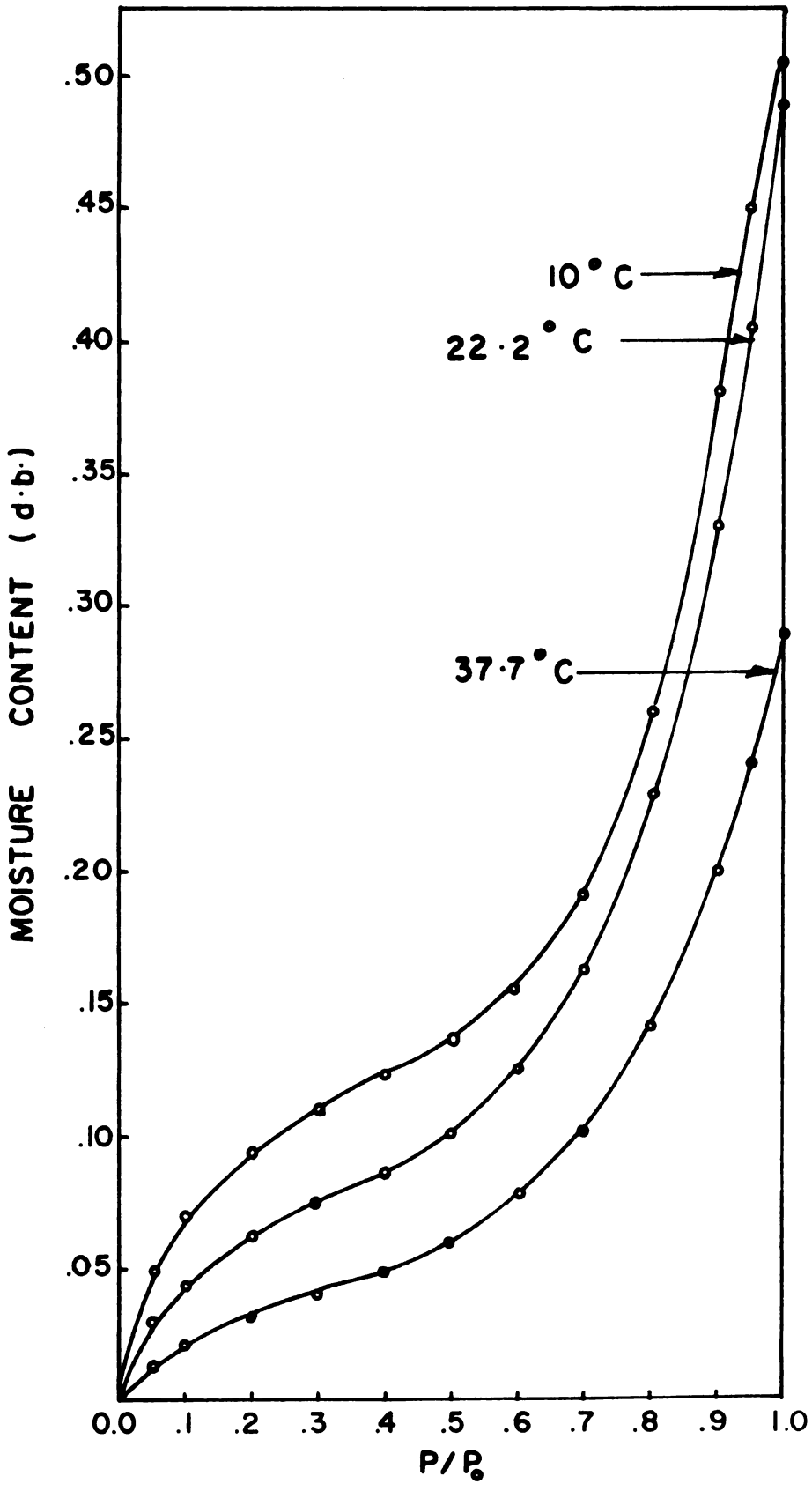

Figure 4.5. Adsorption isotherms for pre-cooked beef powder freeze-dried at 105°F platen temperature. (10°C - 37.7°C)

	← DESORPTION →		
		in (d.b.)	
P/P_o	10°C	22.2°C	37.7°C
0.05	.065	.04	.0427
0.10	.088	.057	.0500
0.20	.110	.075	.0546
0.30	.123	.085	.0682
0.40	.137	.097	.0846
0.50	.156	.113	.109
0.60	.191	.143	.138
0.70	.260	.200	.175
0.80	.425	.280	.213
0.90	.487	.465	.254
0.95	.498	.4755	.273
1.00	.505	.490	.286

Table 4.2.2. Equilibrium moisture content of pre-cooked freeze-dried ground beef.

platen temperature = 105°F

sample size = 100-150 milligrams

fat content = 9.8%

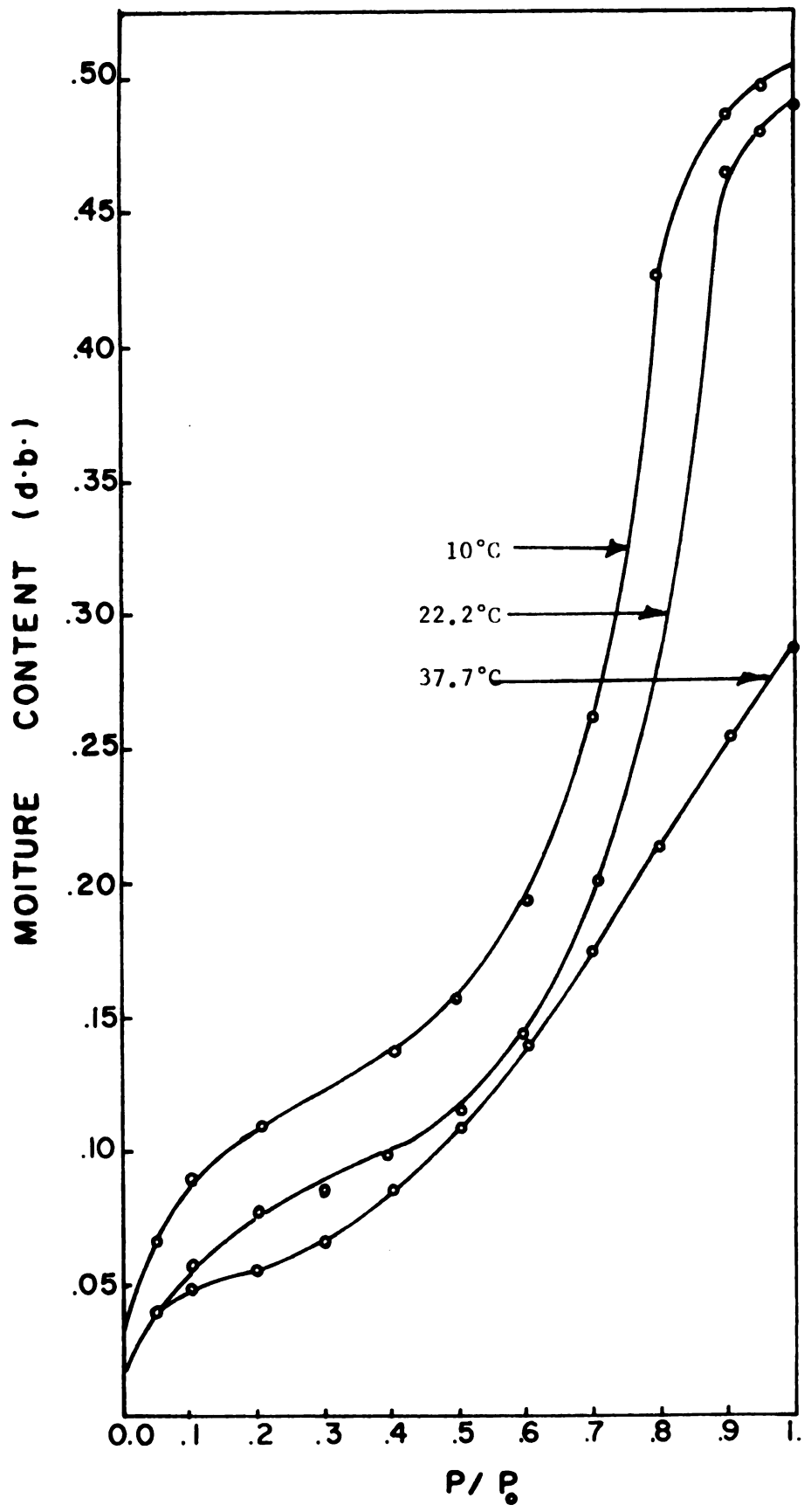

Figure 4.6. Desorption isotherms for pre-cooked beef powder freeze-dried at 105°F platen temperature. (10°C - 37.7°C)

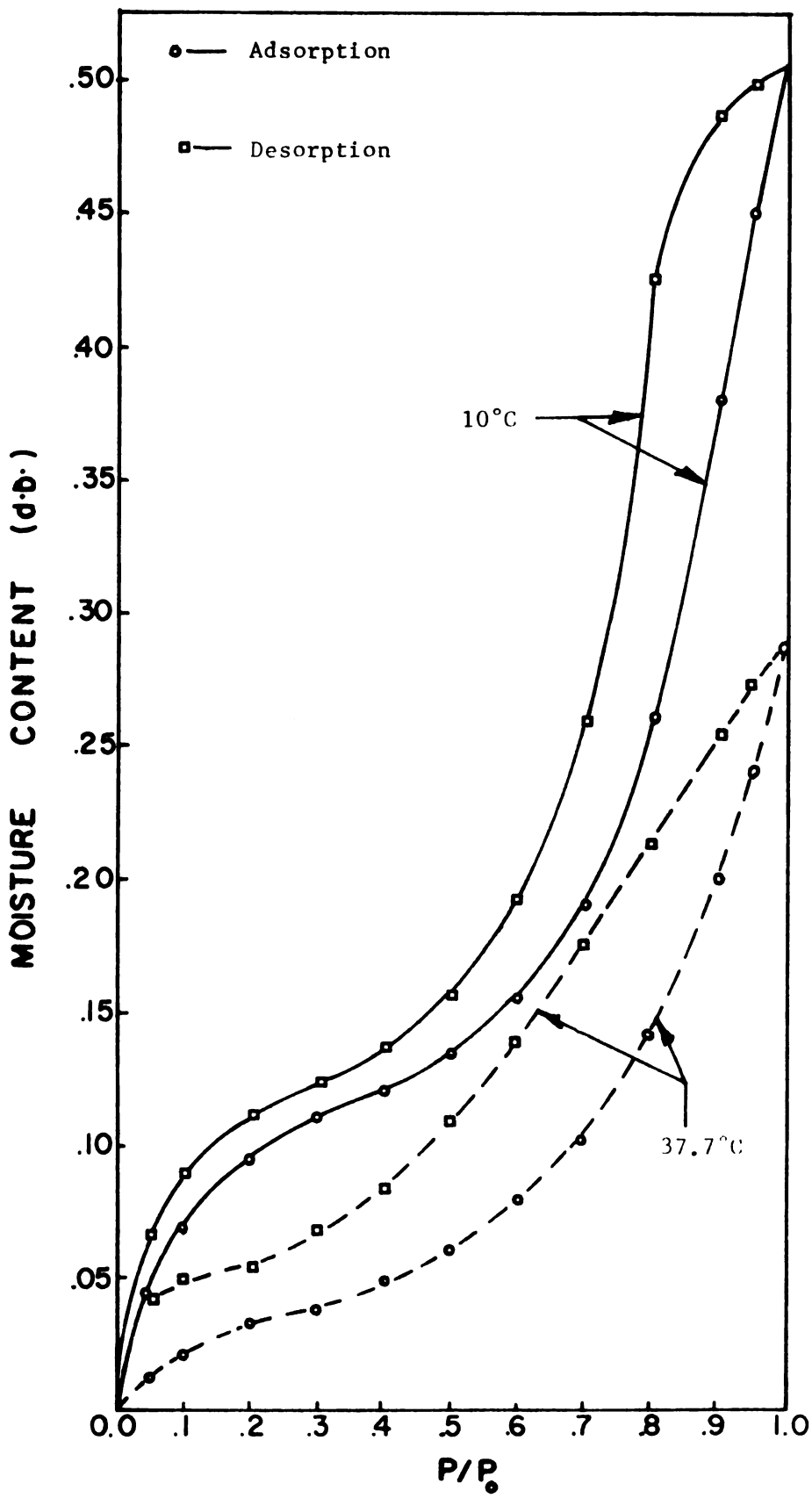

Figure 4.7(a). Plot showing sorption hysteresis in pre-cooked freeze-dried beef powder.

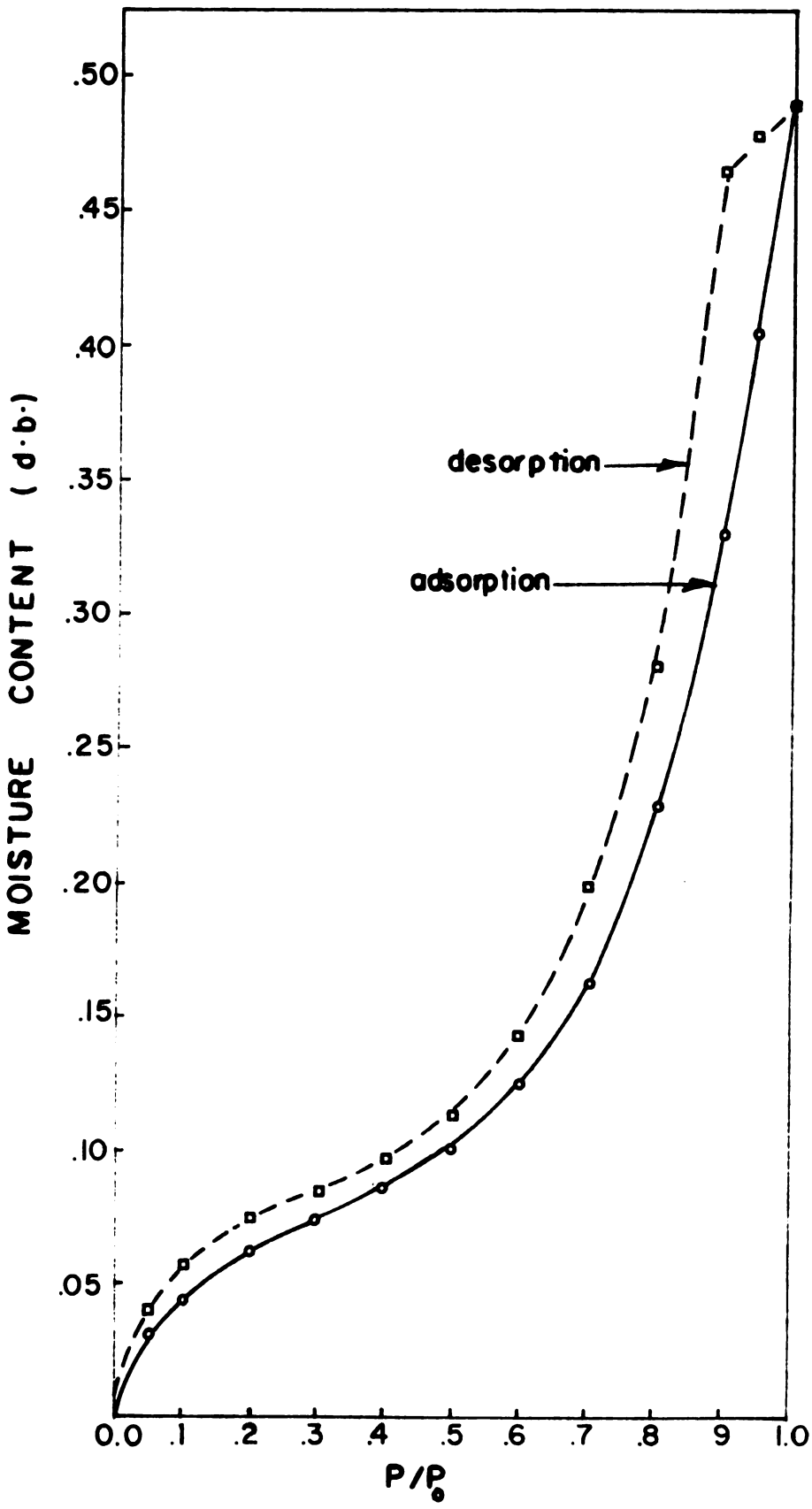

Figure 4.7(b). Plot showing sorption hysteresis in pre-cooked freeze-dried beef powder (22.2°C isotherm)

flattening tendency near saturation vapor pressure - suggesting a type IV classification of the Brunauer type - the adsorption curves are strictly sigmoid-type II, with the "B" point fairly well defined.

These salient features support - as do most sorption isotherms of biological materials - the microporous assumption so fundamental to the development here presented. While a number of biological materials will be used to test the theory as a means of demonstrating its scope, the data presented in this section will in the main, be employed to test the generalized model.

4.3 Verification of the Derived Density Function for Sorbed Water

It is assumed in the interest of simplicity that the B-E-T surface area ($S_{B\text{-}E\text{-}T}$) of a given sorbent can be stretched out into an equivalent flat surface. The mono-layer and subsequent multi-molecular layers are assumed to form a matrix, see Figure 4.8. The individual molecules file into vertical columns. The molecules of each column are forced by virtue of their presence in that column to conform to the cross-sectional area (σ_m, $[A°]^2$) of the first (mono-layer) molecule of that column. The area, σ_m, which one adsorbed molecule would occupy in the completed mono-layer depends among other things, on (a) the sorbate surface tension and (b) the intensity of the sorbent-sorbate interaction represented by the so-called spreading pressure at the surface. Because of the recognized compressive effect of this surface force together with its fundamental polarizability, the adsorbed water molecule is visualized in Figure 4.8 not as a spheroid, but as an ellipsoid, the degree of "flattening" of which is proportional to the gross compressive force acting on the molecule. According to the potential theory, this flattening is expected to be highest in the mono-layer and diminishes progressively outward in the succeeding layers.

With the assumptions enunciated above, the multi-layer thickness t, can be defined as:

$$t(A°) = V_a/S_{BET} \qquad [4.3.1]$$

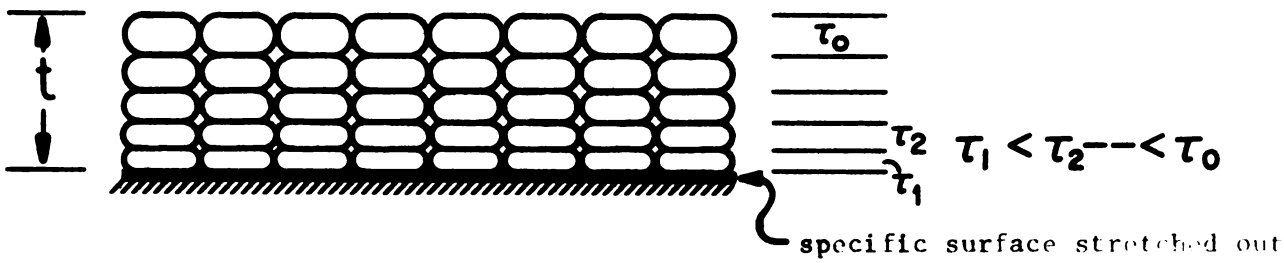

Figure 4.8. Vertical section of stretched out specific surface, showing the multi-layer matrix. Each adsorbed water molecule is visualized as a flattened elipsoid reflecting the degree of compression of the molecule as a result of intermolecular forces of attraction and polarizability effects. Each layer of molecules is subject to a different but uniform compression. The first layer being the most compressed and the top layer the least compressed.

The average thickness of a single layer of adsorbed molecules, τ, previously defined by equation (2.3.7), becomes:

$$\tau_n = t/n = \frac{V_a}{nS_{BET}} = \frac{M_a}{\rho\ nS_{BET}} \qquad [4.3.2]$$

where n is the number molecular layers adsorbed and ρ is the mean density corresponding to n. In accordance with equation (4.3.2), the average thickness at saturation vapor pressure, τ_o is given by:

$$\tau_o(A^\circ) = \frac{M_a}{\rho_o nS_{BET}} \qquad [4.3.3]$$

Combining equations (4.3.2) and (4.3.3) yields:

$$\frac{\rho}{\rho_o} \cong \frac{\tau_o}{\tau_n} \qquad [4.3.4]$$

Equation (4.3.4) implies that the density ratio and the thickness ratio should be approximately equal. This furnishes an approximate verification of the density function derived, tabulated and graphed earlier in chapter II. In Tables 4.3.1 through 4.3.4, the above verification is performed for a number of biological products. A comparison of columns 5 and 9 of each table shows a remarkable agreement between the ratios.

Three things need to be pointed out immediately regarding Tables 4.3.1 through 4.3.4. First, the saturation density, ρ_o, is assumed to be 1 cc/gm, corresponding to the normal bulk liquid density of water. Secondly, since the B-E-T surface area, S_{BET}, determined from H_2O isotherms is known to vary with temperature

Table 4.3.1. Verification table for the density of sorbed water.
Product = Pre-cooked freeze-dried beef powder.
Isotherm temperature = 10°C S_{BET} = 322 (m^2).

1	2	3	4	* 5	6	7	8	9
P/P_o	M_a	$\frac{X}{X_m}$ $X_m = .091$	n	$\rho/\rho_o = \mu^*(\frac{\Delta H}{\Delta H_o})$	$V_a = \frac{M_a}{\rho}$	$t = \frac{V_a}{S_{BET}}$	$\tau_n = t/n$	$\frac{\tau_o}{\tau_n}$
.05	.047	.52						
.10	.070	.769						
			1	1.360	.0669	2.079	2.079	1.351
.20	.095	1.044						
.30	.110	1.210						
.40	.122	1.341						
.50	.135	1.484						
.60	.155	1.703						
			2	1.316	.1380	4.320	2.160	1.300
.70	.191	2.10						
			3	1.164	.2340	7.200	2.400	1.170
.80	.260	2.86						
			4	1.126	.3230	10.000	2.500	1.124
.90	.380	4.18						
.95	.450	4.95	5	1.062	.4280	13.250	2.650	1.060
1.00	.505	5.55	6	1.000	.5050	16.860	2.810	1.000

* In these calculations, $\rho_o \cong$ 1 cc/gm., the normal density of bulk water

Table 4.3.2. Verification table for the density of sorbed water.
Product = Soda boiled cotton (Urquhart and Williams, 1924)
Isotherm temperature = 10°C. $S_{BET} = 126(m^2)$

1	2	3	4	* 5	6	7	8	9
P/P_o	M_a	$\frac{X}{X_m}$ $X_m = .036$	n	$\rho/\rho_o = \mu^*(\frac{\Delta H}{\Delta H^\circ})$	V_a	t $= V_a/S_{BET}$	τ_n	$\frac{\tau_o}{\tau_n}$
.05	.017	.48						
.10	.023	.644						
.20	.032	.896						
			1	1.220	.0295	2.300	2.300	1.217
.30	.041	1.15						
.40	.049	1.372						
.50	.058	1.624						
.60	.068	1.904						
			2	1.120	.0642	5.000	2.500	1.120
.70	.080	2.240						
.80	.099	2.970						
			3	1.089	.0990	7.800	2.600	1.080
.90	.132	3.697						
			4	1.035	.1390	10.800	2.700	1.037
.95	.164	4.593						
			5	1.008	.1780	13.715	2.743	1.02
1.00	.240	6.722						
			6	1.000	.2400	16.980	2.830	1.00

* In these calculations $\rho_o \cong 1$ cc/gm., the normal density of bulk water.

Table 4.3.3. Verification table for the density of sorbed water.
Product = Spruce wood (Stamm, 1938)
Isotherm temperature = 20°C. $S_{BET} = 177(m^2)$.

1 P/P_o	2 M_a	3 $\frac{X}{X_m}$ $X_m = .05$	4 n	* 5 $\rho/\rho_o = \mu^*(\frac{\Delta H}{\Delta H_o})$	6 $V_a = M_a/\rho$	7 t $= V_a/S_{BET}$	8 $\tau_n = t/n$	9 $\frac{\tau_o}{\tau_n}$
.05	.013	.26						
.10	.025	.50						
.20	.025	.99						
			1	1.15	.0434	2.45	2.45	1.14
.30	.063	1.26						
.40	.080	1.6						
.50	.095	1.9						
			2	1.10	.0900	5.2	2.6	1.08
.60	.113	2.26						
.70	.135	2.7						
			3	1.067	.1400	7.98	2.66	1.05
.80	.165	3.3						
			4	1.042	.1910	10.8	2.70	1.04
.90	.225	4.5						
			5	1.035	.2410			
.95	.275	5.5						
			6	1.000	.3000	16.8	2.8	1.00
1.00	.340	6.8						
			7	1.000	.3400	19.6	2.8	1.00

* In these calculations, ρ_o = 1 cc/gm., the normal density of bulk water.

Table 4.3.4. Verification table for the density of sorbed water.
Product = Corn kernels (Rodriguez-Arias, 1956).
Isotherm temperature = 4°C. $S_{BET} = 281(m^2)$.

1	2	3	4	* 5	6	7	8	9
P/P_o	M_a	$\frac{X}{X_m}$ $X_m = .0865$	n	$\rho/\rho_o = \mu^*(\frac{\Delta H}{\Delta H_o})$	$V_a = M_a/\rho$	$t = V_a/S_{BET}$	$\tau_n = t/n$	$\frac{\tau_o}{\tau_n}$
.10	.065	.751						
			1	1.295	.0667	2.37	2.37	1.31
.20	.0925	1.07						
.30	.1100	1.271						
.40	.1275	1.473						
.50	.1425	1.647						
.60	.1625	1.878						
			2	1.145	.1510	5.370	2.685	1.150
.70	.1825	2.109						
.80	.2125	2.456						
			3	1.043	.2480	9.00	3.00	1.02
.90	.2700	3.121						
.95	.3000	3.468						
			4	1.000	.3460	12.4	3.1	1.00
1.00	.3500	4.046						

* In these calculations, $\rho_o \cong 1$ cc/gm., the normal density of bulk water.

(because the mono-layer capacity, v_m, varies with isotherm temperature), the absolute specific surface area of the sorbent is not known. Even though it is customary to use a mean specific surface based on several isotherms, this average value is questionable when wide variations in v_m values occur with isotherm temperature. Because of the doubt in the S_{BET} value used, the t (column 7) and τ_n (column 8) values of these tables do not have absolute but do have relative significance. Consequently, the ratio τ_o/τ_n (column 9), is unaffected by the degree of accuracy of S_{BET}. Finally, the verification performed is insufficient as a test of the validity of the derived density function. At best, it only adds a certain margin of confidence to the derived function. The absolute test for the density relation can be done experimentally by comparing gravimetric sorption data with the corresponding volumetric data for the sorbate, water, on the same sorbent system. There exists in current literature a glaring lack of sufficient data along these lines and thus such a test is not possible at the present time.

4.4 Verification of the Derived Isotherm Equation

4.4 a. Theoretical Isotherms

For illustrative purposes, two sets of isotherms calculated with the volumetric equation (2.3.22) are presented in Figure 4.9. The specific adsorbed volume, V_a, is plotted in its reduced form by dividing each calculated isotherm point by the corresponding calculated adsorbed volume at $P = 0.98\ P_o$. This reduction of all isotherm heights to 1 or 100% allows for a better comparison of characteristic forms of adsorption curves and facilitates the eventual matching of theoretical with experimental isotherms. The adsorbed volume at a relative humidity of 98% is chosen as a relatively well defined point. In contrast, considerable doubt still exists among investigators (see for example, Bangham and Sever, 1925) as to whether equilibrium is ever truly obtained at saturation. As a result, the adsorbed volume at 100% relative humidity is not well defined. In these plots, the volumetric isotherm expression is chosen in preference to its gravimetric equivalent because it lends itself well for consideration on a general basis. The isotherm temperature used for the calculation of Figure 4.9 is 10°C. Two sets of theoretical curves are presented to illustrate the effect of the P_m value on the isotherm shape.

The curves are obviously very characteristic showing (a) well defined initial "knees" at moderately positive values of n [the knees are clearly better defined at lower values of P_m, see Figures 4.9 a and 4.9 b], (b) certain linear parts, and (c) distinctive individual starting angles of the isotherms. All regular types

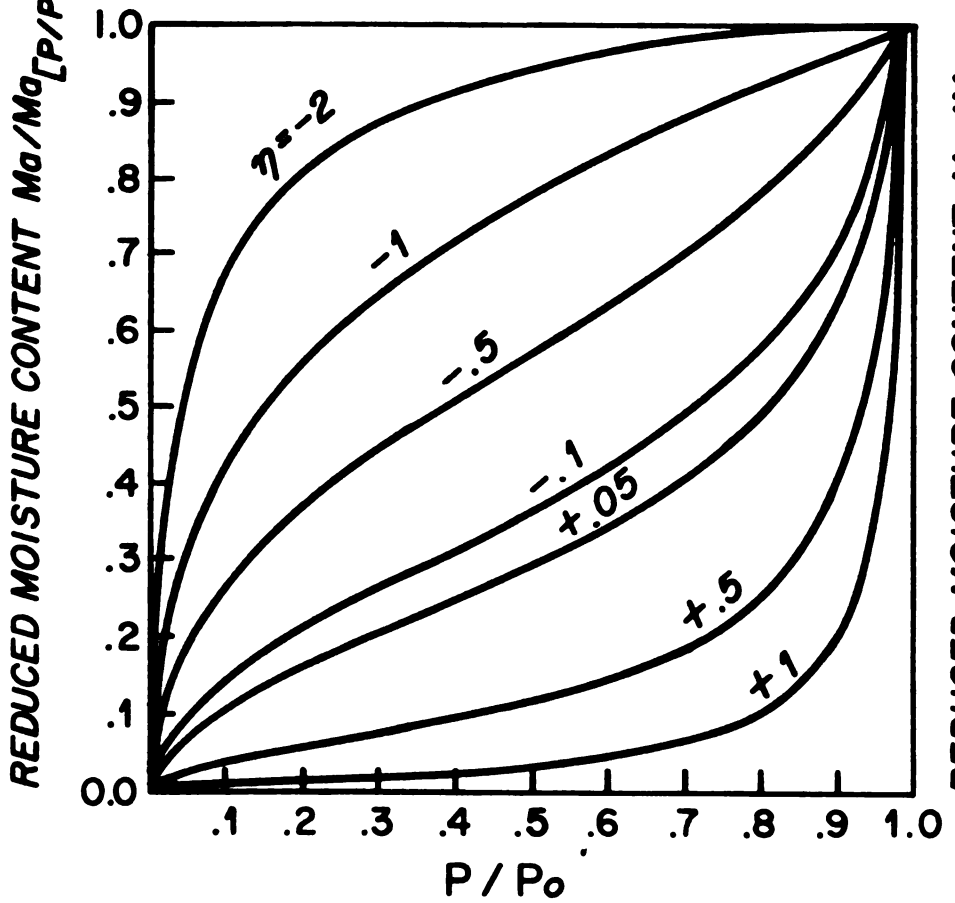

Figure 4.9(a). Theoretical isotherms calculated with eqn. (2.3.22).
$P_m = (.008)P_o$, T = 10°C = 283°K

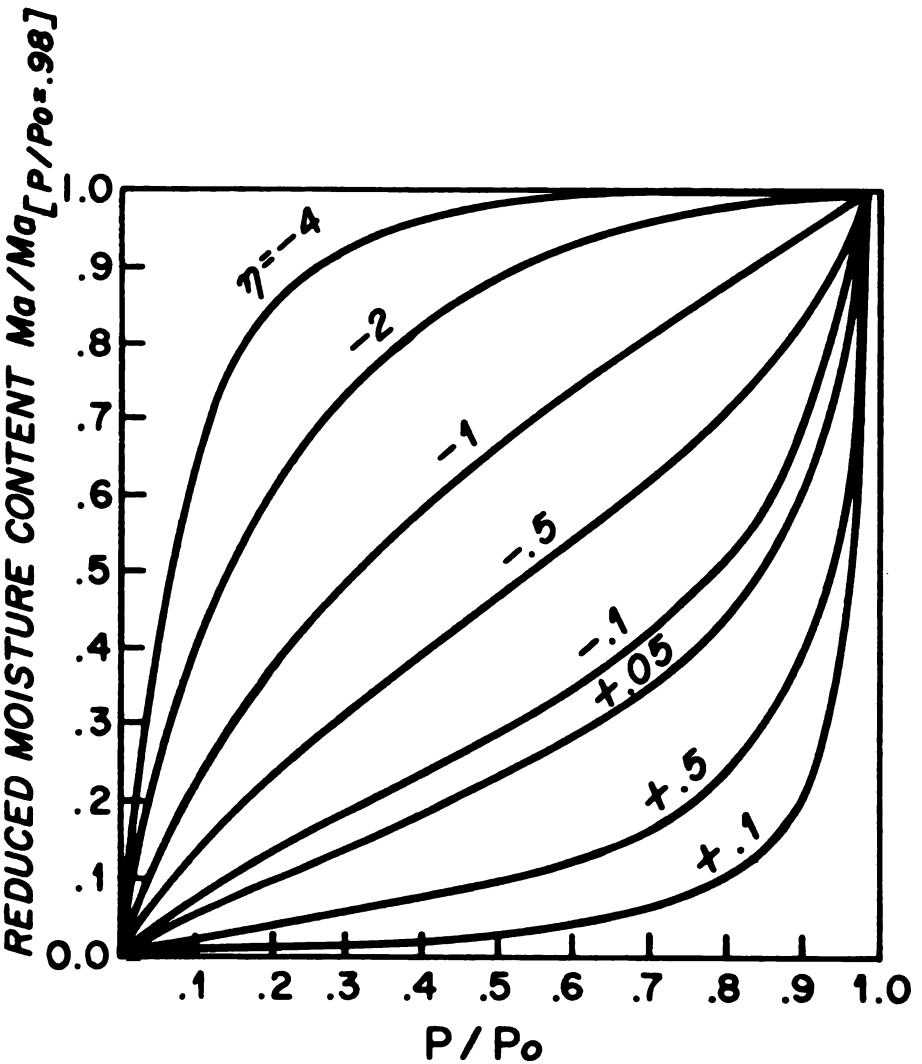

Figure 4.9(b). Theoretical isotherms calculated with eqn. (2.3.22).
$P_m = (0.1)P_o$, T = 10°C = 283°K

of isotherms of the Brunauer classification are obtained merely by the variation of η. This finding is significant in that it vindicates the leading premise of the generalized theory that the three basic concepts in adsorption are complementary and thus can be unified into a self-contained isotherm equation. The present results must also be viewed in their broader context as strengthening considerably the significance of a purely power law distribution concept for the pore-size.

4.4 b. η as the Primary Characteristic Parameter of the Pore Structure

As the primary shape criterion for the set of theoretical isotherms represented in Figure 4.9, η must be viewed as the characteristic value for the representation of the quantitative behavior of a porous sorbent at any relative vapor pressure. In the range $\eta < -1$, the theoretical isotherms are clearly of the Langmuir-type. Thus, this range of η values may be associated with materials characterized by exceedingly narrow pores, probably not more than two molecular diameters in width. These are the so-called micropores. Sigmoid type II isotherms are defined in the range $-1 \leq \eta \leq +1$. Accordingly, pores so characterized fall within the so-called intermediate and lower macroporous range (Brunauer, 1945; Gregg and Sing, 1967). η values in the range $\eta > +1$ define type III isotherms and in consequence may be associated with large pores of the upper macroporous range. It is well recognized that the isotherms of most biological products are sigmoid. Consequently, it would seem logical that the main focus of the present investigation should be restricted to the intermediate range, $-1 \leq \eta \leq +1$.

As defined by equation (2.3.20),

$$\eta = 4 + \gamma \qquad [4.4.1]$$

Ordinarily, this relationship would have provided a convenient computational formula for η. However, it has been previously argued that the pore-size distribution parameter, γ, is not defined with sufficient quantitative accuracy to warrant this usage. This shortcoming notwithstanding, the definition of η as a function of γ in equation (4.4.1) provides a preliminary insight into its qualitative character. It is unique and specific for each sorbent system. It is temperature sensitive, assuming progressively changing values as the isotherm temperature increases [see table 4.1.3]. As a consequence of the previously discussed relationship between η and the characteristic isotherm types, it is apparent that an appreciable temperature-induced change does take place in the sorbent pore structure. Even though the exact nature of this change cannot be specified at this point, it is obvious that in applying the derived isotherm equation to specific products, η must not only be defined for each product, but needs also to be defined for each temperature.

4.4 c ξ as a Secondary Characteristic Parameter of the Pore Structure

According to equation (2.3.19),

$$\xi = \frac{4}{3} \pi K_1 \qquad [4.4.2]$$

ξ is thus a quantity combining the pore-size distribution parameter, K_1, with the factor of pore geometry, $(\frac{4}{3} \pi)$. Since ξ is dependent on K_1, its value is unique for each sorbent system and it is also temperature sensitive (see Table 4.1.3). Because K_1 is not accurately

defined from a quantitative standpoint, the exact value of ξ cannot be determined from equation (4.4.2). A progression from smaller to larger values of ξ is evident as the isotherm temperature is increased (Table 4.1.3). It would seem therefore, that a decreasing η value combined with an increasing ξ value implies a change in the pore structure. This change means that the effective size of each associated pore is affected by a combined hydro and thermo expansion or contraction of the solid component of the sorbing tissue.

4.4 d. Prediction of the Adsorption Isotherms of Certain Biological Materials with the Generalized Isotherm Equation

Since it has not been possible to determine reliable values of η and ξ from a priori considerations, these quantities will be defined empirically to satisfy qualitative criteria stipulated from earlier theoretical considerations. To determine η for a specific product and temperature, the empirical isotherm in its reduced volumetric form is superposed on a set of theoretical isotherms such as shown in Figure 4.9. The best matching η and P_m values are thus selected. Based on these values of η and P_m, the function $[\frac{Z^{\eta} - \lambda^{\eta}}{\eta}]$ is defined for each relative vapor pressure. Combining the approximate density term, ρ_1, with the above function, the best fitting average ξ value, $\bar{\xi}$, is defined. It is now possible to define for each P/P_o value, the first approximation of the specific adsorbed mass, defined by $\rho_1 \cdot \bar{\xi} [\frac{Z^{\eta} - \lambda^{\eta}}{\eta}]$. The discrepancy between this approximate value and its empirical counterpart is minimized by the careful correction of the density term. This gives rise to a new set of density values, designated as ρ_2.

In Tables 4.4.1 through 4.4.5 the relevant parameters for

(a) Pre-cooked freeze-dried beef powder (10°C and 37.7°C)

(b) Raw freeze-dried beef slices (10°C and 40°C)

(c) Whole corn kernels (22°C and 50°C)

(d) Wood cellulose (20°C and 60°C) and

(e) Soda boiled cotton (10°C and 30°C), are shown.

The quantity $\bar{\xi}\ \rho_2[\frac{z^\eta - \lambda^\eta}{\eta}]$ in each table represents the best prediction possible for the product and temperature under consideration. Predicted isotherms based on these tables are represented in Figures 4.10 through 4.14. These plots together with the standard error estimates shown on each table are, for most of the points, within limits of the magnitude of error ordinarily associated with adsorption experiments. The error estimates are also within the limits of variability to be expected on account of the highly specific character of biological materials.

The Corrected Density, ρ_2: In rationalizing the corrected density term, ρ_2, it should be kept in mind that the density function derived in this work, on which ρ_1 is based, is acceptable only as a first estimate. In so far as the isosteric heat values determined by the combined usage of the Clausius-Clapeyron equation and the slopes of the so-called adsorption isostere plots are, at best, crude estimates of the actual quantities (Ross and Olivier, 1964; Gregg and Sing, 1967; Adamson, 1967), the ratio, $(\Delta H/\Delta H°)$, of the derived density function is only as good as the isosteric heat values used. The relatively small correction factors needed to up-grade ρ_1 to ρ_2, in most cases, are justified on the basis of the associated isosteric heat difficiencies discussed above. Moreover, ρ_2 is seen to conform

Table 4.4.1(a). Calculation of theoretical isotherm.
Product = pre-cooked freeze-dried beef powder
Isotherm temperature = 10°C

P/P_o	M_a (Exptl.)	ρ_1	$\bar{\xi}$ = .454	$[\frac{Z^\eta-\lambda^\eta}{\eta}]$ $\eta = 0.1$ $P_m = 0.01$	ρ_2	$\bar{\xi}\rho_2[\frac{Z^\eta-\lambda^\eta}{\eta}]$	Error
.1	.070	1.360	"	.0957	1.612	.070	.000
.2	.095	1.360	"	.1450	1.451	.095	.000
.3	.110	1.316	"	.1870	1.302	.110	.000
.4	.122	1.316	"	.2290	1.160	.132	-.010
.5	.135	1.316	"	.2750	1.160	.144	-.009
.6	.155	1.164	"	.3260	1.160	.171	-.016
.7	.191	1.164	"	.3900	1.160	.205	-.014
.8	.260	1.164	"	.4790	1.160	.252	-.008
.9	.380	1.126	"	.6350	1.160	.334	+.056
.95	.450	1.062	"	.7990	1.160	.420	+.030
.98	.483	1.00	"	1.0400	1.023	.483	.000

Standard Error Estimate = ±.0064

Table 4.4.1(b). Calculation of theoretical isotherm.

Product = pre-cooked freeze-dried beef powder

Isotherm temperature = 37.7°C

P/P_o	M_a (Exptl.)	ρ_1	$\bar{\xi}$ =1.26	$[\frac{Z^\eta - \lambda^\eta}{\eta}]$ $\eta = 0.2$ $P_m = 0.1$	ρ_2	$\bar{\xi}\rho_2[\frac{Z^\eta - \lambda^\eta}{\eta}]$	Error
.1	.0209	1.360		.0089	1.844	.020	+.009
.2	.0309	1.360		.0165	1.532	.031	.000
.3	.0391	1.316		.0240	1.292	.039	+.000
.4	.0500	1.316		.0319	1.248	.049	+.001
.5	.0591	1.316		.0407	1.248	.063	-.004
.6	.0791	1.164		.0512	1.248	.079	.000
.7	.1020	1.164		.0648	1.248	.100	+.002
.8	.1410	1.164		.0844	1.248	.132	+.009
.9	.2000	1.126		.1210	1.248	.190	+.01
.95	.2410	1.062		.1620	1.248	.254	-.013
.98	.2860	1.000		.2260	1.000	.284	+.002

Standard Error Estimate = ±.0064

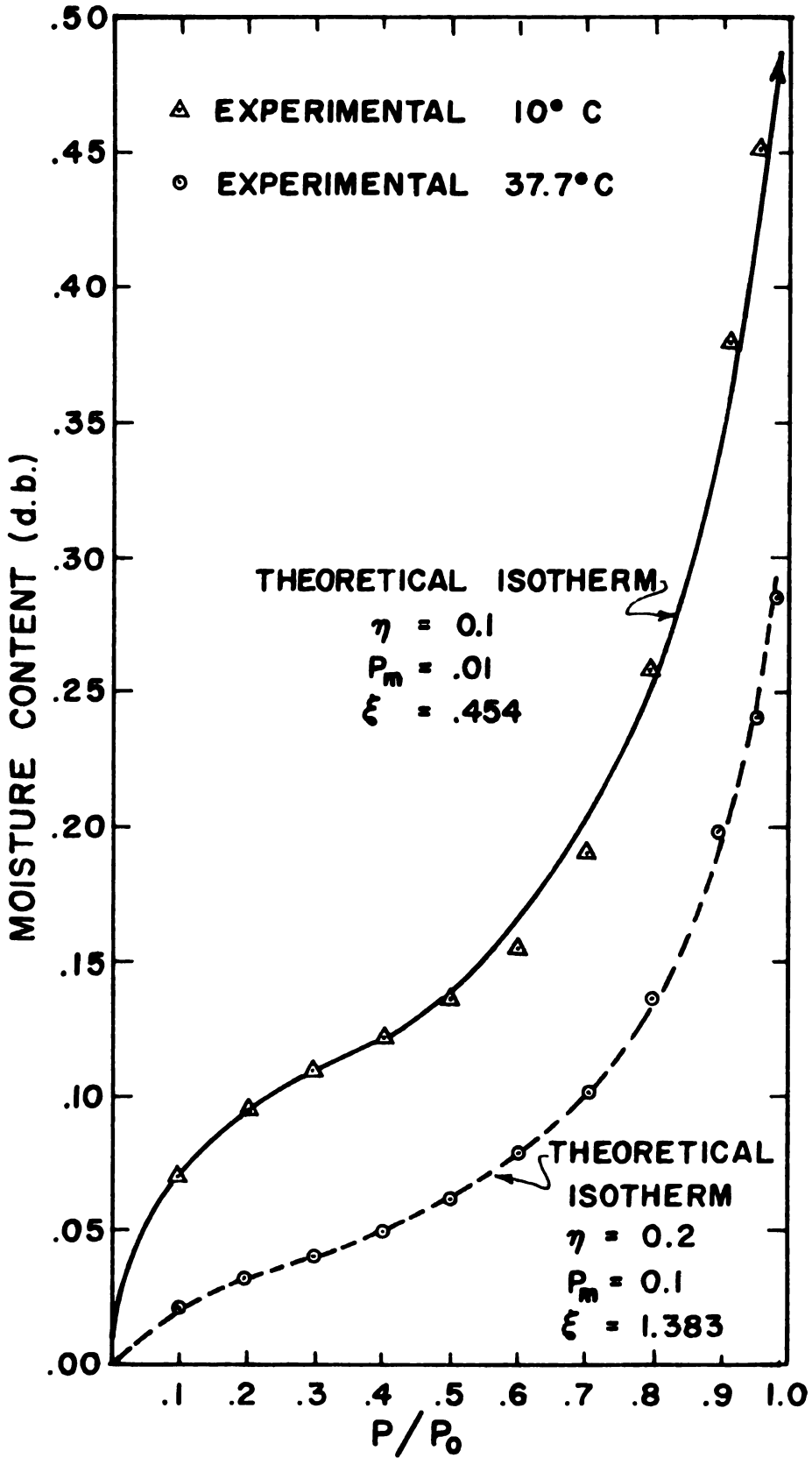

Figure 4.10. Comparison of experimental adsorption isotherms with calculated isotherms for pre-cooked freeze-dried beef powder.

Table 4.4.2(a). Calculation of theoretical isotherm.

Product = raw freeze-dried beef slices
(Data taken from Saravacos, 1965)

Isotherm temperature = 10°C

P/P_o	M_a (Exptl.)	ρ_1	$\bar{\xi}$ = .1047	$\left[\frac{Z^\eta - \lambda^\eta}{\eta}\right]$ η = 0.01 P_m = 0.10	ρ_2	$\bar{\xi}\rho_2\left[\frac{Z^\eta - \lambda^\eta}{\eta}\right]$	Error
.1	.030	1.360	"	.214	1.382	.030	.000
.2	.060	1.360	"	.390	1.382	.055	+.005
.3	.080	1.316	"	.556	1.382	.080	.000
.4	.100	1.316		.724	1.351	.101	-.001
.5	.120	1.316		.906	1.294	.121	-.001
.6	.142	1.164		1.110	1.241	.143	-.001
.7	.170	1.164		1.370	1.204	.172	-.002
.8	.200	1.164		1.710	1.132	.202	-.002
.9	.250	1.126		2.280	1.064	.253	-.003
.95	.310	1.062		2.860	1.050	.313	-.003
.98	.375	1.00	"	3.630	1.00	.38	-.005

Standard Error Estimate = ±0.0027

Table 4.4.2(b). Calculation of theoretical isotherm.

Product = raw freeze-dried beef slices (Saravacos, 1965)

Isotherm temperature = 40°C

P/P_o	M_a (Exptl.)	ρ_1	$\bar{\xi}$ = .136	$\left[\frac{Z^\eta-\lambda^\eta}{\eta}\right]$ $\eta = .04$ $P_m = .10$	ρ_2	M_a (Theoretical) $=\bar{\xi}\rho_2\left[\frac{Z^\eta-\lambda^\eta}{\eta}\right]$	Error
.1	.027	1.36		.126	1.600	.027	.000
.2	.050	1.36		.230	1.600	.049	+.001
.3	.065	1.316		.329	1.520	.066	-.001
.4	.080	1.316		.430	1.380	.080	.000
.5	.090	1.316		.539	1.270	.092	-.002
.6	.100	1.164		.666	1.145	.103	-.003
.7	.120	1.164		.821	1.145	.127	-.007
.8	.155	1.164		1.030	1.145	.160	-.005
.9	.215	1.126		1.400	1.145	.217	-.002
.95	.250	1.062		1.770	1.076	.258	-.008
.98	.300	1.000		2.280	1.000	.310	-.010

Standard Error Estimate = ±0.0048

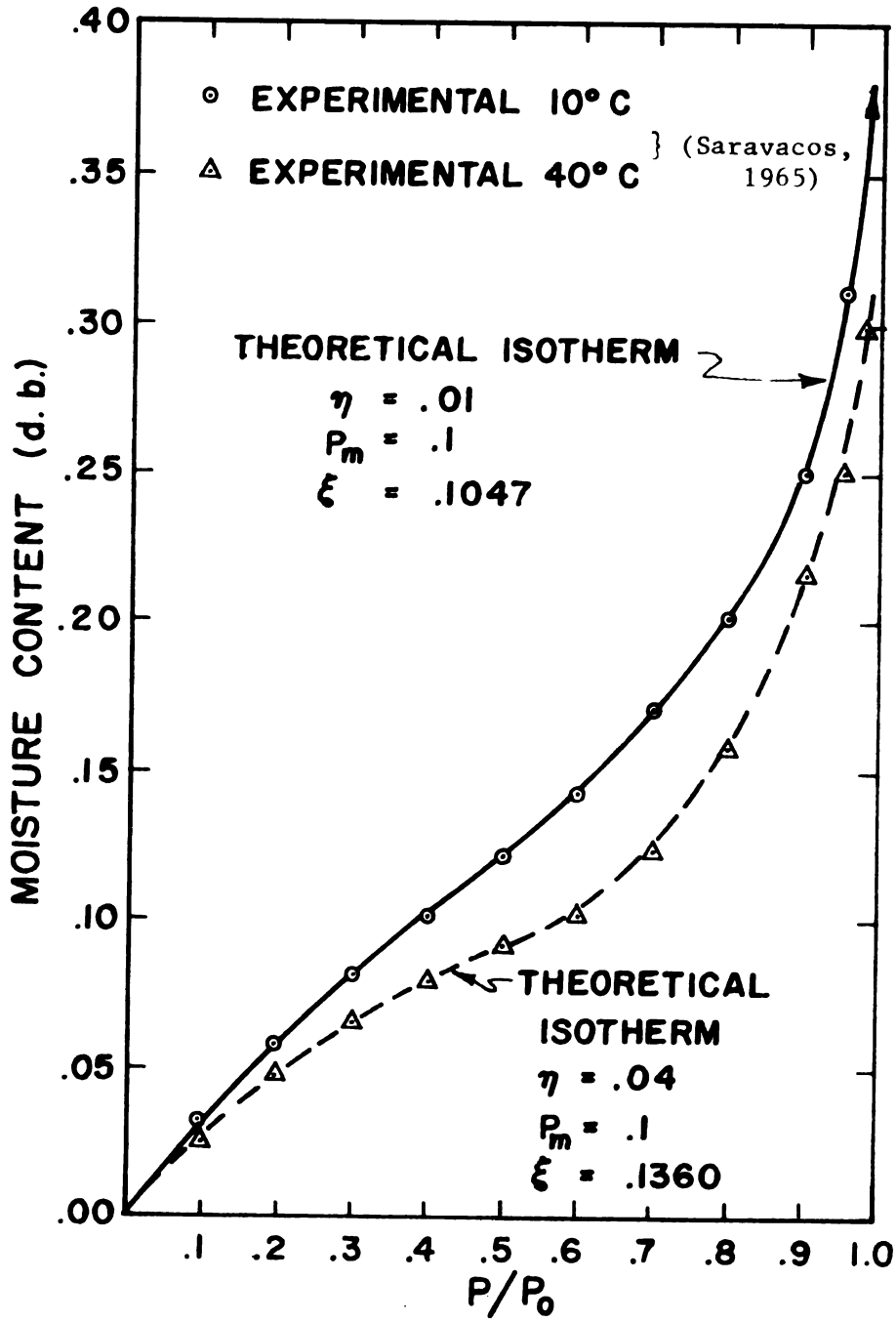

Figure 4.11. Comparison of experimental adsorption isotherms with calculated adsorption isotherms for raw freeze-dried beef in slices.

Table 4.4.3(a). Calculation of theoretical isotherm.

Product = whole corn kernels (Chung and Pfost, 1967)

Isotherm temperature = 22°C

P/P_o	M_a (Exptl.)	ρ_1	$\bar{\xi} = .01415$ $\left[\frac{Z^\eta - \lambda^\eta}{\eta}\right]$ $\eta = -.1$ $P_m = .008$	ρ_2	$\bar{\xi}\rho_2\left[\frac{Z^\eta - \lambda^\eta}{\eta}\right]$	Error
.1	.055	1.295	.0300	1.380	.058	-.003
.2	.072	1.295	.0436	1.215	.074	-.002
.3	.090	1.145	.0548	1.215	.094	-.004
.4	.105	1.145	.0654	1.188	.109	-.004
.5	.118	1.145	.0763	1.129	.121	-.003
.6	.132	1.145	.0882	1.104	.137	-.005
.7	.150	1.043	.1020	1.104	.159	-.004
.8	.182	1.043	.1200	1.104	.187	-.005
.9	.232	1.000	.1490	1.104	.232	0
.95	.266	1.000	.1790	1.081	.273	-.007
.98	.286	1.000	.2080	1.000	.294	-.008

Standard Error Estimate = ±0.0046

Table 4.4.3(b). Calculation of theoretical isotherm.
Product = whole corn kernels (Chung & Pfost, 1967)
Isotherm temperature = 50°C

P/P_o	M_a (Exptl.)	ρ_1	$\bar{\xi}$ =.0184	$[\frac{Z^\eta - \lambda^\eta}{\eta}]$ η = -.08 P_m = .008	ρ_2	$\bar{\xi}\rho_2[\frac{Z^\eta - \lambda^\eta}{\eta}]$	Error
.1	.050			2.08	1.400	.053	-.003
.2	.068			3.04	1.240	.068	.000
.3	.080			3.83	1.146	.080	.000
.4	.092			4.58	1.106	.092	.000
.5	.105			5.36	1.106	.108	-.003
.6	.120			6.21	1.106	.126	-.006
.7	.141			7.22	1.106	.145	-.004
.8	.179			8.54	1.106	.173	+.006
.9	.230			10.70	1.106	.216	+.024
.95	.260			12.60	1.106	.255	+.005
.98	.287			15.20	1.000	.279	-.001

Standard Error Estimate = ±0.0079

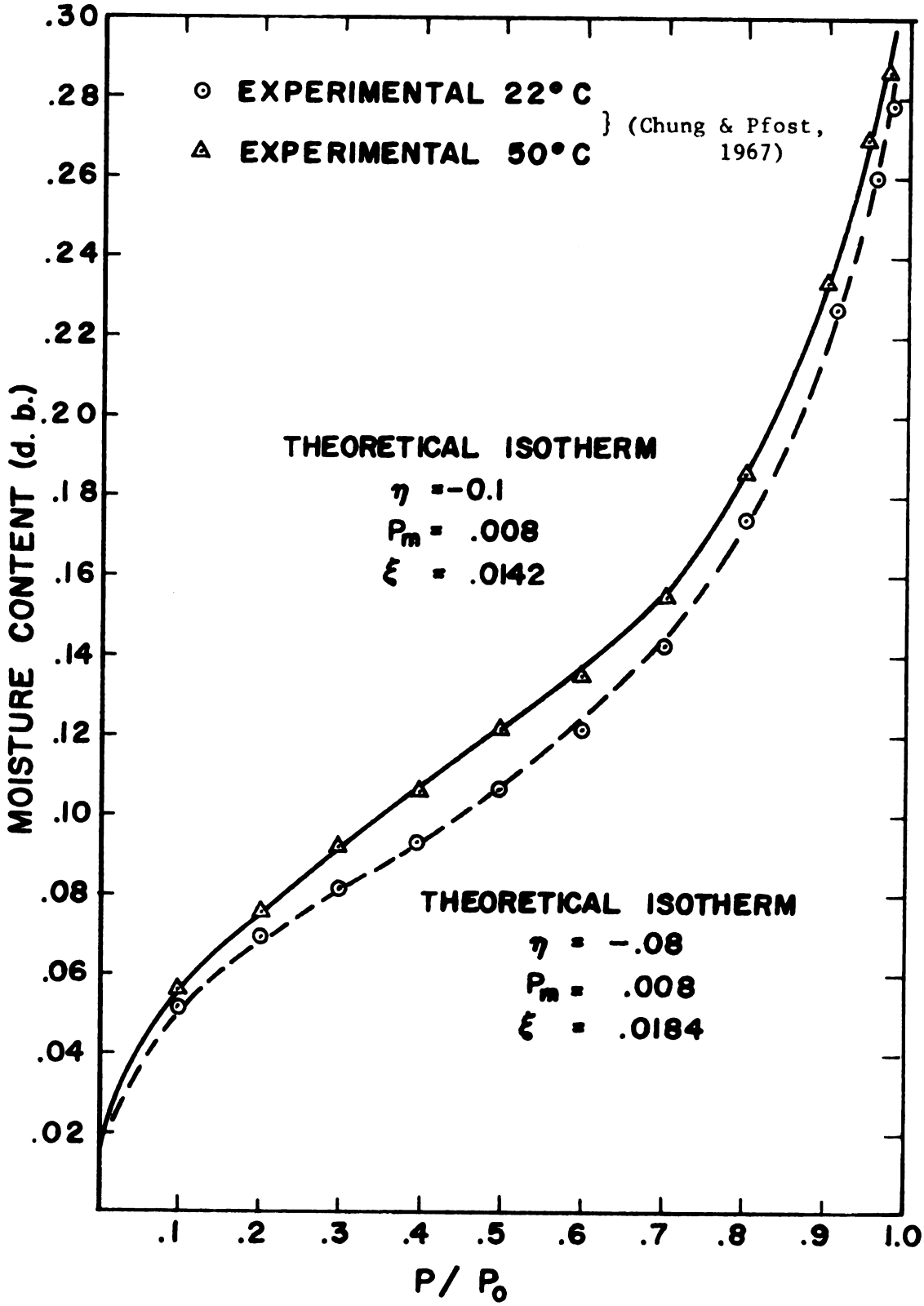

Figure 4.12. Comparison of experimental adsorption isotherms with calculated isotherms for corn (based on the empirical data of Chung and Pfost, 1967).

Table 4.4.4(a). Calculation of theoretical isotherm.
Product = wood (Lewis, 1921)
Isotherm temperature = 20°C

P/P_o	M_a (Expt1.)	ρ_1	$\bar{\xi}$ = .0172	$[\frac{z^\eta - \lambda^\eta}{\eta}]$ η = -.10 P_m = 0.10	ρ_2	$\bar{\xi}\rho_2[\frac{z^\eta - \lambda^\eta}{\eta}]$	Error
.1	.0250	1.153		1.33	1.22	.027	-.002
.2	.0495	1.153		2.40	1.22	.050	.000
.3	.0630	1.101		3.38	1.123	.065	-.002
.4	.0800	1.101		4.36	1.094	.081	-.001
.5	.0950	1.101		5.39	1.050	.097	-.002
.6	.1130	1.067		6.53	1.050	.116	-.003
.7	.1350	1.067		7.90	1.030	.139	-.004
.8	.1650	1.042		9.68	1.030	.171	-.006
.9	.2250	1.024		12.50	1.030	.221	+.004
.95	.2750	1.0065		15.10	1.030	.267	+.008
.98	.3080	1.000		18.30	1.000	.314	-.006

Standard Error Estimate = ±0.00415

Table 4.4.4(b). Calculation of theoretical isotherm.

Product = wood (Lewis, 1921)

Isotherm temperature = 60°C

P/P_o	M_a (Exptl.)	ρ_1	$\bar{\xi}$ =.020	$[\frac{Z^\eta-\lambda^\eta}{\eta}]$ η = -0.07 P_m = 0.10	ρ_2	$\bar{\xi}\rho_2[\frac{Z^\eta-\lambda^\eta}{\eta}]$	Error
.1	.020	1.153		.783	1.249	.020	.000
.2	.035	1.153		1.410	1.224	.035	.000
.3	.045	1.101		2.000	1.145	.046	-.001
.4	.060	1.101		2.590	1.145	.060	.000
.5	.070	1.101		3.210	1.145	.075	-.005
.6	.089	1.067		3.910	1.145	.091	-.002
.7	.110	1.067		4.750	1.145	.111	-.001
.8	.140	1.042		5.870	1.145	.136	+.004
.9	.188	1.024		7.670	1.145	.178	+.010
.95	.225	1.0065		9.390	1.145	.218	+.007
.98	.246	1.000		11.600	1.050	.245	+.001

Standard Error Estimate = ±0.00423

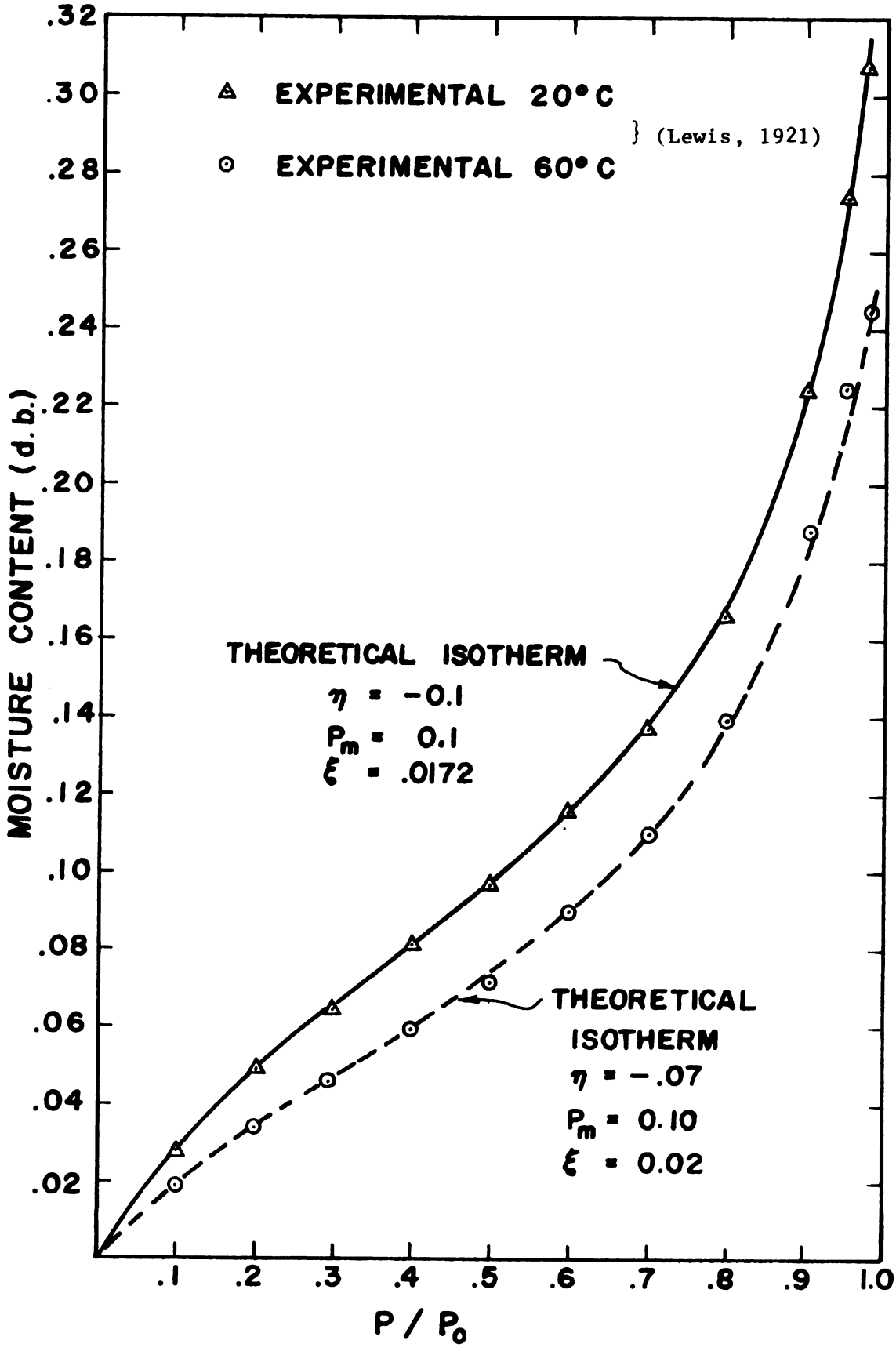

Figure 4.13. Comparison of experimental adsorption isotherms with calculated adsorption isotherms for wood cellulose (based on the data by Lewis, 1921).

Table 4.4.5(a). Calculation of theoretical isotherm.

Product = cotton (Urquhart and Williams, 1924)

Isotherm temperature = 10°C

P/P_o	M_a (Exptl.)	ρ_1	$\bar{\xi}$ =.199	$[\frac{z^\eta - \lambda^\eta}{\eta}]$ η = 0.10 P_m = 0.01	ρ_2	$\bar{\xi}\rho_2[\frac{z^\eta - \lambda^\eta}{\eta}]$	Error
.1	.023	1.19		.0957	1.243	.023	.000
.2	.032	1.19		.145	1.122	.032	.000
.3	.041	1.072		.187	1.122	.041	.000
.4	.049	1.072		.229	1.093	.049	.000
.5	.058	1.072		.275	1.078	.058	.000
.6	.068	1.045		.326	1.078	.070	-.002
.7	.080	1.045		.390	1.045	.081	-.001
.8	.099	1.045		.479	1.045	.099	.000
.9	.132	1.013		.635	1.043	.131	+.001
.95	.164	1.001		.799	1.032	.164	.000
.98	.209	1.000		1.04	1.014	.209	.000

Standard Error Estimate = ±0.000738

Table 4.4.5(b). Calculation of theoretical isotherm.
Product = cotton (Urquhart and Williams, 1924)
Isotherm temperature = 30°C

P/P_o	M_a (Exptl.)	ρ_1	$\bar{\xi}$ =.799	$[\frac{z^\eta-\lambda^\eta}{\eta}]$ η = 0.20 P_m = 0.01	ρ_2	M_a (Theoretical) $\bar{\xi}\rho_2[\frac{z^\eta-\lambda^\eta}{\eta}]$	Error
.1	.018	1.19		.0935	1.388	.018	.000
.2	.027	1.19		.141	1.311	.027	.000
.3	.035	1.072		.183	1.311	.035	.000
.4	.044	1.072		.224	1.311	.044	.000
.5	.052	1.072		.268	1.273	.052	.000
.6	.061	1.045		.319	1.273	.062	-.001
.7	.073	1.045		.381	1.221	.073	.000
.8	.091	1.045		.469	1.221	.092	-.001
.9	.121	1.013		.621	1.178	.121	.000
.95	.147	1.001		.783	1.091	.147	.000
.98	.163	1.000		1.020	1.00	.185	.022

Standard Error Estimate = +0.0066 (based on 11 pts)
= ±0.000447 (based on 10 pts)

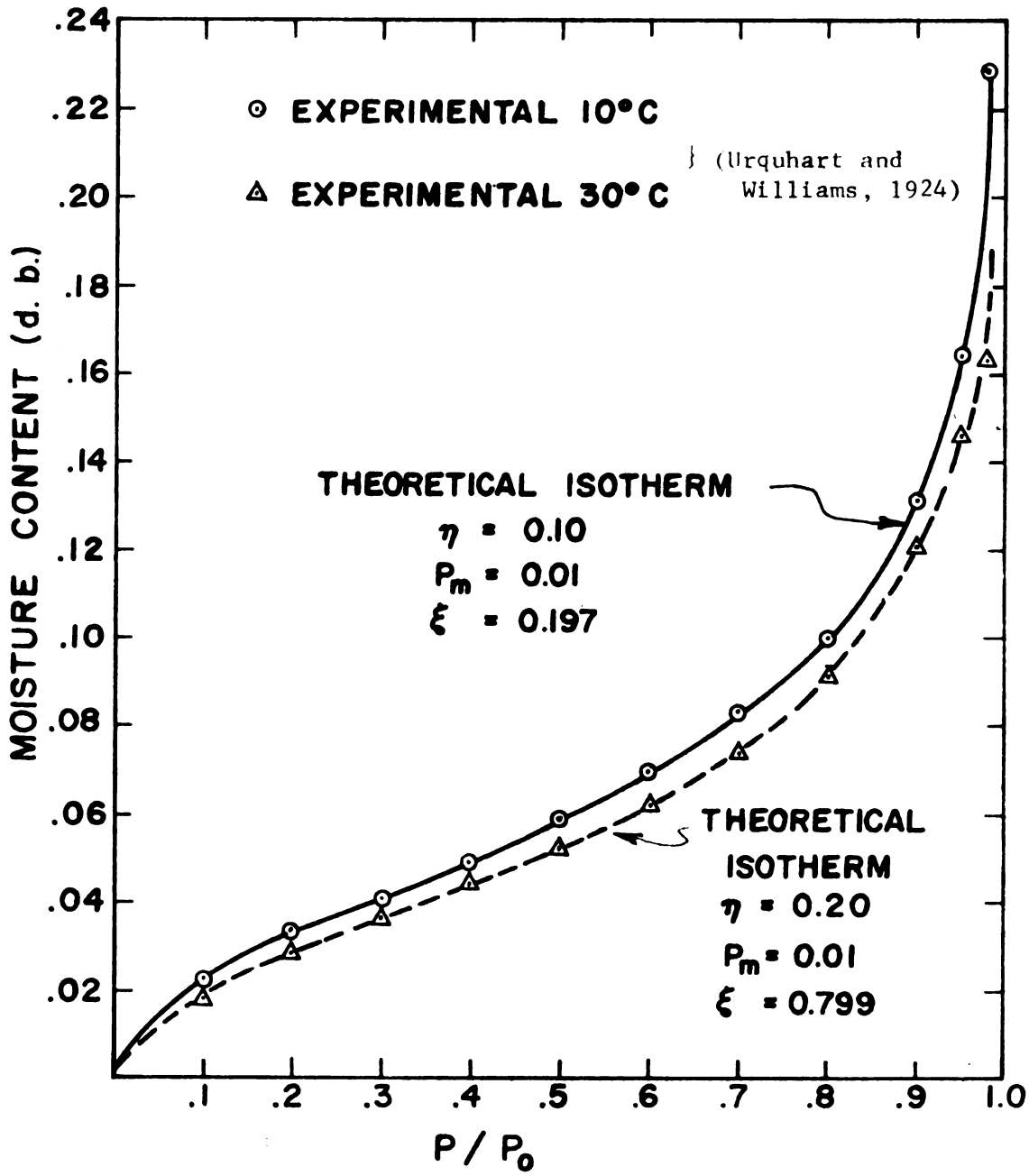

Figure 4.14. Comparison of experimental adsorption isotherms with calculated adsorption isotherms for soda-boiled cotton (data taken from Urquhart & Williams, 1924).

in every case, with the essential implications of the adsorption potential theory. In showing consistently increasing density values with rising isotherm temperatures, ρ_2 reflects the correct temperature dependence of the isosteric heat of adsorption as evident in the well known relation (Ross and Olivier, 1964):

$$\Delta H_{st} = q_{diff} + R_g T$$

where q_{diff} is the differential heat of adsorption.

It appears reasonable, in the absence of conclusive empirical density values, to accept the ρ_2 values on their demonstrated qualitative merit.

Empirical η and $\bar{\xi}$ Parameters: A summary of the empirically determined values of η and $\bar{\xi}$ for corn, cotton, wood, raw freeze-dried beef slices and pre-cooked freeze-dried beef powder is presented in Table 4.4.6. The values are clearly product and temperature dependent. However, when compared with their counterpart semi-theoretically determined η and $\bar{\xi}$ values (Table 4.1.3), drastic differences in magnitude and character are evident. These differences once again emphasize the fundamentally qualitative character of the pore-size distribution parameters, γ and K_1, as determined.

While temperature induced-changes in the pore-structure were generally predictable from the figures of Table 4.1.3, certain interpretations deduced from those figures still need to be revised or finalized. Since the empirical values of η and $\bar{\xi}$ (Table 4.4.6) show increasing trends from smaller to larger values with rising isotherm temperatures, a progression from smaller to larger pores

Table 4.4.6. Summary of empirical η, and $\bar{\xi}$ parameters.

PRODUCT	Temperature °C	η	P_m	$\bar{\xi}$
CORN	22.0	-0.10	.008	.01415
	50.0	- .08	.008	.01840
COTTON	10.0	0.10	0.01	.19900
		0.20	0.01	.79900
WOOD	20.0	- .10	0.10	.01720
		- .07	0.10	.02000
RAW FREEZE-DRIED BEEF SLICES	10.0	0.01	0.10	0.10470
	40.0	0.04	0.10	0.13600
PRE-COOKED FREEZE-DRIED BEEF POWDER	10.0	0.1	0.01	0.45400
	37.7	0.2	0.10	1.26000

is indicated. This expansion in the pores must be accompanied by a concomitant contraction in the solid component of the porous structure.

From tabulated P_m values (Table 4.4.6), it is at once obvious that the P_m parameter as used in this study is quite different from the actual pressure corresponding to the mono-layer capacity. Part of this discrepancy can be traced back to the transformation of coordinate axes which became necessary in the original formulation in chapter II. It would appear that in the attempt to systematize the plots of the derived isotherm equation, the actual physical significance of P_m has been sacrificed.

Stability Considerations in the Sorbent Pore Structure: The standard error estimate of ± 0.021 calculated in Table 4.4.1 a for pre-cooked freeze-dried beef powder is by far the worst recorded. Since this product happens to be the only biological material in its powdered form tested, the comparatively poor error estimate raises a question of structural stability in powdered adsorbents.

It would seem that the pore structure of a powdered adsorbent is basically ill defined. For one thing, the pore sizes and pore-size distributions associated with such sorbents must necessarily change with the degree of sorbent compaction. It is also clear, that both hydro and thermo induced changes in the sorbent pore structure will be more pronounced during the adsorption process. These trends appear to be well reflected not only by the comparatively poor error estimate of Table 4.4.1 a, but also by (a) the change from $\eta = 0.1$ and $\xi = .454$ at 10°C (Table 4.4.1 a) to

η = 0.2 and $\bar{\xi}$ = 1.26 at 37.7°C (Table 4.4.1 b), and (b) the accompanying change in P_m value from 0.01 at 10°C to 0.1 at 37.7°C.

Closure: It has been demonstrated in this section that the derived isotherm equation can be used to reconstruct the adsorption isotherms of biological materials with a fair degree of accuracy. Even though certain quantitative inadequacies of present methods made impossible a priori determination of the structural parameters, η and $\bar{\xi}$, it is still possible to formalize the temperature dependence of these parameters either on a general or specific basis. While no such attempt has been made in the present study because of the limited number of isotherm temperatures investigated, the necessary foundations appear to have been laid to make such an effort a logical extension of the present work.

4.5 Verification of the Proposed "Capillary Condensation - Swelling Fatigue" Double Superposition Theory of Sorption Hysteresis in Biological Materials

As an example, the estimation of desorption isotherms from adsorption data, employing the scheme outlined in section 2.5 c, is implemented in Tables 4.5.1 and 4.5.2 for corn kernels at isotherm temperatures of 22°C and 50°C. Corn is used because, to the knowledge of the author, it is the only bio-material of which the bulk moduli have been empirically determined for a wide range of moisture contents (White, 1966).

The work sheets (Tables 4.5.1 and 4.5.2) are developed as follows: column 2 represents calculated or experimental adsorption data; in this case the data of Chung and Pfost (1967) for whole corn kernels were used. Column 3 gives the number of adsorbed multilayers, $n = X/X_m$. Columns 4 and 5 are the approximate density and volumetric data. The terms of column 6 are obtained by linear interpolation of the incremental volumes; in this case each incremental volume is divided by a factor of 10- to give suitably small adsorption steps. Column 7 gives the bulk moduli data obtained by extrapolation of the data by White (1966). Columns 8 and 9 are calculated in accordance with equations (2.5.17a) and (2.5.18), respectively. Columns 10, 11 and 12 show trial adsorption relative vapor pressure values obtained by the selective variation of the parameter, ω, in the generalized Cohan relation (eqn.(2.5.4)). In this case, ω was found to have the value 1.25. Thus the desorption relative vapor pressure values calculated with the equation:

Table 4.5.1. Work Sheet for the calculation of desorption isotherm.

Product = corn kernel (Chung & Pfost, 1967)

Isotherm temperature = 22°C.

1 P/P_o	2 M_a (Exptl.)	3 # n	4 ρ	5 V_a	6 v_{12} (x 10)	7 K psi ($X10^4$) (White, 1966)	* 8 ΔM_d	9 $M_d = M_a + \Delta M_d$	10 $(P/P_o)^{1.1}$	11 $(P/P_o)^{1.2}$	12 $(P/P_o)^{1.3}$
									(P_d/P_o)		
					.042						
.1	.055		1.295	.042				.0550+	.08	.063	.05
					.013						
.2	.072		1.295	.055		9.30	.0062	.0782	.17	.145	.123
		1			.023						
.3	.090		1.145	.078		8.80	.0069	.0969	266	.236	.209
					.022						
.4	.105		1.145	.090		8.15	.0047	.1097	.364	.333	.302
					.013						
.5	.118		1.145	.103		7.55	.0020	.1200	.466	.435	.406
					.012						
.6	.132		1.145	.115		7.10	.0013	.1333	.57	.542	.516
		2			.028						
.7	.150		1.043	.143		6.50	.00200	.1520	.675	.652	.629
					.031						
.8	.182		1.043	.174		5.80	.0013	.1833	.782	.705	.748
		3			.058						
.9	.232		1.000	.232		4.50	.0011	.2331	.891	.881	.872
					.058						
1.0	.290	4	1.000	.290		4.00	.000	.2900	1.00	1.00	1.00

$$* \Delta M_d = \frac{14.7\ R_g T \ln (P_o/P)\ v_{12}}{\rho\ M\ V_a\ K}$$

Table 4.5.2. Work sheet for the calculation of desorption isotherm.

Product = corn kernel (Chung & Pfost, 1967)

Isotherm temperature = 50°C

1 P/P_o	2 M_a (exptl.)	3 # n	4 ρ	5 V_a	6 v_{12} (x10)	7 K ($x10^4$) (White,1966)	8 ΔM_d*	9 $(M_a+\Delta M_d)$	10 $P_d/P_o = (P/P_o)^{1.25}$
					.0386				
.1	.050		1.295	.0386				.0500	.0580
					.0139				
.2	.068		1.295	.0525		9.30	.0069	.0749	.1330
		1			.0173				
.3	.08		1.145	.0698		8.80	.0058	.0858	.2220
					.0205				
.4	.092		1.145	.0803		8.15	.0049	.0969	.3180
					.0107				
.5	.105		1.145	.0910		7.55	.0018	.1068	.4200
					.0130				
.6	.12		1.145	.1040		7.10	.0015	.1215	.5280
		2			.0300				
.7	.1405		1.043	.1340		6.50	.0023	.1428	.6400
					.0370				
.8	.179		1.043	.1710		5.80	.0016	.1806	.7560
		3			.0590				
.9	.23		1.000	.2300		4.50	.0012	.2312	.8765
					.0600				
1.0	.29	4	1.000	.2900		4.00	.0000	.2900	1.0000

$$* \Delta M_d = \frac{14.7\ R_g T\ \ln(P_o/P)\ v_{12}}{\rho\ M\ V_a\ K}$$

$$P_d/P_o = (P_a/P_o)^{1.25} \qquad [4.5.1]$$

were plotted against the corresponding specific desorbed mass M_d (column 9) to obtain the theoretical desorption curves (Figure 4.15).

Figure 4.15 shows that the theoretical desorption curves fit the experimental points remarkably well for the isotherm temperatures investigated. While broad generalizations must await more extensive application of the theory to other biological products and other isotherm temperatures, this finding indicates that the new approach presented here offers an initial frame-work for more detailed consideration of the complex questions of hysteresis in bio-materials.

4.5 a. The parameter, ω, as a factor of pore geometry

A convenient classification of sorption hysteresis based on (a) the pressure range over which the main boundary loop extends, and (b) the steepness of the adsorption and desorption branches, has been proposed by de Boer (1958). Within the frame-work of this broad classification, the parameter, ω, can be employed to gain more insight into the geometrical shape of the pores of sorbing biological materials (Barrer et al., 1956; de Boer, 1958; Linsen and Van Den Heuvel, 1967).

Thus, for the corn kernel, equation (4.5.1) satisfies the de Boer (1958) criterion:

$$(P_a/P_o)^2 < P_d/P_o \qquad [4.5.2]$$

Consequently, the pores are tubular capillaries with widened spheroidal parts open at both ends. This finding supports the earlier preference in section 4.1 for the interconnected spheroidal ink bottle model.

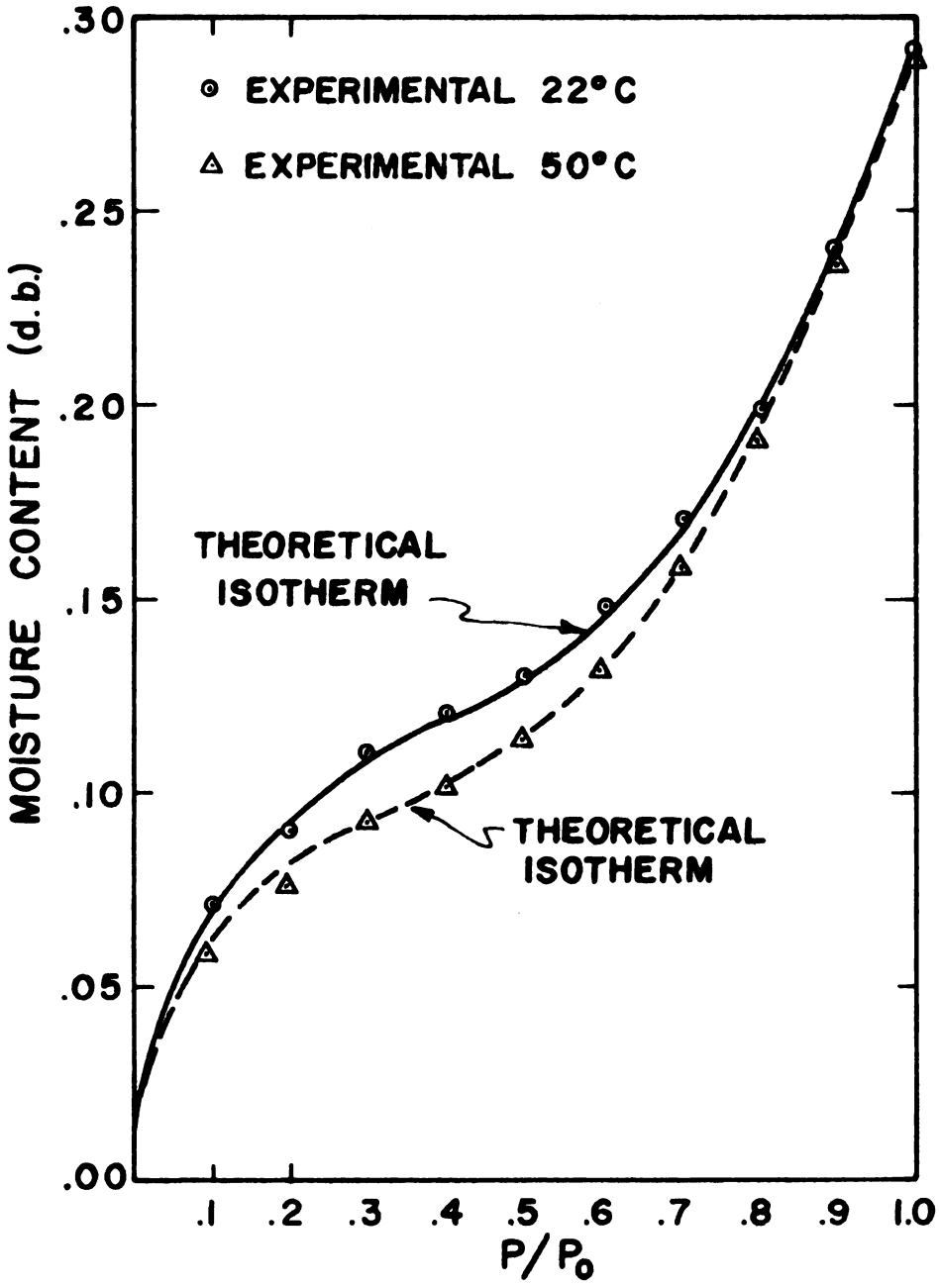

Figure 4.15. Comparison of experimental desorption isotherms with calculated desorption isotherms for corn (expl. data taken from Chung and Pfost, 1967).

V. SUMMARY AND CONCLUSIONS

A generalized model of water sorption is developed and verified for biological materials.

The B-E-T and Capillary condensation theories are combined into an integral isotherm equation for porous biological materials. In order to solve the integral equation explicitly, it became necessary to:

(a) characterize analytically, the physical structure of sorbing bio-materials in terms of a pore-size distribution function and an idealized pore-geometry;

(b) derive, utilizing the general framework of the potential theory in conjunction with the fundamental laws of thermodynamics, an explicit density function for water adsorbed by biological materials. As an essential complement for this method of attack, a new theory of sorption hysteresis is synthesized within the generalized framework.

In consequence of a detailed application of the developed model to the sorption data of several biological products, the following specific conclusions can be drawn.

1. The pores of biological materials are best modeled for transport processes in these systems as interconnected spheroidal "ink-bottles".

2. The numerical distribution of pore-size in bio-materials is well described by a power law distribution function of the type:

$$\varphi_2(R) = K_1 R^{\gamma}$$

where the pore characterization parameters, K_1 and γ are both product and temperature dependent.

3. The density of water sorbed by biological materials can be expressed, in the first approximation, as the semi-theoretical relation:

$$\rho/\rho_o = \mu^* [\Delta H_{st}/\Delta H^\circ_{st}]$$

where ρ is the density associated with the isosteric heat of adsorption, ΔH_{st}; ρ_o and ΔH°_{st} are the corresponding density and isosteric heat values at saturation vapor pressure; and the quantity, μ^*, is empirically defined for the class of biological materials of interest.

4. The interconnected spheroidal ink-bottle pore model, the power law distribution function and the density function are integrated into an isotherm equation of the form:

$$M_a = \frac{\rho \xi}{\eta} [Z^\eta - \lambda^\eta]$$

where η and ξ are the primary and secondary characteristic parameters of pore structure; and Z and λ are functions of relative vapor pressure.

The derived isotherm equation,

(a) reflects through its density term, the well established fact that the heat of adsorption varies with moisture content,

(b) reconstructs the empirical adsorption isotherm and its dependence on temperature reasonably well,

(c) yields most characteristic isotherm types principally through the variation of the principal structural parameter, η.

It thus appears conclusive that the three basic concepts in adsorption, namely: (a) the Kinetic concept as exemplified by the B-E-T theory of multi-molecular adsorption, (b) Polanyi's adsorption potential theory, and (c) Zsigmondy's capillary condensation theory, play complementary and possibly overlapping roles and can be unified into a coordinated theory of water sorption by biological materials.

5. A new theory of sorption hysteresis based on the superposition of (a) Capillary Condensation hysteresis, and (b) Swelling Fatigue hysteresis, is developed in quantitative terms and has been successfully employed to predict the desorption isotherms of whole corn kernels.

VI. SUGGESTIONS FOR FURTHER STUDY

As a consequence of the present study, it is recommended that further investigations should be undertaken in the following areas:

1. The Density of Sorbed Water. The function derived in this study for the density of water can be improved considerably if (a) more precise isosteric heat values are measured and (b) the determinative function, u^*, is revised to reflect a wider spectrum of biological materials. Furthermore, because of the almost complete absence of reliable experimental data on the density of water sorbed on biological materials, the derived density function is yet to be conclusively verified.
2. The Structural Parameters, η and ξ. The dependence of η and ξ on temperature needs to be formalized in order to make it possible to extrapolate from a set of empirical η and ξ values at one isotherm temperature to another. If these parameters are determined for a sufficiently large number of biological materials (over a wide enough temperature range) formalization on a general basis would be possible. Furthermore, water-induced changes in biological materials should be studied in terms of the η and ξ parameters. In this case the structural parameters determined from a desorption isotherm can be compared with those resulting from the adsorption branch. This type of parametric study can conceivably furnish additional information on the phenomenon of hysteresis.

3. Mechanical Properties of Biological Materials. The bulk modulus of most biological materials as a function of moisture content and temperature has not been experimentally determined. Therefore, it was not possible to test the "Capillary Condensation - Swelling Fatigue" superposition concept of sorption hysteresis developed here in sufficient detail to establish its general validity. Additional work should be done along these lines.

REFERENCES

Adamson, A. W. (1967). The Physical Chemistry of Surfaces. (second edition), Interscience Publishers, New York.

Alfrey, T. and P. Doty (1945). The Methods of Specifying the Properties of Viscoelastic Materials. J. of Appl. Physics. 16:700.

Allamand, A. J., P. G. T. Hand and J. E. Manning (1929). The Sorption of Water by Activated Charcoals, Part V. J. of Physical Chemistry. 33:1694.

Bakker-Arkema, F. W. (1961). Desorption and Adsorption Isotherms for Alfalfa of Four Growth Stages in the Temperature Range of 40° to 120°F. Unpublished M.S. Thesis, Agricultural Engineering Department, Michigan State University.

Barrett, E. P., L. G. Joyner and P. P. Halenda (1951). The Determination of Pore Volume and Area Distributions in Porous Substances. J. Am. Chem. Soc. 73:373.

Babbitt, J. D. (1942). On the Adsorption of Water Vapor by Cellulose. Canadian J. of Research. 20(A), No. 9, pp. 143-172.

Bangham, D. H. and W. Sever (1925). An Experimental Investigation of the Dynamical Equation of the Process of Gas-Sorption. Phil. Mag. 6(49):935.

Barkas, W. W. (1953). Part A, Mechanical Properties of Wood and Paper. R. Meredith, Editor, Interscience Publishers, New York.

Barrer, R. M., N. McKenzie and J. S. S. Reay (1956). Capillary Condensation in Single Pores. J. of Colloid Science. 11:479.

Becker, H. A. and H. R. A. Sallans (1956). A Study of Desorption Isotherms of Wheat at 25°C and 50°C. Cereal Chem. 33:79.

Bernal, J. D. and R. H. Fowler (1933A). A Theory of Water and Ionic Solutions, with Particular Reference to Hydrogen and Hydroxyl ions. J. Chem. Physics. 1:515.

Bernal, J. D. and R. H. Fowler (1933B). Pseudocrystalline Structure of Water. Transactions Faraday Soc. 29:1049.

Benson, S. W., D. A. Ellis and R. W. Zwanzig (1950). Surface Area of Proteins III. Adsorption of Water. J. Am. Chem. Soc. 72:2102.

Benson, S. W. and J. W. King (1965). Electrostatic Aspects of Physical Adsorption: Implications for Molecular Sieves and Gaseous Anesthesia. Science. 150:1710.

Bewig, K. W. and W. A. Zisman (1964). Surface Potentials and Induced Polarization in Nonpolar Liquids Adsorbed on Metals. J. Physical Chemistry. 68:1804.

Bradley, R. S. (1936). Polymolecular Adsorbed Films. Part I. The Adsorption of Argon on Salt Crystals at Low Temperatures and the Determination of Surface Fields. J. Chemical Society. 1467-1474.

Brunauer, S., P. H. Emmett and E. Teller (1938). Adsorption of Cases in Multi-molecular Layers. J. Am. Chem. Soc. 60:309.

Brunauer, S., L. S. Deming, W. E. Deming and E. Teller (1940). On a Theory of Van Der Waal's Adsorption of Gases. J. Am. Chem. Soc. 62:1723.

Brunauer, S. (1945). The Adsorption of Gases and Vapors Vol. 1. Princeton University Press, Princeton.

Brunauer, S., L. E. Copeland and D. L. Kantro (1967). The Langmuir and B-E-T Theories. In Solid-Gas Interface Vol. 1, p. 77. Edited by Flood. Marcel Dekker Inc., New York.

Burrage, L. J. (1934). Studies on Adsorption. Part VII. The Form of Isothermals of Vapor on Charcoal and Its Relation to Hysteresis. Trans. Faraday Soc. 30:317.

Cassel, H. M. (1944). Cluster Formation and Phase Transitions in the Adsorbed State. J. Phys. Chem. 48:195.

Chung, D. S. and H. B. Pfost (1967). Adsorption and Desorption of Water Vapor by Cereal Grains and Their Products. Parts I, II and III. Transactions A.S.A.E. 10(4):552.

Clampitt, B. H. and D. E. German (1958). Heat of Vaporization of Molecules at Liquid-Vapor Interfaces. J. Phys. Chem. 62:438.

Coelingh, M. B. (1938). Thesis, University of Utretch.

Coelingh, M. B. (1939). Optische Untersuchungen über das Flüssigkeit Dampfgleichgewicht in Kapillaren Systemen. Kolloid Z. 87:251.

Cohan, L. H. (1938). Sorption Hysteresis and the Vapor Pressure of Concave Surfaces. J. Am. Chem. Soc. 60:433.

Cohan, L. H. (1944). Hysteresis and the Capillary Theory of Adsorption of Vapors. J. Am. Chem. Soc. 66:98.

Coulson, C. A. (1959). Hydrogen Bonding. Edited by D. Hadzi. Perganon Press Ltd., London.

Cranston, R. W. and F. A. Inkley (1957). The Determination of Pore Structures from Nitrogen Adsorption Isotherms. Advances in Catalysis. 9:143.

Davidson, G. F. (1927). The Specific Volume of Cotton Cellulose. J. Textile Institute. 18:T 175.

Day, D. L. and G. L. Nelson (1965). Desorption Isotherms for Wheat. Trans. A.S.A.E. 8(2):293.

de Boer, J. H. and C. Zwikker (1929). Adsorption als Folge von Polarisation die Adsorptionsisotherme. Z. Physik Chem. B3:407.

de Boer, J. H. (1953). The Dynamical Character of Adsorption. Clarendon Press, Oxford.

de Boer, J. H. (1958). The Shapes of Capillaries. In Structure and Properties of Porous Materials. Edited by Everett and Stone. Butterworths Scientific Publications, London. p. 68.

Defay, R., I. Prigogine, A. Bellemans and D. H. Everett (1966). Surface Tension and Adsorption. Wiley and Sons, Inc. New York.

Dellyes, R. (1963). Modification A La Théorie B-E-T Et Nouvelles Possibilitiés D' Application. J. Chim. Phys. 60:1008.

De Vries, Thos. (1935). Densities of Adsorbed Gases I. Carbon Dioxide on Charcoal. J. Am. Chem. Soc. 57:1771.

Dollimore, D. and G. R. Heal (1964). An Improved Method for the Calculation of Pore-Size Distribution from Adsorption Data. J. of Appl. Chem. pp. 109-114.

Dorsey, N. E. (1940). Properties of Ordinary Water Substance. Reinhold Publishing Co., New York.

Dubinin, M. M. (1955). A Study of the Porous Structure of Active Carbons Using a Variety of Methods. Quarterly Review (London). 9:101.

Dubinin, M. M. (1965). Theory of Bulk Saturation of Microporous Activated Charcoals During Adsorption of Gases and Vapours. Russian J. of Phys. Chem (English Trans.). 39:697.

Everett, D. H. (1958). Some Problems in the Investigation of Porosity by Adsorption Methods. In Structure and Properties of Porous Materials. Edited by Everett and Stone. Butherworths Scientific Publications, London. p. 95.

Everett, D. H. (1967). Adsorption Hysteresis. In The Solid-Gas Interface. Edited by Flood. Marcel Dekker, Inc. New York. p. 1055.

Ewing, A. (1881). Proc. Royal Society (London), 33:22.

Ewing, D. T. and C. H. Spurway (1930). The Density of Water Adsorbed on Silica Gel. J. Am. Chem-Soc. 52:4635.

Filby, E. and O. Maass (1932). The Volume Relations of the System, Cellulose and Water. Can. J. of Research. 7(2):162.

Flood, E. A. (1967). The Solid-Gas Interface Vols. I & II. Marcel Dekker, Inc., New York.

Foster, A. G. (1932). The Sorption of Condensable Vapors by Porous Solids. Part I. The Applicability of the Capillary Theory. Trans. Faraday Soc. 28:645.

Foster, A. G. (1934). The Sorption of Methyl Alcohol by Silica Gels. Proc. Royal Soc. (London). A. 146:129.

Foster, A. G. (1948). Pore Size and Pore Distribution. Discussions Faraday Soc. 3:41.

Foster, A. G. (1951). Sorption Hysteresis I. Some Factors Determining the Size of the Hysteresis Loop. Journal of Physical and Colloid Chemistry. 55:638.

Frenkel, Y. I. (1946). Kinetic Theory of Liquids. The Clarendon Press, Oxford. Reprinted by Dover Publications, 1955.

Gibbson, R. E. (1934). The Influence of Concentration on the Compression of Aqueous Solutions of Certain Sulfates and a Note on the Representation of the Compression of the Aqueous Solution as a Function of Pressure. J. Am. Chem. Soc. 56:4.

Gorter, C. J. and H. P. R. Frederikse (1949). A Few Remarks on Physical Adsorption. Physica. 15:891.

Gregg, S. J. and K. W. Sing (1967). Adsorption Surface Area and Porosity. Academic Press, London and New York.

Guggenheim, E. A. (1967). Thermodynamics. North Holland Publishing Co., Amsterdam.

Halsey Jr., G. D. (1948). Physical Adsorption on Non-Uniform Surfaces. Journal of Chemical Physics. 16:931.

Halsey Jr., G. D. (1950). The Role of Heterogeneity in Adsorption and Catalysis. Discussions Faraday Soc. 8:54.

Hammerle, J. R. (1968). Failure in a Thin Viscoelastic Slab Subjected to Temperature and Moisture Gradients. Unpublished Ph.D. Thesis Penn. State University.

Harkins, W. D. and D. T. Ewing (1921). A High Pressure Due to Adsorption, and the Density and Volume Relations of Charcoal. The Compression of Liquids by Charcoal. J. Am. Chem. Soc. 43:1787.

Harkins, W. C. and G. Jura (1944). Surfaces of Solids XIII. A Vapor Adsorption Method for the Determination of Area of Solids Without Assumption of a Molecular Area and Areas Occupied by Nitrogen and other Molecules on the Surface of a Solid. J. Am. Chem. Soc. 66:1366.

Harvey, E. N. (1943). Surface Areas of Porous Materials Calculated from Capillary Radii. J. Am. Chem. Soc. 65:2343.

Henderson, S. M. (1952). A Basic Concept of Equilibrium Moisture. Agricultural Engineering 33(1):29.

Henderson, S. M. (1969). Equilibrium Moisture Content of Small Grain Hysteresis. A.S.A.E. paper No. 69-329 presented at Purdue University, June 22-25, 1969.

Hill, T. L. (1952). Theory of Physical Adsorption. Advances in Catalysis. 4:211.

Hill, T. L. (1960). Introduction to Statistical Thermodynamics. Addison-Wesley Publishing Co., Inc., Reading, Mass. and London.

Hüttig, G. F. (1948). Zur Auswertung der Adsorptions-Isothermen. Monatsh. Chem. 78:177.

Jastrzebski, Z. D. (1957). Nature and Properties of Engineering Materials. Wiley and Sons, Inc., New York.

Jungh (1965). Ann Phys. Chem. 125:292.

Katz, S. M. (1933). The Laws of Swelling. Transactions Faraday Soc. 29:279.

Katz, S. M. (1949). Permanent Hysteresis in Physical Adsorption. J. Phys. Chem. 53:1166.

Kraemer, E. O. (1931). A Treatise on Physical Chemistry. Edited by H. S. Taylor. D. Van Nostrand Co., New York.

Kuprianoff, J. (1958). Bound Water in Foods. In Fundamental Aspects of Dehydration of Foodstuffs. London, England: Society of Chemical Industries.

Kühn, I. (1964). A New Theoretical Analysis of Adsorption Phenomena. Introductory Part: The Characteristic Expression of the Main Regular Types of Adsorption Isotherms by a Single Simple Equation. J. Colloid Science. 19:685.

Labuza, T. P. (1968). Sorption Phenomena in Foods. Food Technology. 22:263.

Lamb, A. B. and A. S. Coolidge (1920). The Heat of Adsorption of Vapors on Charcoal. J. Am. Chem. Soc. 42:1146.

Lambert, B. and A. G. Foster (1932). Studies of Gas-Solid Equilibria. Part IV. Pressure-Concentration Equilibria between Ferric Oxide Gels and (a) Water, (b) Ethyl Alcohol, (c) Benzene, directly Determined under Isothermal Conditions. Proc. Roy. Soc. (London) A136, 363.

Langmuir, I. (1918). The Adsorption of Gases on Plane Surfaces of Glass and Mica and Platinum. J. Am. Chem. Soc. 40:1361.

Lewis, W. K. (1921). The Rate of Drying of Solid Materials. The Journal of Industrial and Engineering Chemistry.

Lippens, B. C., B. G. Linsen and J. H. de Boer (1964). Studies on Pore Systems in Catalysis.
I The Adsorption of Nitrogen; Apparatus and Calculation.
II The Shapes of Pores in Aluminum Oxide Systems.
III Pore-Size Distribution Curves in Aluminum Oxide Systems.
J. of Catalysis. 3:32.

Lisen, B. G. and A. Van den Heuvel (1967). Pore Structure. In The Solid-Gas Interface. Edited by Flood. Marcel Dekker, Inc. New York. p. 1025.

Lowry, H. H. and P. S. Olmsted (1927). The Adsorption of Gases by Solids with Special Reference to the Adsorption of Carbon Dioxide by Charcoal. J. Phys. Chem. 31:1601.

Lykov, A. W. (1955). Experimentelle und Theoretische Grunlagen der Trocknung. V.E.B. Verlag Technik. Berlin, Germany.

Matz, S. A. (1965). Water in Foods. A.V.I. Publishing Co., Inc., Westport, Connecticut.

McBain, J. W. (1935). An explanation of Hysteresis in the Hydration and Dehydration of Gels. J. Am. Chem. Soc. 57:699.

McMillan, W. G. and E. Teller (1951). The Role of Surface Tension in Multi-layer Gas Adsorption. J. Chem. Phys. 19:25.

McMillan, W. G. and E. Teller (1951). The Assumptions of the B-E-T Theory. J. Phys. Chem. 55:17.

McGavack, J. and W. A. Patrick (1920). The Adsorption of Sulfur Dioxide by the Gel of Silicic Acid. J. Am. Chem. Soc. 42:946.

Müller, H. (1882). On the Relation between Moisture Present in Textile Fabrics and that in the Atmosphere. J. Soc. of Chem. Industries. 1:356.

Parks, G. J. (1902). On the Heat Evolved or Absorbed when a Liquid is Brought in Contact with a Finely Divided Solid. Phil. Mag. 4:240.

Patrick, W. A. and F. V. Grimm (1921). Heat of Wetting of Silica Gel. J. Am. Chem. Soc. 43:2144.

Patrick, W. A. (1929). Colloid Symposium Annual. 7:129.

Pichler, H. J. (1956). Sorptionisothermen für Getreide und Raps. (Sorption isotherms of wheat and rape-seed). Landtechnische Forschung 2:47.

Pickett, G. (1945). Modification of the B-E-T Theory of Multimolecular Adsorption. J. Am. Chem. Soc. 67:1958.

Pierce, C. and R. N. Smith (1950). Adsorption-Desorption Hysteresis in Relation to Capillary of Adsorbents. J. Phys. Chem. 54:784.

Pierce, C. and R. N. Smith (1950). Heats of Adsorption IV. Entropy Changes in Adsorption. J. Phys. Chem. 54:795.

Pierce, C. (1953). Computation of Pore Sizes from Physical Adsorption Data. J. Phys. Chem. 57:149.

Pierce, F. T. (1929). A Two-Phase Theory of the Absorption of Water Vapor by Cotton Cellulose. J. Textile Inst. 20:133.

Polanyi, M. (1914). Verhandl. Deutsch. Physich. Ges. 16:1012.

Polanyi, M. (1916). Verhandl. Deut. Physik. Ges. 18:55.

Polanyi, M. (1920). Z. Elektro. Chem. 26:370.

Rao, K. S. (1941). Hysteresis in Sorption. I, II, III, IV, V, VI. J. Phys. Chem. 45:501.

Rodriquez-Arias, J. H. (1956). Desorption Isotherms and Drying Rates of Shelled Corn in the Temperature Range of 40 to 140°F. Unpublished Ph.D. Thesis, Dept. of Agri. Eng., Michigan State University.

Rose (1849). Ann. Phys. 73:1.

Ross, S. and J. P. Olivier (1964). On Physical Adsorption. Interscience Publishers, New York, London, Sidney.

Saravacos, G. D. and R. M. Stinchfield (1965). Effect of Temperature and Pressure on the Sorption of Water Vapor by Freeze-Dried Food Materials. J. of Food Science. 30(5):779.

Shull, C. G. (1948). The Determination of Pore-Size Distribution from Gas Adsorption Data. J. Am. Chem. Soc. 70:1405.

Stamm, A. J. and R. M. SeBorg (1935). Adsorption Compression on Cellulose and Wood I. J. Phys. Chem. 39:133.

Stamm, A. J. and W. K. Loughborough (1935). Thermodynamics of Swelling of Wood. J. Phys. Chem. 39:121.

Stamm, A. J. and L. A. Hansen (1937). The Bonding Force of Cellulose Materials for Water (from Specific Volume and Thermal Data). J. Phys. Chem. 41:1007.

Stamm, A. J. (1938). Calculations of Void Volume in Wood. Industrial and Engr. Chem. 30(11):1280.

Strohman, R. D. and R. R. Yoerger (1967). A New Equilibrium Moisture-Content Equation. Trans. A.S.A.E. 10(5):675.

Swan, E. and A. R. Urquhart (1927). Adsorption Equations - A Review of the Literature. J. Phys. Chem. 31:251.

Ter Haar, D. (1950). Phenomenological Theory of Visco-Elastic Behavior. Physica. 16:719, 738, 839.

Thompson, T. L., R. M. Peart and G. H. Foster (1967). Mathematical Simulation of Corn Drying - A New Model. A.S.A.E. Paper No. 67-313. Presented at Saskatoon, Saskatchewan, Canada, June 27-30, 1967.

Thomson (Lord Kelvin), W. (1871). On the Equilibrium of Vapor at a Curved Surface of Liquid. Phil. Mag. S.4 Vol. 42, No. 282: 448.

Triebold, H. O. and W. A. Aurand (1963). Food Composition and Analysis. D. Van Nostrand Co., Inc. Princeton, New Jersey.

Tuck, N. G. M., R. L. McIntosh and O. Maass. The Density of Adsorbates. Can. J. of Research. 26B:21.

Urquhart, A. R. and A. M. Williams (1924). The Moisture Relations of Cotton. The Effect of Temperature on the Absorption of Water by Soda-Boiled Cotton. J. Textile Institute. 21:T559.

Urquhart, A. R. (1929). Adsorption Hysteresis. J. Textile Inst. 20:T117.

Urquhart, A. R. (1929). The Mechanism of the Adsorption of Water by Cotton. J. Textile Inst. 20:125.

Urquhart, A. R. and N. Eckersall (1930). The Moisture Relations of Cotton. VII. A Study of Hysteresis. J. Textile Inst. 21:T499.

Van Laar (1924). Zustandsgleichung von Gasen und Flussigkeiten. Quoted by Lowry and Olmsted (1927), J. Phys. Chem. 31:1601.

Van Arsdel, W. B. and M. J. Copley (1963). Food Dehydration. Vol. 1. A.V.I. Publishing Co., Westport, Connecticut.

Viswanathan, B. and M. V. C. (1967). Computation of Pore Size Distribution in Terms of Surface Area. J. of Catalysis. 8:312.

Ward, A. G. (1962). The Nature of the Forces Between Water and the Micromolecular Constitutents of Food. In Recent Advances in Food Science. Vol. 3:207. Edited by Keitch and Rhodes. Butterworth's London.

Wheeler, A. (1945). Report #S-9829. Circulated to the PAW "Recommendation 41 Group" of the Petroleum Industry, June 1945; presented at A.A.A.S. Gordon Conference on Catalysis 1945 and 1946.

Wheeler, A. (1955). Reaction Rates and Selectivity in Catalyst Pores. In Catalysis - Fundamental Principles. Vol. II, p. 105. Edited by P. H. Emmett.

White, H. J. and H. Eyring (1947). The Adsorption of Water by Swelling High Polymeric Materials. Textile Research Journal. 17(10):523.

White, R. K. (1966). Swelling Stress in Corn Kernel as Influenced by Moisture Sorption. M.S. Thesis in Agricultural Engineering Penn. State University.

Young, D. M. and A. D. Crowell (1962). Physical Adsorption of Gases, Butterworth, London.

Young, J. H. and G. L. Nelson (1967). Research of Hysteresis Between Sorption and Desorption Isotherms of Wheat. Trans. A.S.A.E. 10(6):756.

Young, J. H. and G. L. Nelson (1967). Theory of Hysteresis Between Sorption and Desorption Isotherms in Biological Materials. Trans. A.S.A.E. 10(2):260.

Zsigmondy, R. (1911). Z. Anorg. Chem. 71:356.

APPENDICES

APPENDIX A

Isosteric heat of adsorption plotted as a function of moisture content for several materials.

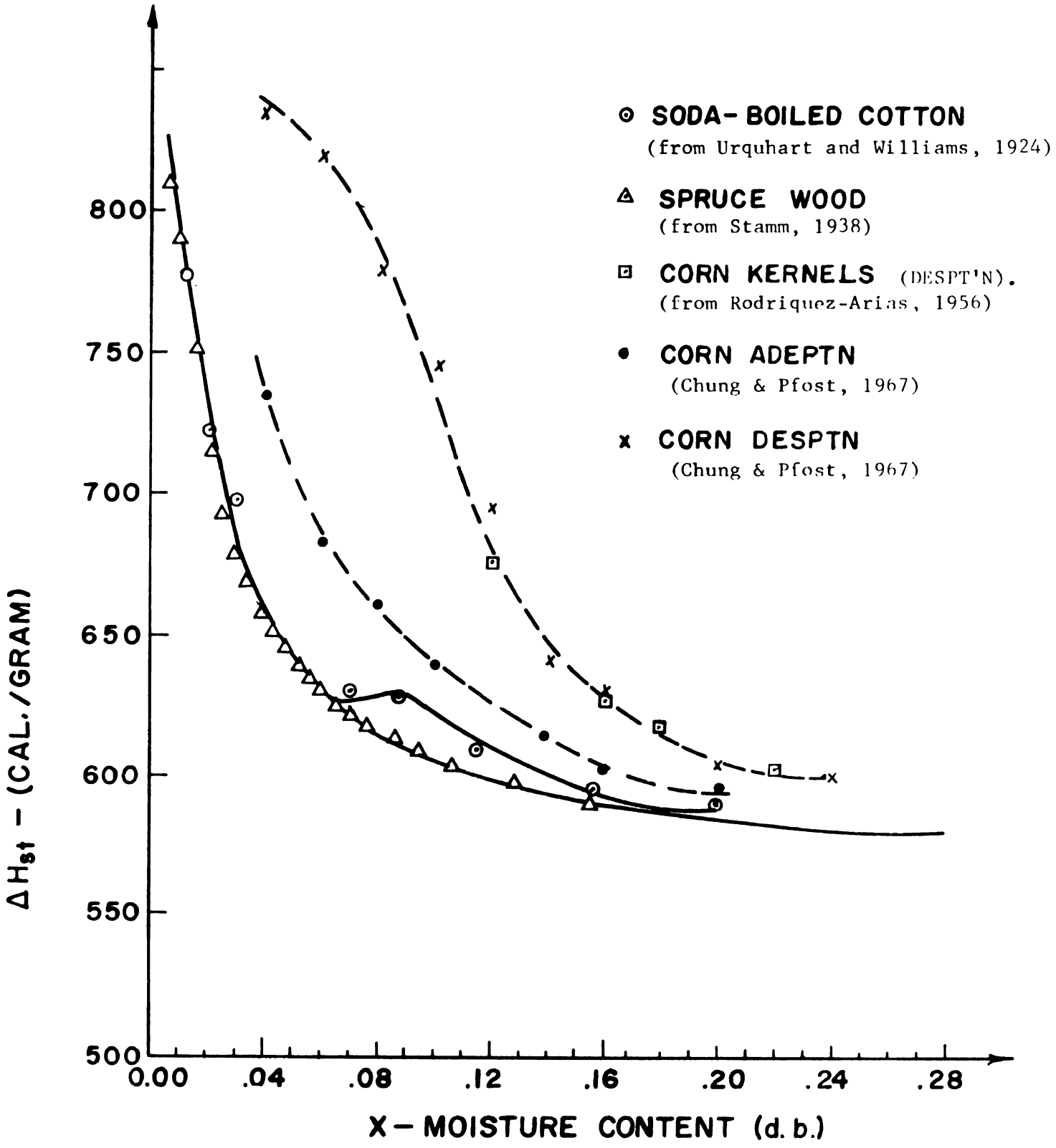

Figure A-1. The isosteric heat of adsorption as a function of moisture content.

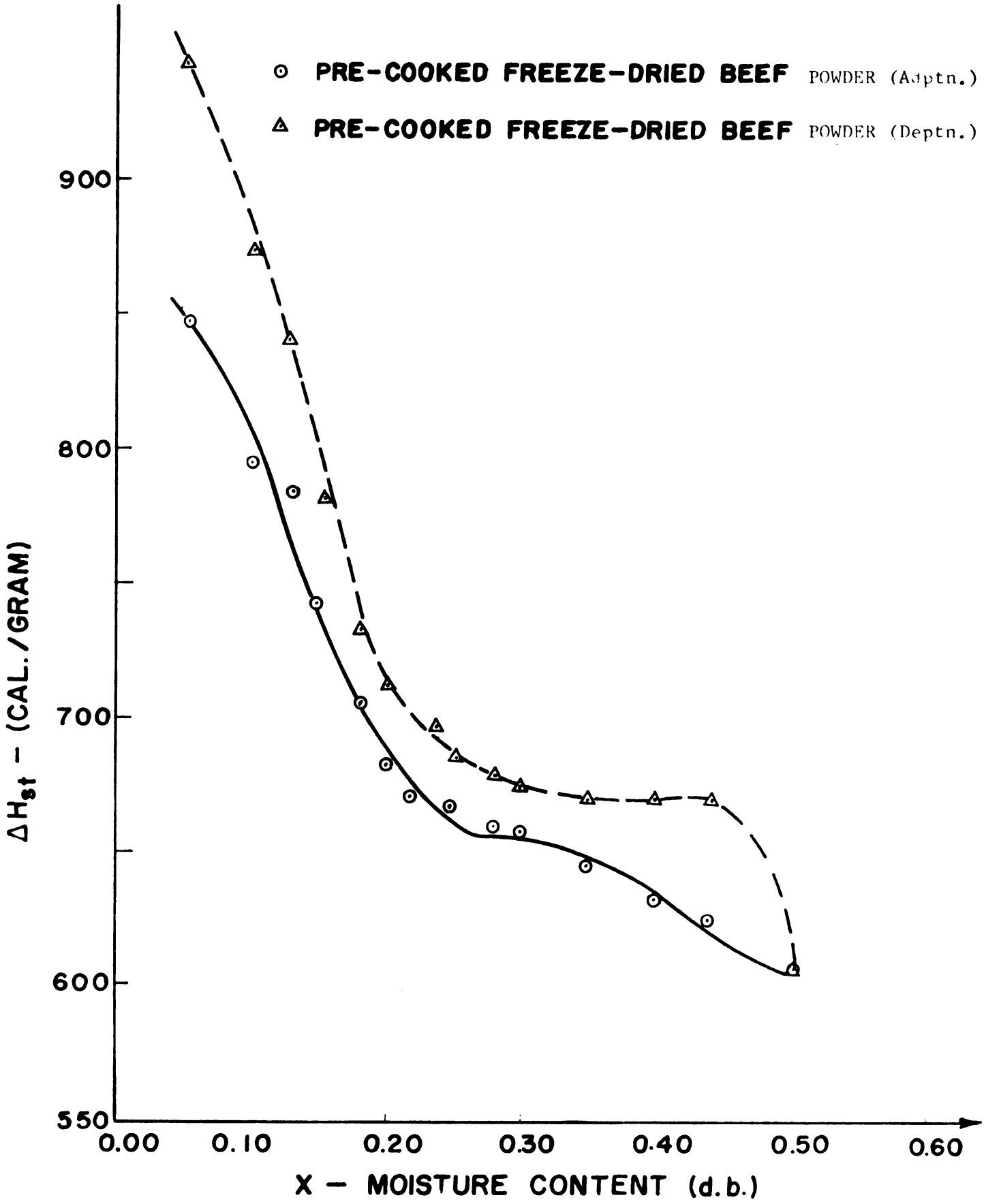

Figure A-2. The isosteric heat of sorption as a function of moisture content.

APPENDIX B

Development of the working equation of the Cranston and Inkley (1957) method for the calculation of pore-size distribution from sorption isotherms.

Let $V_r \delta r$ be the volume of pores having radii between r and $r + \delta r$, where δr is small compared with r. Consider an adsorption step from a relative pressure P_r such that the small pore in the range is about to fill with condensate, to a pressure $P_{(r+\delta r)}$, such that the largest pore in the range has just filled with condensate. During this pressure change, pores in the range considered became filled with condensate, smaller pores are already filled, while in larger pores the thickness of the adsorbed layer on their walls increases from t_r to $t_r + \delta t$. The total volume of liquid water adsorbed in this step is given by the volume of liquid condensed in pores with average radius $\bar{r} = (r_1 + r_2)/2$, and the volume of water condensed in larger pores contributing to the thickness of the adsorbed layer. Thus, assuming a cylindrical geometry,

$$v_{\bar{r}} \delta r = \pi(\bar{r} - t_r)^2 L_r + c(t_r - t_{r+\delta r}) \Sigma S_{r-\delta r} \qquad [A\text{-}1]$$

where $L_{\bar{r}}$ = total length of pores with mean radius $\bar{r}$,

$\Sigma S_{\bar{r}-\delta r}$ = surface of pores covered with multi-layer thickness t_r,

c = correction factor for the curved surface

The volume of pores with radius $\bar{r}$ is given by:

$$V_{\bar{r}} = \pi \bar{r}^2 L_{\bar{r}} \qquad [A\text{-}2]$$

so that $L_{\bar{r}} = V_{\bar{r}}/\pi \bar{r}^2$ [A-3]

Also the capillary surface $S_{\bar{r}}$ is given by:

$$S_r = 2\pi \bar{r} L_{\bar{r}} = 2V_{\bar{r}}/\bar{r} \quad [A-4]$$

If equations (A-3) and (A-4) are substituted in equation (A-1) and the summation sign is replaced by an integral sign:

$$v_{\bar{r}}\delta r = \frac{(\bar{r}-t_{\bar{r}})^2}{\bar{r}^2} V_{\bar{r}}\delta r + \delta t \int_{\bar{r}+\delta r}^{\infty} \frac{\bar{r}-t_r}{\bar{r}} \frac{2V_{\bar{r}}}{r} dr \quad [A-5]$$

where $c = \frac{\bar{r} - t_{\bar{r}}}{\bar{r}}$, and

$V_{\bar{r}}\delta r$ is the total volume of pores in the range δr considered.

In the limiting case, where $\delta r \to 0$, equation (A-5) becomes:

$$v_r dr = \frac{(r-t_r)^2}{r^2} V_r dr + dt \int_r^{\infty} \frac{2V_r(r-t_r)dr}{r^2} \quad [A-6]$$

where v_r derived from experimental measurements, while r, t_r, dr and dt are all functions of pressure which can be evaluated. Thus, V_r can in theory, be evaluated by applying equation (A-6) to the experimental results. In practice, however, it is not convenient to use the equation as it stands and it is preferable to integrate it over small finite ranges of radii.

Consider a finite adsorption step from pressure P_1 to pressure P_2, where P_1 corresponds to the critical radius r_1 and P_2 to radius r_2. The total volume of water adsorbed during this step is:

$$v_{12} = \int_{r_1}^{r_2} v_r dr$$

$$= \int_{r_1}^{r_2} \frac{(r-t_1)^2}{r^2} V_r dr + (t_2-t_1) \int_{r_2}^{\infty} \frac{V_r(2r-t_1-t_2)}{r^2} \quad [A-7]$$